Hydrodynamic Modelling for Flood Management in Bay of Fundy Dykelands

By
Michael Fedak

A Thesis Submitted to
Saint Mary's University, Halifax, Nova Scotia
in Partial Fulfillment of the Requirements for
the Degree of Master of Science in Applied Science

July 16, 2012, Halifax Nova Scotia

Approved: Dr. Danika van Proosdij
Supervisor
Department of Geography

Approved: Dr. Ryan Mulligan
External Examiner
Department of Civil Engineering
Queen's University

Approved: Dr. Timothy Webster
Supervisory Committee Member
COGS, NSCC

Approved: Dr. Peter Secord
Graduate Studies Representative

Date: July 16, 2012

Library and Archives Canada

Published Heritage Branch

395 Wellington Street
Ottawa ON K1A 0N4
Canada

Bibliothèque et Archives Canada

Direction du Patrimoine de l'édition

395, rue Wellington
Ottawa ON K1A 0N4
Canada

Your file Votre référence
ISBN: 978-0-494-89992-2

Our file Notre référence
ISBN: 978-0-494-89992-2

Abstract

"Hydrodynamic Modelling for Flood Management in Bay of Fundy Dykelands"

By Michael Fedak

Storm surge in the coastal Bay of Fundy is a serious flood hazard. These lands are low-lying and adapted to farming through the use of coastal defences, namely dykes. Increasing rates of sea level rise due to climate change are expected to increase flood hazard in this area. In this thesis, flood risk to communities in the Avon River estuary of the Upper Bay of Fundy is investigated through computer based modelling and data management techniques. Flood variables from 14 possible storm surge scenarios (based on sea level rise predictions) were modelled using TUFLOW software. A GIS was used to create a database for simulation outputs and for the analysis of outputs. TUFLOW and a geographic information system (GIS) flood algorithm are compared .It was found that obstructions to flow controlled flooding and drainage and these features required the use of a hydrodynamic model to represent flows properly.

July 16, 2012

Acknowledgements

Funding Sources:

- Atlantic Canada Adaptation Solutions Association part of the Natural Resources Canada Regional Adaptation Collaboratives (RAC) Project.
- Environment Canada
- Nova Scotia Department of Agriculture, Land Protection, Resource Stewardship
- Nova Scotia Community College: Centre of Geographic Sciences (NSCC-COGS)
- Saint Mary`s University

Important Contributors:

- My Parents; Janos and Beata
- My Grandfather: Musci Sàndor
- Phillip Ryan, Hydraulic Engineer: BMT-WBM Australia
- Kevin McGuigan and Nathan Crowell: Applied Geomatics Research Group
- Ken Caroll & Darrell Hingley: NS Dept of Agriculture
- Emma Poirier, Jennie Graham, Barbara Perrot-Pietersma, Casey O`Laughlin, Ben Lemieux, Greg Baker, In_CoaST Research Unit, and MP_SpARC: Saint Mary's University
- Drs. Paul Muir and Tim Webster: Supervisory Committee
- Dr. Danika van Proosdij: Main Supervisor
- Dr. Ryan Mulligan: External Examiner

Table of Contents

Figures

Tables

Equations

List of Symbols

A = *Wetted area of a channel cross section*
Q = *Discharge*
t = *Time*
g = *Acceleration due to gravity*
Δt = *Timestep*
x *and* y = *Distance in x and y directions*
Δx, Δy = *Computational cell dimensions in x and y directions (2D Model)*
H = *depth of water*
c = *speed of a shallow water wave given by* $(gH)^{1/2}$
u = *Depth and width averaged velocity (1D model)*
u *and* v = *Depth average velocity components in x and y directions*
ζ = *Water surface elevation*
So = *Channel Slope*
Sf = *Friction Slope (Roughness Formulation such as Chezy or Manning's n)*
R = *hydraulic radius*
Cr = *Courant Number*
HR = *(flood) hazard rating*
DF = *debris factor*
c_f = *Coriolis force coefficient*
f_l = *Form Loss coefficient*
μ = *Horizontal diffusion of momentum coefficient*
p = *Atmospheric pressure*
ρ = *Density of Water*
F_x *and* F_y = *Sum of external forces in X and Y directions*

CHAPTER 1: Introduction and Literature Review

Flooding is the most commonly occurring natural disaster in Canada (PSC, 2012). In Nova Scotia flooding may result from a number of sources depending on the location and time of year. Since 70 per cent of the population of Nova Scotia lives on (or near) the coast, flooding due to elevated water levels from storm surge and extreme events, such as hurricanes, is of particular concern (Provincial Oceans Network, 2011). The coastlines of Nova Scotia are varied due to large differences in coastal geomorphology. This thesis focuses on the Bay of Fundy area of Nova Scotia, which is known for having the largest tidal range in the world (NOAA, 2011). Settlement along the coast of the Bay is centered on dykelands, which are salt marshes that have been cut-off from tidal influence using embankments known as dykes and converted into farmland (see Section 2). Without the dykes, these lands would be flooded regularly at high tide. Unusually high tides, caused by storm surge, are of major concern for flooding the Bay of Fundy (Desplanque and Mossman, 1999; Bleakney, 2004; Provincial Oceans Network, 2011). Compounding flood risks to the dykelands are climate change driven sea level rise, local geological subsidence, increasing tidal amplitude as well as sediment deposition in channels. Sea level rise in the Bay of Fundy has increased the risk associated with storm surges (Daigle and Richards, 2011).

Land use planning in flood prone areas requires the delineation of total risk associated with differing land uses. Flood risk assessment is ideally based on integrating data and models over varying temporal and spatial scales, and then organizing the results in a spatial decision support system which makes them accessible to decision makers.

Models are an abstraction of reality consisting of entities and their relationships which are deemed important in understanding some aspects of the behaviour of a system. Modelling for flood risk assessment can be done by computer-based or physical means whereby variables related to flooding are examined.

This thesis is concerned with hydrodynamic (hydraulic) and geographic information systems (GIS) modelling techniques which are computer-based. Hydrodynamic models consist of a mathematical model based on a set of physical equations describing water flow through time based on the conservation of mass and momentum, boundary conditions which represent the evolution of the system through time, a domain representing the terrain, and initial conditions. The mathematical model is solved by software which provides approximate solutions at defined intervals. Examples of hydrodynamic modelling software are TUFLOW and MIKE21 which solve the Shallow Water Equations. GIS models consider the spread of water across a grid representing the terrain elevations (digital elevation model). These models are not based on physical equations and do not represent the evolution of a system through time but are less data intensive and time consuming to run.

1.1 Thesis Statement

This research investigates the use of a hydrodynamic model (TUFLOW) as a tool to inform decisions relating to future flood risk in the dykelands of the Bay of Fundy. This study presents results from computer simulations of possible flood scenarios as well as an examination of the implications of these results for flood management. The anticipated outcomes of the research were the delineation of areas at risk, a better

understanding of the important components of the natural and man-made drainage systems in the dykelands for dealing with storm surge flooding and the construction of a database containing outputs which can be associated with features of interest to decision makers (buildings, dykes). A method was developed to organize the results in a database that allows the data to be queried and transformed into multiple different formats. The outcome of this study will assist planners, engineers, GIS professionals and emergency managers in decision making relating to flooding and the application of flood models to the Upper Bay of Fundy.

1.2 Rationale

Increased coastal flood risk has been identified as one of the major impacts of climate change in Atlantic Canada (Provincial Oceans Network, 2011; ACASA, 2012). Low lying coastal communities are at particular risk from storm surge driven flood events. Delineating areas prone to flooding is useful for land use planning because it can inform policies around mitigating risk to communities. Outputs from flood prediction are useful for implementing structural and non-structural measures of flood prevention. Structural methods use engineered features such as dams and dykes to control flooding. Non-structural methods include regulations preventing development on floodplains and economic instruments discouraging development in hazardous areas. Different technologies for hydrodynamic modelling and geographic information systems can be combined for effective flood risk management (Cunge, 1998; Zerger and Wealands, 2004; Haile, 2005; Blackburn et al., 2012).

1.3 Purpose and Objectives

This research focuses on hydrodynamic flood modelling to predict flood hazard in a macrotidal estuary with dykelands. This thesis covers potential uses, advantages and challenges of hydrodynamic modelling and makes suggestions as to how it can be used in a flood management strategy. The specific objectives are to:

1. Determine the flood hazard extent, duration, depth and velocity for an ensemble of storm surge scenarios with varying water levels and drainage characteristics in the study area.

2. Assess the vulnerability of dykes and buildings to storm surge flooding and explore hazard reporting and data organization methods.

3. Investigate the added value and challenges around applying a hydrodynamic model for flood hazard assessment compared with past studies using GIS based analysis.

1.4 Interdisciplinary Approaches in Flood Modelling

Proactive land use planning in flood prone areas is based on useful flood risk prediction, mapping and community consultation. Obtaining useful predictions depends on the integration of multiple sources of data and analysis methods. The overall framework for flood prediction may be considered a part of geoinformatics (Haile, 2005), or more specifically, hydroinformatics (Cunge, 1998). Hydroinformatics came through recognition that the science of hydraulics was being applied for practical purposes by a growing number of people from different disciplines. By bringing different skills and

perspectives together, it was thought that hydraulics could be applied to a larger selection of meaningful problems (Cunge, 1998). The focus of hydroinformatics is not entirely technical. One of the goals is to analyze the social dimensions of water related problems and to provide support to decision makers using technologies and frameworks for flood management (Cunge, 1998).

1.5 Data Requirements

Data requirements for modelling can be quite extensive depending on the model used and the accuracy requirements. A list of necessary and desirable data for coastal modelling may include; bathymetry and coastal topography, tides and currents, sea level rise, surface roughness, temperature and salinity, particulates, and winds (Hardisty, 2007; Haslett, 2009). Validation data is also desirable, especially when a model is used in an environment different from where it was developed. For assessing coastal hazards due to sea level rise, all of these processes and conditions may be considered, however this requires coupling several models together, each simulating a particular aspect of the overall system. Limits on data availability, resources in terms of time and expertise make running a model of all the physical processes in an estuary very difficult and, as per Bonini's Paradox, the resulting model may be just as difficult to understand as the natural processes being modeled (Lakhan, 2005). Therefore the relevant environmental conditions need to be identified and included in the model, while others may be left out.

1.5.1 Terrain Data and Bathymetry

A high resolution terrain model is essential so that the features of the intertidal areas may be captured and the dykes properly represented. Purvis et al, (2008) indicated

that a high quality terrain model is as important as proper boundary condition data and Haile, (2005) demonstrated that a sufficient resolution terrain model (under 10m cell size) is necessary in order to limit the overprediction of inundation extents. Ideally the surface model would be created from a combination of Light Detection and Ranging (LiDAR) LiDAR and multibeam bathymetry points and cover a large enough area so that the numerical model is able to simulate all physical processes properly. Terrain models based on LiDAR have been demonstrated to provide the high resolution necessary for numerical and GIS based flood prediction (French, 2003; Haile, 2005; Webster et al., 2008; National Research Council, 2009). Mason et al., (2011) states that for rural flood inundation modelling a digital terrain model representing bare earth (surface features removed) with a vertical accuracy of about 0.5 m and a spatial resolution of 10 m is required. For urban areas a higher resolution model of a vertical accuracy of 5 cm and a spatial resolution of 0.5 m may be required to resolve gaps between buildings (Mason, et. al, 2011). For dykes, they recommend that data with ~10 cm vertical accuracy and 2 m spatial resolution be used. Saul, et.al, (2011) indicate a desirable vertical accuracy of 0.05 to 0.15 m and 0.5-1.0 m spatial resolution for urban flood modelling. However, in their study they use a DEM (constructed from LiDAR points) with a grid cell size of 2 m by 2 m.

Past studies in Nova Scotia (Webster, 2004; Webster et al., 2011; van Proosdij, 2009) have explored the usefulness of high resolution terrain data and geographic information systems in predicting flood extents. These methods produced predictions of maximum

flood extent based on terrain elevations derived from LiDAR data. The vertical accuracy of these data was between 0.15 to 0.30 m with a spatial resolution of 1 to 2 m.

1.5.2 Boundary Conditions

According to Beven (2009), "Boundary conditions are constraints and values of variables required to run a model for a particular domain and time period".

The following boundary conditions can be used in flood inundation modelling in an estuary:

- Tidal Data (Harmonics and Water Levels)
- Storm surge levels
- Design Storm Hydrographs of Flow or Rainfall
- Wind Forcing
- Atmospheric Pressure
- Impenetrable zones or edges of the domain (high elevation areas).

In a coastal model, boundary conditions are typically water level elevations, or currents originating from the offshore edges of the domain (Hearn, 2008). The boundaries may be open or closed depending on whether or not they allow flows of matter and energy to and from the domain. Observed water levels are available at tide gauges. In the absence of a reliable tide gauge, a prediction model may be used such as the one used by WebTides service in the Maritimes (DuPont et al., 2005). Predicted tides for a local area may be based on a larger regional scale, particularly if local tide gauge data is unavailable. This may be coupled with a meteorological model acting at the same scale; provided that data are available and a framework has been set up so that a model can be run in a relatively short period of time (Barnard et al., 2009). This can be an effective method to predict risk due to an oncoming storm (Cheung et al., 2003).

In order to provide data for long term planning, researchers calculate probabilities of a high water event based on past water level data or through simulation modeling (Irish et al., 2009; Thompson et al., 2009). Using the probabilities of occurrence of different water levels, models can use expected water level data as boundary conditions. These predicted high water events usually include considerations of global and local sea level rise and meteorological effects that are based on a number of years of water level measurements. Ideally, a statistical model would be used to generate probabilities of meeting certain water levels (return periods) but this requires a continuous gauge record of 20-30 years in order to produce a reliable model (Thompson et al, 2009; Webster et al., 2008). Thompson et al, (2009) showed that using joint probability methods it may be possible to create estimates of water level return periods using 10 years or less of reliable data.

Wind forcing, atmospheric pressure and rainfall boundary conditions may also be necessary if individual storm events are to be simulated (Zerger and Wealands, 2004). However, Pender and Neelz, (2011) point out that wind effects are primarily important over very large floodplains where they may have some effect on water depths.

The sensitivity of the model should be tested for the different boundary conditions to determine which are the most responsible for changes in model results as errors in these data will translate to uncertainties in the model (Brown et al, 2007).

1.5.3 Surface Roughness

Surface roughness values are empirically derived coefficients describing the resistance of a channel or floodplain to water flow. They are used in numerical models

and may be assigned by a number of different methods. The required number of surface roughness values should be determined before their values are selected. Categories may be assigned to areas using different methods including examination of aerial photography, an automated classification algorithm for delineating areas based on LiDAR returns, and classification of Synthetic Aperture Radar imagery (such as RADARSAT) (Wamsley et al., 2010; French, 2003; Schumann et al., 2007). The advantage of using classification algorithms and LiDAR returns is that derived areas will be based on some actual physical boundaries whereas manual estimation of boundaries is prone to human input error. Werner et al, (2005) showed that sensitivity analysis using the Generalized Likelihood Uncertainty Estimation (GLUE) method can assist in determining the number of necessary roughness categories. In Werner et al, (2005), the sensitivity of the LISFLOOD-FP hydrodynamic model to changing floodplain and land use values was evaluated. Results indicated that the model was much more sensitive to changes in channel roughness than floodplain roughness. However they cautioned that their results may be area and model specific. Cunge, (2003) brought up another issue concerning roughness areas, namely, the need to know if there are any significant flow obstructions (such as bridges) because not accounting for these features will cause chosen roughness values to be much higher than realistic.

However, methods for the assignment of roughness coefficients assume that there is an optimal set of roughness coefficients, even though this is often not the case (Aronica et al., 2002; Beven, 2009; Pappenberger et al., 2005). Roux & Dartus, (2008) and Aronica et al., (2002) used an inverse modelling approach for assigning surface roughness coefficients.

In this approach, a range of possible roughness values was investigated by running simulations using different combinations of the values and then comparing the simulated inundation extents with observed results. Roughness values were chosen based on simulations which matched the observations more closely. Aronica et al, (2002) showed that a range of acceptable roughness values could be tested based on observed data to determine the optimal values.

Empirically derived roughness coefficients, such as Manning's n, are widely and effectively used (Cunge, 2003; Wamsley et al., 2010), but there is concern that these coefficients are incapable of properly describing the complex interactions between features such as vegetation and water (Wamsley et al., 2010; Lane, 2005; Pappenberger et al., 2005). The variation of roughness parameters with seasonal changes in surface cover would need to be investigated as it has been shown that vegetation can attenuate waves and reduce the severity of flooding (Moller, 2006; Wamsley et al, 2010).

1.6 GIS Based and Numerical Modelling Methods

1.6.1 GIS based methods

A flood prediction can be generated using algorithms within a GIS that predicts how water spreads across a terrain (Bates et.al, 2005). For this procedure, very accurate and properly processed terrain data are required (Webster, et al., 2004). The reasons why GIS methods are being considered are that they allow predictions to be made faster than numerical models and require less input data (Krupka, 2009). There are various levels of complexity within these models. The simplest is a planar approach where the predicted

extent of flooding is obtained by selecting all the areas of a surface which are equal in elevation to the maximum flood elevation.

Bates et al., (2005) concluded that the planar method overpredicts flooded areas and does not ensure connectivity of water flow to the main channel. However, Webster and Forbes, (2005) demonstrated that it is easy to preserve connectivity as long as the main flow path is known. The open source GIS GRASS provides an algorithm (r.lake) which predicts the flooding of an area based on its connectivity with a seed point (GRASS Development Team, 2009). Bates et al., (2005) showed that planar methods are inappropriate for areas where friction and inertia and important determinants of flood extent. The GIS based approached has been widely used in Nova Scotia with high resolution LiDAR DEMs (van Proosdij, 2009; Webster, 2010; Webster et al, 2011).

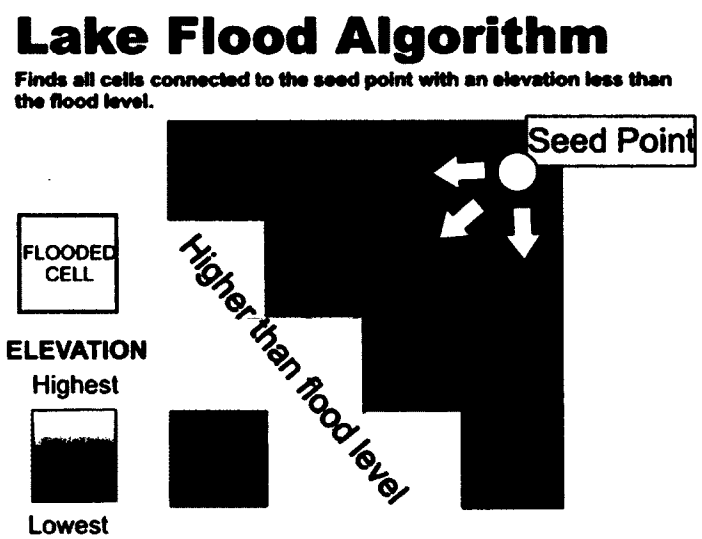

Figure 1: Lake Flood Algorithm which finds all DEM cells connected to the seed point greater than or equal to an absolute flood elevation.

Rapid flood inundation models (RFIM) are a more complex method of GIS based flood prediction that takes flood volumes and resistance into account, in addition to connectivity (Lhomme et al., 2009; Krupka, 2009). These models are being developed for cases where a large number of model runs need to be completed in a short time or a large

study area needs to be modelled (Lhomme et al., 2009). The model works using a GIS-based algorithm whereas depressions in the landscape are identified and filled based on connectivity to a start point. Volumes of water, defined at the beginning of the simulation, are spread between depressions in the landscape and resistance to flow is taken into account as a function of spreading extent with greater losses due to resistance at greater extents. Lhomme et al., (2009) tested their model in a variety of environments and compared their results with those from Two Dimensional Unsteady Flow (TUFLOW), a software package based on a mathematical model of the Shallow Water Equations (Section 3.3.1). They found that results from the models matched closely in areas with constrained floodplains where the pressure and inertia terms in the Shallow Water Equations were not important. However, neither GIS based method will produce results matching a hydrodynamic model in areas where fluid dynamical processes are important since they use only static water levels.

1.6.2 Numerical Methods

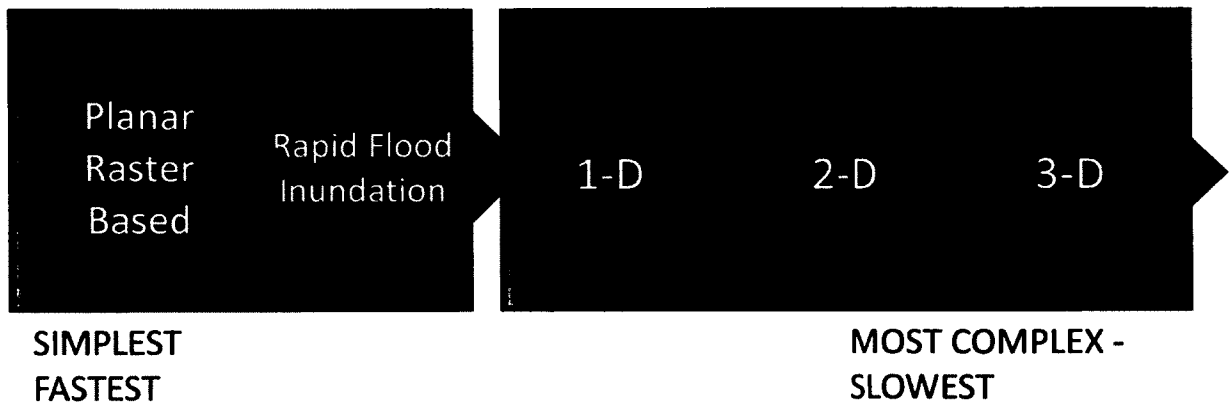

Figure 2: Computer based modelling methods organized by complexity and run time. Complexity refers to the solution procedure, and data and modeller expertise requirements. The simpler methods have shorter run-times, discounting the set-up times for each method.

Non-linear systems of partial differential equations (PDEs) are used to model water flow. Since these continuous equations are too complex to solve analytically, numerical methods are used to provide approximate solutions. Hydrodynamic models may be applied in one, two, or three spatial dimensions (we will refer to these as 1D, 2D and 3D respectively). Any of these schemes may be useful depending on the problem being investigated and the complexity with which the real world is to be modelled. Practically, a 1D scheme is much less computationally expensive than a 2D scheme for the same area (Figure 2). For urban areas with obstacles to water flow such as buildings, a 2D scheme is recommended since it can resolve the frequent changes in flow velocity and direction more suitably than a 1D scheme (Néelz and Pender, 2009; Bates et al., 2005). A 3D scheme is very computationally expensive compared to a 2D and its practical use is therefore limited (Pender and Neelz, 2011; Hearn, 2008).

1D flood models tend to be applied in areas where change happens along a single path with channel geometry defined at cross sections (Hearn, 2008). They are commonly used for modeling hydrological systems such as rivers but can also be applied to estuaries if the variation in the properties of interest occurs longitudinally. In a 2D model, properties are allowed to vary both laterally and longitudinally. Bekic et al, (2006) compared the effectiveness of a 1D and 2D hydrodynamic models for predicting water flow in a mesotidal estuary in Glasgow Scotland (Bekic et al, 2006). The software packages used for this experiment were MIKE21 (2D) and ISIS (1D). They found that under certain conditions, the two models predicted very similar water levels. However, when meteorological and wind boundary conditions were considered, the 2D model gave more accurate water level estimates (Bekic et al, 2006). Therefore, they concluded that 2D models are better for estuaries with strong wind shear and atmospheric pressure effects (Bekic et al, 2006). While a 1D model can be effective in determining the magnitude of water flow along a single path, coastal hazards such as flooding require that the flow of water be considered in areas outside of the main channel. Here, it is likely that water does not flow along a single path (Haile, 2005). Coastal defenses as well as infrastructure such as roads and buildings need to be modeled. This can be better achieved with 2D and 3D modelling methods (Haile, 2005; Pender & Neelz, 2011).

The 1D model is less flexible than the 2D when dealing with multiple channels in a floodplain (Lin et al., 2006). A coupled 1D/2D model can be very effective for modelling flood hazards. Lin et al., (2006) demonstrated the use of such a model for simulating the breach of an embankment along the River Thames due to flooding. Their study compared

the results of a software package implementing a coupled model (DIVAST 2D and ISIS 1D) with a software package using a 1D model (ISIS Floodcell) and concluded that a coupled model was able to simulate flooding more accurately. The coupled model preserved connectivity between the embankment breach and the flooded areas while the 1D model presented areas with no connection to the breach as being flooded (Lin et al., 2006). The coupled model also showed reduced computational times compared to a purely 2D model (Lin et al., 2006).

Since 2D models are depth averaged, they do not simulate the vertical distribution of current or density variations throughout the water column. A 3D model is able to simulate both horizontal and vertical movement of water and suspended matter. This type of model can simulate most of the physical processes acting in an estuary; however, the data requirements and computational time are greater than those in other types of models (Hearn, 2008; Hu et al., 2009). An example of a commercially available 3D hydrodynamic model is the Delft3D model which was used by Hu et al., (2009) in the Yahtzee River Estuary to simulate storm surge and morphological change. Using Delft3D allowed them to simulate sediment transport due to natural processes and storms, and to make predictions about the effects land use change would have on morphology (Hu et al., 2009). Through coupling Delft3D with the SWAN wave model software package, they were also able to hindcast wave heights during the Typhoon Forrest with some accuracy (Hu et al., 2009). However, their data requirements were much greater than those for a 1D/2D simulation of flooding and included water salinity, suspended sediment loads, erosion, deposition stresses, deposition rates, and bed densities (Hu et al., 2009).

There are also hybrid models in addition to the previously mentioned modelling methods. For example, LISFLOOD-FP is a software package implementing a hydrodynamic model which was developed to take advantage of high resolution raster terrain data (Bates et al., 2005). This model uses a 1D diffusive wave equation (Section 1.6.2.1) to solve for the motion of water in the longitudinal direction. For flow in the transverse direction, the method uses volume transfers similar to rapid flood inundation modelling. The advantage of this method is a reduced computational requirement. The other advantage is the ability to use a raster as the simulation domain without the need to construct a specialized grid or mesh.

1.6.2.1 Equation Choice

Different simplifications of the Navier Stokes system of PDEs can be used for simulating water flow. The choice of equations depends on the flow characteristics being modelled. Open channel flows can either be steady or unsteady and uniform or non-uniform. Steady flow is flow that does not change with time at a single point whereas uniform flow is where velocity does not change along the channel. Flow regime is another important characteristic which relates water velocity to wave velocity. When wave velocity is greater than water velocity, the flow is considered sub-critical; when water velocity is greater than wave velocity, flow is considered supercritical. A hydraulic jump occurs when flow transitions from a subcritical to supercritical state which is a change in the velocity and the cross section of flow. An example where supercritical flow may occur is on the landward side of a dyke or embankment during flood overtopping (Chinnarasri et al, 2003).

Bates et al, (2005) and Sutherland et al., (2004) suggest that for flood prediction the 1D Saint Venant Equations (Equations 1a and 1b), and in 2D form the Shallow Water Equations (Section 3.3.1), are most commonly used because they describe the movement of the various flow types. These are formulations of the 3D Navier Stokes Equations which assume incompressible flows and negligible vertical change (hydrostatic pressure distribution). In the case of the 1D Saint Venant Equations, flow is assumed to occur in the longitudinal direction. The Saint Venant Equations are a dynamic model with terms for inertia and local acceleration. There are simplified forms of these equations known as diffusive and kinematic wave equations which omit the inertia and pressure terms, respectively (Equation 1b). Richardson and Julien, (1994) investigated the importance of the pressure and inertia terms in the Saint Venant Equations. They concluded that a kinematic wave approximation is suitable for steeply sloping channels where the effects of pressure and inertia are negligible compared to the channel bed slope. For instance for when using the HEC-RAS hydrodynamic modelling software package in channels with slopes greater than 10%, the assumption of hydrostatic equilibrium may not be valid (HEC, 2008). The pressure terms were found to be dominant in subcritical overland flow (mildly sloping channels) while the local and convective acceleration (inertia) terms were dominant in supercritical overland flows (such as in dam breaks or dyke overtopping).

$$\frac{\partial Q}{\partial x} + \frac{\partial A}{\partial t} = 0$$

Equation 1a: Saint Venant Equation: Conservation of Mass (no lateral inflow),
Where:
A = Wetted area of the cross section
x = Distance
t = Time
Q = Discharge

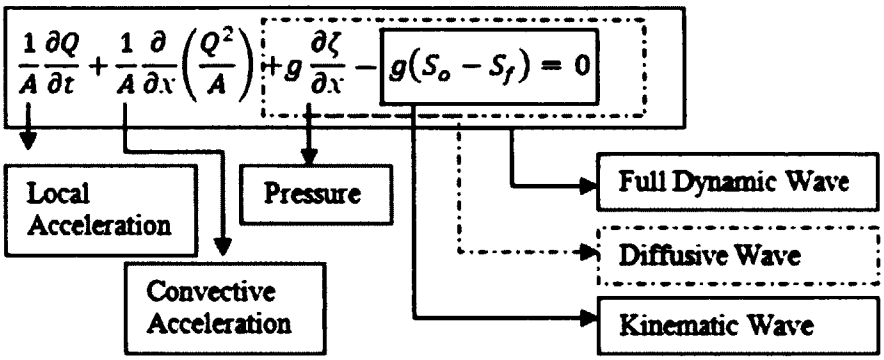

Equation 1b: Saint Venant Equation: Momentum Terms,

Where:
A = Wetted area of the cross section
Q = Discharge
t = Time
x = Distance
u= Depth and width averaged velocity
ζ= Water surface elevation
g = Acceleration due to gravity
S_o= Channel Slope
S_f= Friction Slope (Roughness Formulation such as Chezy or Manning's n)
$S_f = \frac{n^2}{R^{4/3}} u|u|$ for Manning's n roughness where n= Manning's n coefficient and R= hydraulic radius

1.6.2.2 Solution Procedure

After the equations are chosen, boundary and initial conditions set up and a computational grid has been chosen to represent the physical domain; a numerical solution procedure must be developed. The continuous form of the equations is discretized, i.e., the non-linear partial differential equations are approximated by a large system of linear algebraic equations which allow numerical solutions to be obtained for specific times using values from the boundary conditions and locations based on a grid, mesh or sub-regions; this is known as discretization. Since the solution node values are extracted from terrain data, there is a process of interpolation of elevations which creates

the domain. This process can lead to errors and uncertainties in model results as information is lost due to interpolation (Haile, 2005; National Research Council, 2009).

The variables in the linear system of equations resulting from the discretization are given values according to the initial and boundary conditions. Then, in order to move the model forward in time, a timestep needs to be specified in order to define the values for which the model will be solved. At each timestep the linear system of equations is updated with new values from the boundary conditions and from solution values at the previous timestep, and solved again to obtain solution values for the current time.

However, there are certain factors to which have to be considered when selecting the timestep. The limitations due to time step differ based on the way that the PDEs are discretized, i.e., explicitly or implicitly. In an explicit scheme, rates of change are evaluated in terms of known quantities at the previous time step while in an implicit scheme new quantities are calculated at each time step based on the previous and current solution values. Explicit schemes are limited to a smaller time steps than implicit schemes because an explicit scheme depends on information travelling across a cell so that the next value can be calculated, while an implicit scheme is not entirely dependent on the previous solution (Hearn, 2008). The limit on the timestep in an explicit model is expressed as the Courant- Friedrichs- Lewy (CFL) condition,

$$c\left(\frac{\Delta t}{\Delta x}\right) < 1$$

Equation 2: CFL condition for explicit schemes,

Where:
t = timestep
x = length of the model element (distance between nodes)
g = gravity
d = depth of water
c = speed of a surface gravity wave ($\sqrt{gd}$)

This condition states that the timestep (Δt) of an explicit scheme must be smaller than the time it takes for a wave with speed c to travel across a spatial cell of size Δx. This number is known as the Courant number (Cr). Since even an implicit scheme begins to show errors at higher Cr, Hearn (2008) recommends Courant numbers less than 10.

1.6.2.3 Numerical Modelling Limitations

The cell size of a rectangular grid is a limiting factor in a finite difference type discretization of a hydrodynamic model. Courant numbers allow the time step and speed of the solution process to be increased. Courant numbers are related to the CFL condition in that Cr< 1 satisfies the condition while Cr>1 does not which means that at Cr>1 an explicit solution is not valid. However, dropping the cell size of the computational domain increases the number of solution nodes and thus the size of the linear system of the equations and the computational time required for a solution.

To try to improve the speed of the solution computation, methods have been developed to reduce the number of nodes involved in a computation. The ideal method for a region is based on the shape of the coastal land forms and the relevant physical processes (Hearn, 2008). Nesting grids of different sizes allow the cell size to be varied across the area.

Smaller cells can therefore be used in areas where additional detail is required. The TUFLOW and MIKE 3 hydrodynamic software packages are both capable of linking grids with different cell sizes. Another method involves using a grid with curvilinear elements which vary in cell size to accommodate local bathymetry and coastal features (Hearn, 2008). The DELFT 3D, SLOSH and CEST packages are all capable of operating with a curvilinear grid and are well suited for areas with curving topography such as rivers or canals and areas with barrier islands (Zhang et al, 2008).

The third type of grid is a flexible unstructured mesh. This type of grid is composed of triangles which vary in size to accommodate bathymetry (Hearn, 2008). The MIKE 3 and MIKE21 software packages are capable of using a flexible mesh and the Surface Water Modeling System (version 10.0) is able to generate meshes with a combination of rectangular and triangular shapes. Varying the type of grid does not change the limitations associated with the time step; however it reduces the number of cells required while still maintaining detail in areas of interest (Hearn, 2008).

There are also limitations due to the non-linear nature of the equations. Pender and Neelz, (2011) point out that shallow water flows are subject to shocks which result in discontinuous solutions of the equations causing large errors and model instability. Shocks typically occur where there is a hydraulic jump which may be caused by changes in bottom slope (abrupt changes typically lead to the most error) as well as the effects of friction. These errors are not dependent on cell size or grid type; discontinuities can arise between two elements depending on the geometry of the grid (Falconer et al, 2007). Newer numerical models typically include some shock-capturing or shock-fitting scheme

for handling flow transitions to reduce errors and instabilities (Pender and Neelz, 2011; Falconer et al, 2007).

1.7 Model Evaluation

Model evaluation typically consists of analyzing the model errors and comparing simulated results with those from an observed event. The goal of evaluation is to learn about the usefulness of a model in simulating inundation and judging the predictive ability of the model. French, (2009) makes a distinction between the replicative and predictive abilities of a model. The replicative ability means that the model can simulate a past event; while predictive ability concerns the simulation of a future event. Cunge, (2003) notes that if a proper deterministic model is used then its predictive capability should be high. He states that replicative abilities should be the strength of data driven statistical models which make predictions based on trends from years of data (such as water levels from tide gauges). Deterministic models may be used in areas without extensive past observations as their ability to make predictions is based on known scientific laws such as conservation of mass, and continuity of momentum. Beven, (2009) adapts a view he calls pragmatic realism in which the complexity of environmental systems makes it difficult to know the system well enough to take an approach which places trust in the model. He argues that the limitations of models needs to be known as they are an imperfect representation of a system which may be beyond our capacity to ever fully understand. By taking the approach Beven suggests, assessment of uncertainty in model predictions becomes critical. Cunge, (2003) is more supportive of the use of a

mathematical modelling approach but still acknowledges the need to assess the uncertainty of model results.

1.7.1 Model Calibration and Sensitivity Analysis

Model calibration involves the adjustment of model inputs and parameters so that simulated outputs match observed data more closely. Calibration is part of standard modelling practice[1] but Cunge, (2003) argues that it is a useless exercise in some cases as there are insufficient data available for calibration and the predictive ability of the model would be better assessed through validation and uncertainty assessment. He presents the case of modelling tides in coastal areas where the data available for calibration are sparse. Furthermore, when data originates mostly near the coast, Cunge observes that local influences will distort the data. If calibration is possible, there are a number of measures for comparing observed and predicted data. French, (2009) and Sutherland et al, (2004) present a set of conventional performance measures, such as root mean square error (RMSE), for the calibration of hydrodynamic models. Using conventional performance measures for calibration assumes that an optimal parameter set can be found for a model. According to Beven, (2009); very seldom does an optimal parameter set exist for a model because of limited knowledge of the environmental system being modelled. There may be a number of possible models that can fit with the observed data and this characteristic is known as equifinality (Beven, 2009).

---

[1] Standard modelling practice is 1. Model Set-up 2. Calibration 3. Validation 4. Application of a validated model for flood prediction.

A sensitivity analysis consists of evaluating the change in results produced by the model when parameter values are changed. The response of the model to a change in a parameter indicates how sensitive the model is to that parameter. The relative importance of parameter values for useful flood prediction can be judged through sensitivity analysis as errors in parameters which the model is more sensitive to will cause greater errors in model results. Beven, (2009) compares point and global methods of sensitivity analysis and argues that global methods should be used because they provide a better representation of changes in model behaviour throughout the domain. Global sensitivity analysis is a statistical method of analyzing the variance in model results at points throughout the domain based on variations in parameters or other inputs (Beven, 2009). In addition to capturing the sensitivity of the model to changes in a single parameter, global methods can be used to examine the interactions between parameters (Beven, 2009).

However, multiple runs are required to assess the sensitivity of the model to different parameters. French, (2009) suggests that knowledge of the environmental system being modelled can constrain the number of values one is required to investigate. In an investigation of the Blyth estuary, he chose roughness values for the intertidal (salt marsh) and subtidal areas and ran 30 simulations using different combinations of Manning`s n coefficients. He chose to concentrate on simulations using higher roughness values for the intertidal zone and lower values for the deep channel since these combinations showed a better match with the validation data.

1.7.2 Model Validation

For validation, the calibrated model is used to predict another observed event, apart from the ones used for calibration. The degree to which the model can predict this event is a measure of its predictive ability. Cunge, (2003) argues that, in most cases, the calibration step may be skipped and validation carried out since the environmental conditions between the calibration and validation events have likely changed and the parameters are therefore uncertain. According to Cunge; during validation, discrepancies between observed and modelled results should be explained using logical reasoning relating to model approximations and uncertainty.

French, (2009) suggests that, for tidal hydrodynamic modelling validation be undertaken using a sequence of tides covering a spring-neap cycle. He also suggests that for the comparison of modelled and observed time-series, quantitative measures such as mean absolute error, root mean square error and relative mean absolute error be calculated.

1.7.3 Model Errors and Uncertainty

Errors are differences between observed and simulated values (Haile, 2005). Beven, (2009) extends the concept of error evaluation to model selection. He specifies three types of errors:

- Accepting a poor model because of a lack of good validation data.
- Rejecting a good model because of poor validation data which suggests the model is poor.
- Using a model structure that does not properly account for all important processes, possibly because they are not known.

Haile, (2005) identifies six main sources of error in flood modelling as:

- Systematic or random errors in input data
- Systematic or random errors in observations
- Errors due to improper parameters
- Errors due to incomplete or biased model structures
- Errors due to discretization of the model domain
- Errors due to rounding off (or truncation) (i.e., numerical computation errors)

Uncertainty assessment is necessary since a model is not a complete representation of reality. Processes take place in reality which are unknown or not present in the model causing discrepancies between predictions and observations. Beven, (2009) suggests that an uncertainty assessment based on Bayes theorem is ideal for the assessment of uncertainty in flood inundation models. This approach assumes that multiple different models may be equally valid representations of a system given that available observations are incomplete. He contends that only Bayesian methods are capable of assessing model uncertainty given imperfect observations and model structures.

Examples of the Bayesian Generalized Likelihood Uncertainty Estimation method applied to flood inundation studies are provided in Aronica et al, (2002); Horrit, (2006); Mason et al., (2009); Baldassarre et al., (2009). In these studies, remotely sensed images of flood extent were used as the observed data. Multiple simulations were performed with varying parameters and initial conditions to determine a set of models considered to be acceptable representations of reality. In Baldassarre et al, (2009) the problem of uncertain satellite image extents was investigated. When used as observed data in a Bayesian approach, it was found that images of the same event from different satellites did not result in the same set of models being considered valid.

The problem with a Bayesian uncertainty assessment method is the number of modelling software runs that may be required to fully sample the model domain. For example, Beven, (2009) suggests, that in a model with two parameters, at least 100 values should be tested for each parameter, which requires 10,000 model runs. Complex hydrodynamic software packages which solve the full dynamic wave form of the Shallow Water Equations on high resolution domains tend to have run times in hours or days. Software packages running simplified models, such as LISFLOOD-FP, have been used for sensitivity analysis since their run times are significantly lower (Aronica et al, 2002). The run times are lower because simplified formulations of the governing equations are used; see section 1.6.2.1.

Uncertainty assessment of modelling software results is identified by several sources as a topic requiring further research (NRC, 2009; Beven, 2009; Haung, 2005; Haile, 2005). Multiple methods of uncertainty assessment exist but there are no set standards of uncertainty assessment for flood inundation models. Temporal uncertainty of model results would also need to be assessed based on continuing observations as environmental change will make modelling software predictions continuously more uncertain (Cariolet, 2010, Manson, 2007, de Vriend et al., 1993).

In terms of flood risk management, uncertainties may be classified as source, pathway and receptor (Beven et al., 2011). A source uncertainty concerns the source of the flood, a receptor is the subject of harm in the pathway of a hazard which receives impact from the hazard (Mirfenderesk, 2012). Note that this approach can also be used for defining exposure and vulnerability as discussed in the next section.

1.8 Definitions of Risk, Hazard and Vulnerability.

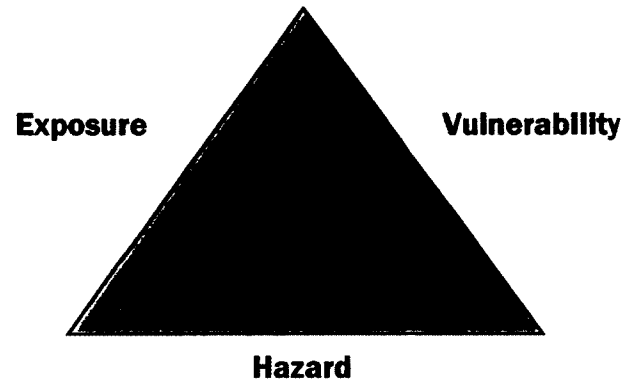

Figure 3: Total risk represents the area of the triangle while the sides represent the components of risk. If one of the sides gets larger, so does the total risk.

The definition of risk used in this study is based on Ken Granger's (2003) total risk concept which is expressed as:

Risk (total) = Hazard x Elements at Risk x Vulnerability

By this logic, risk results from the interaction between the flood hazard (i.e., storm surge), the exposure of the elements (e.g., buildings or dykes) to the event of flood and the vulnerability of the elements that are being impacted (i.e., the stability of the buildings) (Granger, 2003; Kelman, 2002). Hazard addresses the probability of an event occurring. Return periods are usually associated with the probability of a storm occurring, for instance a 1 in 100 year storm is one that is expected to occur once every 100 years. Longer return period storms have a lower probability of occurrence but are more intense than more frequently occurring storms. The total risk definition is appropriate because it recognizes the interdependence between components of risk.

In the context of climate change adaptation, the hazard element cannot be reduced (that would be the role of mitigation) so the elements at risk (exposure) and vulnerability are of interest. Vulnerability can be thought of as the resilience of elements in the face of exposure to a hazard. Elements in this study are physical features but it is important to understand that there are several social and economic dimensions to vulnerability which need to be considered both for flood management and climate change adaptation planning (Davidge and Gladki, 2010).

To manage exposure and vulnerability, it is possible to adapt a source-pathway-receptor approach. The **source** is the source of the hazard (i.e. storm surge), the **pathways** are the physical elements (i.e. floodplain) through which the flood may travel to the **receptor** (Mirfenderesk, 2012). If viewed this way, altering elements controlling flooding in the pathway or altering the receptors of flooding may change overall flood risk.

1.9 Hazard and Vulnerability Determining Factors

Depth is typically used as the primary indicator of flood hazard to communities (Kelman, 2002). Depth-damage curves are used by FEMA (Federal Emergency Management Agency) in the United States to delineate flood hazard. These curves are for different types of structures and they assess loss in terms of property value (NRC, 2009). Velocity by itself is not that often used as an indicator of flood hazard (Kreibich et al., 2009). However, taken together with depth; velocity can be an effective indicator of hazard and useful for delineating flood risk to people, and vehicles (HR Wallingford et al., 2006; Xia et al., 2011). In Australia and the United Kingdom, flood management policy has been influenced by empirical relationships derived from studying the effects of

different combinations of velocity and depth (WRL, 2010; HR Wallingford, et al., 2006; Pistrika and Jonkman, 2010; New South Wales Government, 2005).

$$HR = d \times (v + 0.5) + DF$$

Equation 3: Flood Hazard to People Formula,

where,
HR = (flood) hazard rating;
d = depth of flooding (m);
v = velocity of floodwaters (m/sec);
DF = debris factor = 0, 1, 2 based on expected debris associated with land uses.

Equation 3 is the flood hazard to people rating formula presented in HR Wallingford, et al., (2006). This rating is used in the United Kingdom. For Australia; WRL, (2010) describes a similar approach to evaluating hazard to people but omits a debris factor since they claim it is arbitrary and not supported by experimental evidence. They also use a pure velocity depth product for their classification (V×D) and break their hazard categories up by height and mass product (HxM).

In addition to flood hazard to people, the hazard to buildings has also been studied in an attempt to link velocities and depths with flood damage; see Kelman, (2002) for a complete overview. However, the link between velocities, depths and flood damage is inconclusive as Pistrika and Jonkman, (2010) point out. They suggest using FEMA's Hazus depth damage curves which relate flood depth, duration and construction type to potential flood damage.

Kelman, (2002) points out that, in addition to velocity and depth, there are many other hazards related to flooding which can cause additional damage depending on the duration and intensity of flooding. One of these hazards is sediment. It is important to note that

large storms in the Bay of Fundy are known to mobilize large amounts of sediment and therefore sediment concentrations and settling times may be a significant component of storm surge flood damage that would warrant further investigation (O'Laughlin and van Proosdij, in review).

1.10 Data Management and Decision Support

The prediction of flooding is a very complex and data intensive task. A Geographic Information System (GIS) allows spatially referenced data from flood simulations to be stored in a database. Data can be retrieved from the database by multiple different applications for processing and analysis. Numerical models can be parameterized, run, and results analyzed using a GIS. Cesur, (2007) showed that execution of the 1D model software HEC-RAS could be triggered automatically using ArcGIS (a commercial GIS software) as new data was added to the ArcGIS database. A GIS database can assist in data collection for a modelling exercise as data models can be developed which define the data requirements, formats, processing steps, and relationships between elements (Nyerges, 2007). Zerger and Wealands, (2004) showed the potential for a GIS to be used for efficient data output management from a numerical model. They showed how relationships between entities representing components of the natural system and attributes can be modeled and incorporated into a database using a GIS.

When model predictions are meant for decision making, a spatial decision support system (SDSS) is commonly used for organizing the inputs, tools, and results (Haung, 2005;

Zerger and Wealands, 2004; Webster et al, 2008; Nyerges and Jankowski, 2010). A SDSS is a computerized method of providing the information necessary for decision making including inputs of spatial and data relating to the area of interest, models for predicting the behaviour of the environmental system, methods of analysis to determine the usefulness of predictions, and ways of outputting the results so that they are useful to decision makers. A spatial decision support system has the core functions of integrating data management, analysis techniques, and visual representation (Nyerges and Jankowski, 2010).

A decision system for assessing coastal hazard due to sea level rise in an estuary may include several different simulation models depending on the conditions present in the area, the number of parameters deemed important to the problem, and the desired level of detail (temporal and spatial). A simple decision system may only consider the maximum flood inundation extent, while a more complex system may consider morphological changes, slope failure probabilities and maximum wave runup (Barnard et al., 2009).

The usefulness of a SDSS to planners is a matter of debate, Brommelstroet, (2010) wrote that SDSS do not assist planners. Data stored in an SDSS is based on abstractions from reality which make facts provided by the system difficult to understand and use in planning practice. He suggests that modellers should commit to finding ways of implementing their systems in planning practice instead of just trying to improve the tools. Janssen and Stewart, (2009) point to additional shortcomings of SDSS, namely poor communication between developers and decision makers which leads to unrealistic expectations and a final product which does not answer the initial question. Their

recommendation is to limit the scope of the problem and to focus the SDSS so that its contents can be better understood and the results communicated to stakeholders who participate in the project through workshops.

CHAPTER 2: Study Area and Background

The study area is near Windsor in the Avon River estuary located within the Minas Basin of the Bay of Fundy in Nova Scotia (Figure 5; Figure 6). The Minas Basin has a macrotidal regime (tidal range greater than 4m according to Haslett, 2009) which has led to the development of extensive intertidal areas composed of salt marshes and mudflats. European settlers dyked the intertidal areas to protect them from flooding at high tide. Once cut off from the tidal regime, the salt was washed off the surface of the marsh and the soil was used as farmland (Bleakney, 2004). Since the 1940s the dykes have been maintained by the Nova Scotia Department of Agriculture and the historic dyke system was replaced with an engineered line of dykes. To reduce dyke maintenance costs, a causeway was built across the Avon River in 1969, cutting areas upstream of Windsor off from tidal influence.

To drain areas behind the dykes, there are culverts which pass under the dykes and have tidal flaps which allow outflow during low tide. These drainage features (aboiteaux) are linked to creeks in both the dyked and intertidal areas (Figure 4). The original purpose of the dykes was to protect farmland, however new development in the area has placed important infrastructure at risk of flooding in the event of a breach or overtopping (Browning, 2011).

Figure 4: Aboiteaux Structure

Figure 5: Study Area Satellite Image and Context Inset Map. Dykes are shown in orange

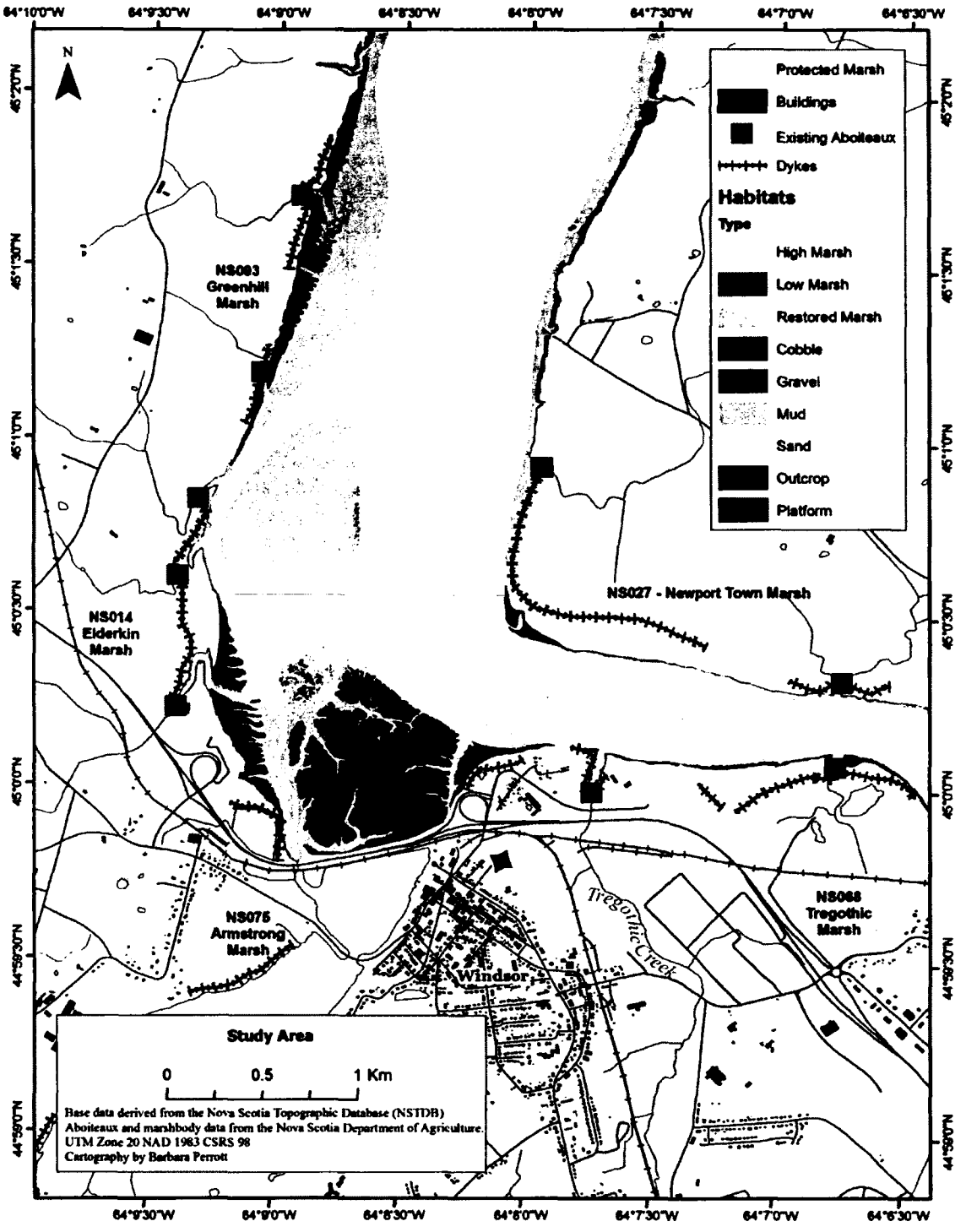

Figure 6: Study area detailed map with incorporated marsh bodies, aboiteaux and waterways

2.1 Geomorphological Characteristics and Tidal Dynamics

The morphology of the area is typical of a macrotidal environment with an extreme tidal range of up to 16 m (Bird, 2000; Carter and Woodroffe, 1994). Macrotidal estuaries are generally funnel shaped features with broad mouths and linear banks with diminishing widths upstream and extensive intertidal areas (Bird, 2000). These features occur where the continental shelf is wide and the sides of the estuary converge and cause the tide wave to be compressed laterally thus magnifying the height of the tide (Dyer, 1997). Macrotidal estuaries were created at the end of the last glacial maximum approximately 18,000 years ago (Carter and Woodroffe, 1994). The high tides in the Bay of Fundy are due to the geometry of the Bay which causes 'resonance'. Resonance means that time it takes for a wave of water to travel the length of the bay and back is equal to the time between high tides.

Morphology of these areas is shaped largely by tides and tidal currents. Surface gravity waves have very little influence on the high tide shoreline but may have an influence on the intertidal areas (Bird, 2000). Tides push sediments upstream which results in deposition in the upper intertidal zone and near the mouth of the estuary (Bird, 2000). This net deposition of sediment results in the formation of sandbanks, mudflats and/or salt marshes (Dyer, 1997). Once these features become colonized by vegetation, they act as a positive feedback for sediment balance since they cause additional sediment accretion (Bird, 2000).

At low tide, there are usually a number of channels leading from the river to the sea. These channels are subject to rapid change due to tidal currents. In macrotidal estuaries,

these channels tend to be straight and parallel (Bird, 2000). Currents can rapidly change the size and position of these channels although a pattern of change can usually be identified (Bird, 2000).

In the study area, there are extensive intertidal areas composed of mudflats within the channel of the river and salt marshes along the edges covered by vegetation. Within the marshes and mudflats, there are tidal creeks which play a role in drainage (Davidson Arnott et al., 2002) In the winter, ice blocks are deposited throughout the intertidal areas and vegetation is sheared off the salt marshes (Davidson-Arnott et al, 2002). The area is subject to strong storms in both summer and winter seasons. The Windsor Causeway has caused rapid sediment accretion and salt marsh formation in the Avon River estuary (van Proosdij et al., 2009). Due to the tidal range, water is well mixed since the tidal flow is much greater than river flow and there is minimal stratification (Dyer, 1997).

Literature around expected changes to estuaries focuses on the effect that sea level rise will have on tides. Tides are expected to penetrate further inland and tidal ranges and amplitudes may increase (Carter and Woodroffe, 1994; Bird, 2000). Due to increasing amplitudes and reaches, channels may be widened which will cause an increase in velocities (Pugh, 2004). Coastal flooding is also expected to be more extensive and longer lasting as rising sea levels may block river floods (Bird, 2000). However, rising sea levels may be offset by greater sediment supply from inland regions due to increased precipitation (Bird, 2000). Coastal defenses such as levees may be overtopped either due to rising tides or an increase in tidal amplitude (Carter and Woodroffe, 1994). Greenberg, et al. (in press) studied the expected changes in tidal dynamics in the Bay of Fundy and

concluded that due to sea level rise and subsidence, the amplitude of the tides will change causing higher peak water levels. By 2055 total sea level rise is expected to be 0.41 – 0.79m in the Upper Bay of Fundy (Greenberg et al, in press). Greenberg also stated that this change was happening independent of sea level rise and will only be magnified by global sea level rise (Greenberg, et al, in press).

2.2 History of Flood Management in the Dykelands

Since the end of the 1960s, the Nova Scotia Department of Agriculture has been tasked with maintaining the dykes which protected farmland around Nova Scotia. Land uses behind the dykes have changed since the Department was given their mandate. In the Tregothic marsh, the total assessed value of land parcels is $31,003,300 (in 2011 Canadian Dollars) but only 0.6% of this value is agricultural land (Browning, 2011). Changing land uses put pressure on dyke managers as development moves away from agricultural uses and potential losses from flooding increase. Additional pressure on dyke maintenance comes from local sea level rise. Over the past century, sea level has risen at a rate of two millimetres per year, which was approximately 20 centimetres per century (Desplanque and Mossman, 2004). Furthermore, dykes in some areas are actively eroding which increases the chance of a breach (van Proosdij D., 2009). Gradual changes in water level and constant erosion are an ongoing challenge but large storm events also pose a major danger to the dykelands. The most significant storm in the recorded history of the dykelands was the October 1869 Saxby Gale. During this event, a storm surge, occurring during a Saros peak tide, of at least 1.5m overtopped most dykes in the region causing damage which took years to repair (Desplanque and Mossman, 2004; Bleakney, 2004).

Storm surges coinciding with a high spring tide, as during the Saxby Gale, can result in dyke overtopping and flooding. The highest tides occur in the Bay of Fundy during the peak of the 18.6 year Saros cycle. Desplanque and Mossman (1999) showed that dyke overtopping events coincide with Saros cycle peaks when tidal ranges in the Avon River estuary increase to above 16 m. The next Saros peak is expected in 2012-2013.

Currently, Nova Scotia's flood management policies pertaining to the dykelands are based on the Maritime Marshlands Rehabilitation Act (MMRA), the Flood Damage Reduction Program (FDRP), the Agricultural Marshland Conservation Act (AMCA) and land-use by-laws of the communities with dykelands. The draft Nova Scotia Coastal Strategy has also highlighted coastal flooding in the dykelands as a serious hazard (Provincial Oceans Network, 2011). The MMRA and the FDRP were based on federal/provincial partnerships. The MMRA was concerned with structural flood management and agricultural land preservation. It resulted in the surveying of marsh body boundaries (for the creation of administrative units), the reconstruction of the dykes, and the creation of the Windsor causeway. The program ended in 1968 and all responsibility for dykelands management was transferred to the province. The AMCA was implemented in 2000 and reaffirmed the provincial commitment to preserving the dykelands for agricultural uses. The marsh body boundaries have not been updated since they were surveyed in the 1950s-1960s under the MMRA. The FDRP (ended in 1999) was concerned with the Truro dykelands. It used hydraulic modelling and a two-zone floodway/floodway fringe approach to delineating areas of hazard. As a result of the FDRP, a statement of provincial interest was added to the Municipal Government Act

(MGA) tasking municipalities with managing flood hazard in their planning policies. Recent LiDAR surveys have made it possible to update the marsh body boundaries and carry out new floodplain delineation using high resolution digital elevation models (DEMs) (van Proosdij, 2009).

In the study area, the Town of Windsor and the District of the Municipality of West Hants have added environmental constraint areas to their land use by-law based on the incorporated marsh body boundaries (Town of Windsor, 2010). In the Town of Windsor, developments within environmental constraint areas must prove they have considered flood hazard in their plans (Town of Windsor, 2010). West Hants forbids the construction of most new buildings in the dykelands (Municipality of the District of West Hants, 2011). Flood events caused by overtopping have occurred more recently than the Saxby Gale but their effect has been largely limited to agricultural land (Personal communication Ken Carroll; van Proosdij, 2009).

Flood water can become trapped behind the dykes, during high tide when outlets are blocked, and compound flooding problems (van Proosdij, 2009; Personal Communication Ken Carroll). Culverts may also become blocked with silt and debris, causing a greater risk of inland flooding. During an overtopping event, if there is already freshwater trapped behind dykes, additional saltwater will lead to greater depths, durations and extents of flooding.

CHAPTER 3: Methods

This research focuses on the investigation of hydrodynamic and GIS flood modelling to predict flood hazard in a macrotidal estuary with dykelands. In addition to modelling, data management methods and challenges were also investigated.

The modelling process consists of the following steps:

(1) Surveying the environmental characteristics of the study area to determine modelling requirements.

(2) Choosing a hydrodynamic model that was determined to be appropriate to the purpose of the study.

(3) Consulting with decision makers and stake holders to determine the required types of output for flood management purposes.

(4) Collecting validation data during perigean spring high tides.

(5) Validating the model using collected data and testing its sensitivity to changing parameters.

(6) Simulating different levels of flood risk through an ensemble of possible storm surges at high tide. These tides range from more probable water levels close to the current higher high water large tide (HHWLT) to extreme events comparable to the historic Saxby Gale. The range of maximum water levels predicted for Hantsport by Daigle and Richards, (2011) was covered.

After the simulations were complete, all outputs were transferred to commonly used raster formats and associated the flood variables with important features such as buildings. Identifying pathway and physical receptor elements is started in this thesis and modelling errors and uncertainties are assessed based on the source-pathway-receptor approach (see section 1.7.3).

3.1 Flood Modelling Process

To achieve the objectives, consultations were carried out with dykeland administrators, aboiteau superintendents and concerned decision makers to determine their experiences with flood management and learned the challenges they wanted to address. Analysis was carried out using the following software:

- TUFLOW hydrodynamic modelling package (version 2011-AB) – Used for simulating flooding.
- Surface Water Modelling System (SMS) 11.0 – Used for pre-processing simulation data.
- ArcGIS 10.0- Used for pre-processing and result management.
- SAGA GIS 2.0- Used for creating GIS based flood predictions.
- Web Tides 0.65- Used for generating a time series of tidal water levels.
- Python 2.6.5 (Programming language).

3.2 Relevant Environmental Processes and Characteristics

3.2.1 Bathymetry and Coastal Topography

Since there is a quantifiable relationship between water depth and tidal behaviour in an estuary, having accurate measurements of depth is essential. Since behaviour of a tidal wave in shallow water is also related to the bottom friction of an estuary, an accurate representation of the bottom will give a more exact result as to how the tidal wave or flood wave will respond to bottom friction. Getting accurate measurements of intertidal features requires LiDAR terrain data that is obtained at low tide (Bartlett and Smith, 2005). Another advantage of high resolution surface data is the ability to more accurately determine boundary conditions since coastlines, and other physical features, are shown in greater detail. The study area contains complex intertidal features that are important to

consider when choosing the limits of the domain and the resolution of the model since the drainage of intertidal areas is dependent on these features.

Working with a large DEM of high resolution ground data can be computationally costly; therefore a DEM may be re-sampled at a lower resolution. As long as features of interest, such as flood defenses, are stored in another dataset, they may be reinserted into a grid for simulation (Purvis et al., 2008). When terrain models are re-sampled, it is important to know the effect that a re-sampling method will have on the data. Surfaces for dynamic modeling should be smooth and not have too many artifacts created by the re-sampling method. A high resolution LiDAR dataset with a vertical accuracy of ± 0.15m was acquired from the Applied Geomatics Research Group (AGRG). These data were acquired at low tide in May 2007 and used in Webster et al, (2011). Older bathymetric surveys were also available for the main channel but were not used since they are of much lower resolution than the LiDAR and sediment accretion in the channel has caused significant morphological change since they were acquired. However, for Lake Pisiquid, which was cut off from the main channel when the causeway was constructed, it was possible to use older bathymetric surveys since there has been minimal morphological change.

All inputs to the modeling process need to be referenced to the same horizontal and vertical datum (see glossary for definition of terms). The vertical datum is usually referred to as mean sea level or orthometric height, which in Canada is the Canadian Geodetic Vertical Datum of 1928 CGVD28 (Webster et al., 2004). LiDAR data is usually referenced to the WGS84 datum ellipsoidal heights while tidal gauge data and

bathymetry may be referenced to height above lowest low water (chart datum). To convert LiDAR data in WGS84 ellipsoidal height to a vertical datum and orthometric height, a separation model (HT1_01E) is used. This model consists of the difference between WGS84 height and CGVD28 height in any given area (Webster et al., 2004). Converting from chart datum to orthometric height is done by finding the offset between chart datum and mean sea level for a given area either by contacting the hydrographic service responsible for the chart datum used or trying to find the offset by comparing height from a chart datum to orthometric height from LiDAR points in an intertidal area (Webster et al., 2004). For the horizontal datum the NAD83 datum with a Universal Transverse Mercator (UTM) projection to have coordinates in meters as Eastings (x-coordinate) and Nothings (y-coordinate) was used.

Being able to model the wetting and drying of cells in a simulation is one of the strengths of hydrodynamic modelling software. For modeling wetting and drying processes, having a high resolution terrain model can be useful as it gives a more accurate representation of terrain slope and flow path than models created from low resolution data sources. The model domain was constructed using the LiDAR dataset described above. Where the dataset was lacking, for instance at culvert entrances and the tops of dykes (due to interpolation, see Appendix A), it was augmented with ground survey data taken with a high accuracy real time kinematic (RTK) GPS receiver (horizontal accuracy was ± 0.01m while vertical was ± 0.05m) (See Appendix.A).

3.2.2 Implications of Geomorphology for Model Selection

As discussed in section 2.1, the study area is a macrotidal estuary. The complexity of the terrain, as well as the volumes of water and suspended sediment which are exchanged through tides creates special challenges for modelling. High resolution terrain data are required, as well as robust numerical schemes able to handle large amounts of wetting and drying as well as discontinuities (shocks) caused by rapid changes in terrain slope and flow characteristics.

In a macrotidal estuary, the intertidal zone tends to be extensive so a significant amount of area is covered by high tide and exposed during the low tide. The numerical modelling software has to have different criteria for determining whether an element should be considered wet or dry and needs to provide realistic solutions in areas of wetting and drying. The 2D numerical inundation modelling software used by Dupont et al, (2005) was built to predict tides in the Upper Bay of Fundy but did not provide reliable results in areas that fully dry during a tidal cycle in the Avon River estuary. These predictions are used as part of the WebTides service and are considered reliable for areas with an orthometric height of 0 m or less.

Due to the large tidal influence, the water in macrotidal estuaries tends to be well mixed. If the tidal range is large relative to the water depth then the water column may become completely mixed which makes the estuary vertically homogenous (Dyer, 1997). For this to happen, the tidal flow needs to be much larger than the river flow (Dyer, 1997). In the Avon River estuary, this is the case. If the estuary were significantly stratified, a 3D model may have needed to be used; otherwise a 2D or 1D representation may be

sufficient. Additionally, van Proosdij, (2009) indicated that freshwater inflow from the St. Croix River was negligible compared to the tide.

If predictions are to be made over a long period of time, morphological change will need to be considered. Modelling potential changes in morphology is possible but beyond the scope of this thesis. Instead it is recommended that morphological change in the channel and on the intertidal zones continue to be observed and this type of modelling redone if the morphology of these zones changes significantly. The frequency of these updates would need to be determined by decision makers and scientists.

3.2.3 Tides and Currents

Tides are long waves generated in the open ocean that propagate into the shallow water of estuaries. Gravitational tides, which are caused by the moon and the sun, cause water levels to rise and fall in a regular and predictable manner (Hardisty, 2007). The number of ebb and flood tides which take place daily vary from place to place. Most coastlines have a semi-diurnal tide which creates two flood and ebb tides every day. The ebb and flood cycle reaches peak levels when the sun and moon are aligned with respect to Earth (full moon), this is known as the spring tide and occurs approximately once every 14 days (Haslett, 2009). The opposite is known as the neap tide. Mean sea level is based on the longest known tide cycle which lasts 18.6 years (Saros cycle). The study area has semi-diurnal tides. Elevation of tides in the study area varies between the neap and the spring cycle. Storm surges at high tide during a spring cycle are more likely to cause dyke overtopping. The most likely tides to cause overtopping are spring tides occurring during the Saros cycle peak. The storm surge associated with the Saxby Gale

happened during a spring tide at the peak of the Saros cycle. Simulations were carried out on a spring tide with varying levels of storm surge added.

When a tidal wave enters an estuary, the shallow water causes the tide wave to slow down since the velocity of a tide wave is given by $\sqrt{gh}$, where g is the acceleration due to gravity and h is the total depth. The tidal range in a given estuary is primarily determined by the size and topography of the estuary. As the tide wave travels inland, the bottom friction eventually overcomes the increase in velocity due to decreasing channel width and the tide wave slows down leading to an asymmetrically shaped tidal curve (Dyer, 1997). The effects of roughness needed to be included in the model so equations with friction terms were essential.

Once a tide enters shallow water, the tidal current intensifies. Tidal current are responsible for the advection of materials and properties of the water column (Hearn, 2008). Flows due to currents are defined based on their velocities, variation through time, and the flow regime (Hardisty, 2007). Flow properties are important to understand because models treat flow differently depending on their governing equations (Section 1.6.2). A model needed to be chosen which can simulate unsteady and supercritical flows.

3.2.4 Sea Level Rise and Tidal Changes

An attempt was made to calculate water level return periods using the method described in Webster et al, (2008) using tide gauge data gathered at the Windsor Causeway. However, the record was too short (2001-2009) to be able to generate reliable return periods. Predictions created by Daigle and Richards, (2011), who presented a

series of water level return period predictions (10, 25, 50, 100 year for the present and for 20 year intervals to the year 2100) for the Town of Hantsport (which is downstream from Windsor) , were used. Their predictions indicate a maximum water level of approximately 8.7-10.3 m CGVD28 possible between now and the year 2100. They used the tide gauge in Saint John New Brunswick to create their predictions since that is the only long term gauge record available in the area. Daigle and Richards, (2011) used the method described in Bernier, (2005) to arrive at their water level predictions. However, Webster et al, (2008) were critical of the method employed in Bernier, (2005) because they believed it filtered out high water levels during storms since it used a 6-hour average of water levels. Daigle and Richards, (2011) acknowledged this criticism and pointed out that higher than predicted water levels may occur due to events like the Saxby Gale. Also consulted was Greenberg, et al, (in press) for information on potential changes in tidal dynamics since the Daigle and Richards report did not consider the effects of increasing tidal range due to glacial rebound and sea level rise.

3.3 Hydrodynamic Modelling Methods

In this study, an approximate numerical solution to a hydrodynamic model based on the Shallow Water Equations is calculated. Mass and energy are conserved by the model; this means that when a defined volume of water enters the model domain, it is not lost until it exits the domain through a boundary. Other physical effects, such as roughness and acceleration of water, are also included.

3.3.1 Hydrodynamic Model

The TUFLOW (Two-Dimensional Unsteady FLOW) hydrodynamic modelling package was used to simulate storm surge (Syme, 1991). TUFLOW is a software package running a 1D/2D finite difference hydrodynamic model that provides a numerical solution of the full dynamic shallow water equations using an alternating difference implicit scheme (ADI) (Syme, 1991). This software was developed in the early 1990s and has since been actively updated by BMT-WBM in Australia. It includes a scheme created specifically for handling wetting and drying in intertidal areas (Syme, 1991). It also contains a scheme for handling transitions to supercritical flow (BMT-WBM Personal Communication, 2011).

A test against other models by the United Kingdom Environment Agency showed the performance of TUFLOW to be comparable to other widely used models, such as MIKEFLOOD, for flood hazard assessment (Néelz & Pender, 2009). TUFLOW was used as part of the ESPACE (European Spatial Planning: Adapting to Climate Events) project to predict potential flooding from different water level and coastal defence scenarios (ESPACE, 2006; Wicks et al, 2011). Equations 4a, b, and c show the major physical processes handled by the TUFLOW 2D algorithm. As mentioned earlier, TUFLOW implements a 1D/2D coupled model and there is an implementations (ESTRY) of a 1D model linked with the 2D scheme, which is used in this study to simulate underground drainage through culverts, aboiteaux (as unidirectional culverts) and the tide gate under the causeway. ESTRY solves the full dynamic 1D form of the Shallow Water Equations, known as the Saint-Venant equations (Equations 1a & 1b).

$$\frac{\partial \zeta}{\partial t} + \frac{\partial (Hu)}{\partial x} + \frac{\partial (Hv)}{\partial y} = 0$$

Equation 4a: Conservation of Mass

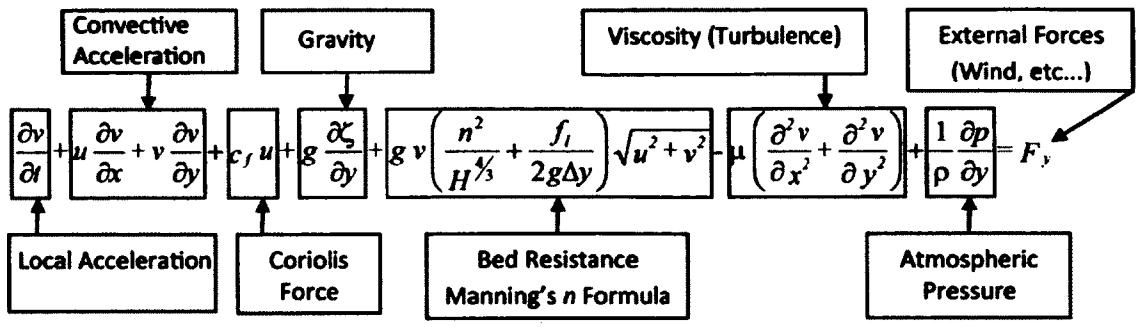

Equation 4b: Momentum in the y-Direction. Terms are annotated by associated physical processes,

$$\frac{\partial u}{\partial t} + u\frac{\partial u}{\partial x} + v\frac{\partial u}{\partial y} - c_f v + g\frac{\partial \zeta}{\partial x} + g\,u\left(\frac{n^2}{H^{4/3}} + \frac{f_l}{2g\Delta x}\right)\sqrt{u^2+v^2} - \mu\left(\frac{\partial^2 u}{\partial x^2} + \frac{\partial^2 u}{\partial y^2}\right) + \frac{1}{\rho}\frac{\partial p}{\partial x} = F_x$$

Equation 4c: Momentum in the x-Direction, See equation 5b for identification of terms.

Where:
ζ= Water surface elevation
u and v= Depth averaged velocity in x and y directions
H= Water Depth
t = Time
g = Acceleration due to gravity
x and y = Distance in x and y directions
Δx and Δy = Computational cell dimensions (see Appendix A for TUFLOW computational cell diagram)
C_f = Coriolis force coefficient
n = Manning's n coefficient
f_l = Form (energy) loss coefficient
μ = Horizontal diffusion of momentum coefficient
p = Atmospheric pressure
ρ = Density of Water
F_x and F_y= Sum of components of external forces (e.g., wind) in the x and y directions

3.3.2 Requirements for Decision Making and Data Collection

Policy makers and managers responsible for the dykelands from the Department of Agriculture, Town of Windsor and the Municipality of West Hants were consulted. Hydrodynamic modeling was briefly introduced and flood scenarios, which could be investigated, were discussed. Insights were gained regarding drainage patterns and infrastructure in the study area. The following lists detail the data requirements, desirable outputs and scenarios that were discussed.

The following features needed to be in the simulations:

1. Aboiteaux structures which are one-way culverts that allow drainage from the marsh bodies at low tide (Figure 4).
2. Dykes with the latest surveyed elevations.
3. Hydraulic structures within the marsh bodies, such as culverts.
4. Lake Pisiquid and the tide gate.
5. Variable surface roughness based on land uses/surface cover.

The following outputs were desirable:

1. More detailed estimates of flood hazard, using more variables than depth.
2. Duration of flooding along with depths and velocities (maximums for the entire flood, incremental outputs from the simulation).
3. Investigation of dyke overtopping considering locations and durations.
4. Determination of probabilities of water levels using Windsor tide gauge data.
5. Flood risk to infrastructure and buildings.

All of the desired outputs were provided except for the determination of water level probabilities. Exact dyke overtopping durations for all dyke segments were not calculated (see Appendix A for explanation).

These are possible flooding scenarios for the study area:

1. Storm surge overtopping/breaching dykes.

2. Inland flooding from rivers being trapped by aboiteaux structures.
3. Excessive rainfall.
4. Ice-jams blocking outflow.
5. Some combination of the above factors.

Storm surge overtopping of dykes was primarily investigated. Partial blockage of aboiteaux structures during the highest water level flood scenario was also investigated as well as a dyke breach. The other scenarios are important but would require more data collection and model configuration which was not possible due to time and budget constraints.

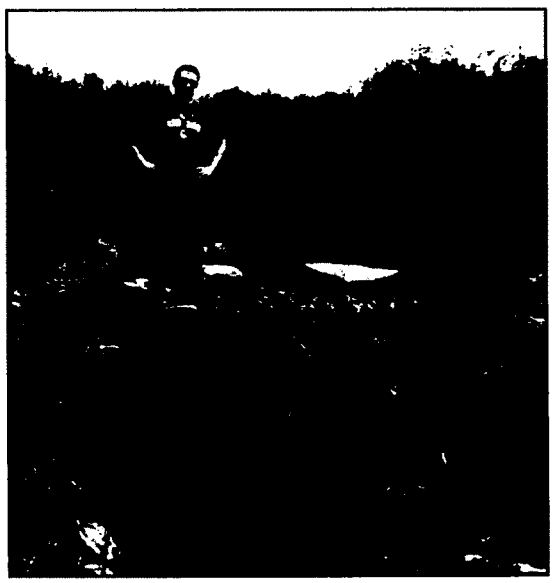

Figure 7: Culvert Survey
Photo credit: Fedak, 2011

3.3.2.1 Hydraulic Structures

The Department of Agriculture provided the locations and some specifications (size, material, inlet types, flow estimates for some structures) of their aboiteaux structures. Additional information, such as images of aboiteaux and dyke condition, came from the Marshlands Atlas (Pietersma-Perrot and van Proosdij, 2012). Within the marsh body, spatial data was collected from the Nova Scotia 1:10,000 topographic database but it was found, through ground truthing, that these data were out of date and contained no specifications of the drainage features. Data was also received from the Town of Windsor relating to the drainage features along Tregothic Creek. Culverts were surveyed as well as aboiteaux and overpasses with GPS devices in the Tregothic, Elderkin and Newport Town marshes

(Figure 7). Note was taken of the size, geometry, condition, materials, and inlet/outlet types and took pictures of each culvert at the inlet and outlet. All these data have been incorporated into the Marshlands Atlas (Pietersma-Perrot and van Proosdij, 2012). However, this dataset is incomplete and thus the model does not include all of the important hydraulic structures but there is now substantially more information in a database which may be built upon.

3.3.2.2 Validation Event Data Collection

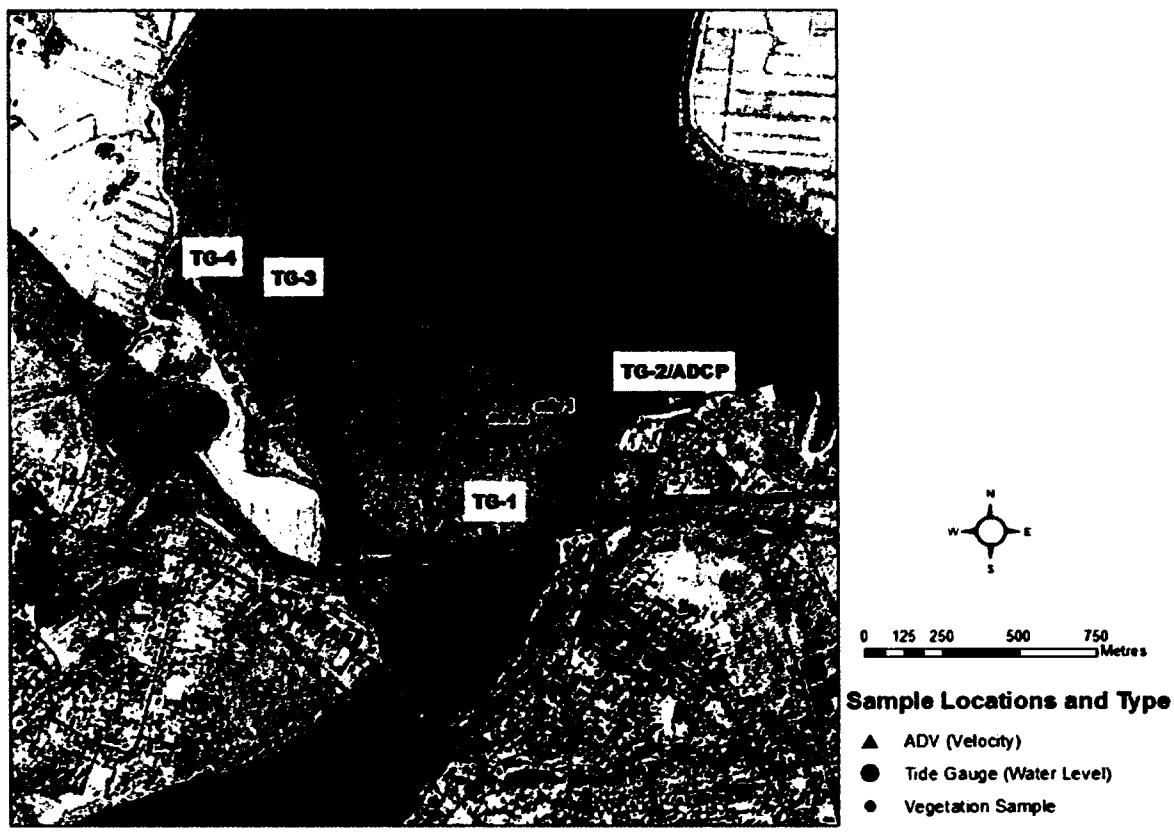

Figure 8: Validation Data Collection Locations

Data were collected in tidal creeks and on the surface (low marsh) of the Windsor and Elderkin Marshes for a perigean spring high tide event (Figure 8). The maximum water level that was recorded was 7.9m (CGVD28) and there was no recorded dyke overtopping. Depth measurements were collected using Solonist[tm] tide gauges (TG), within stilling wells, with a sampling frequency of five minutes. Four of these units were placed in marsh creeks and three recorded usable data from May 13th to 20th (Figure 9). A barologger was used to record atmospheric pressure for correcting tide gauge readings. The height of these instruments was determined using a RTK GPS system to an accuracy of ± 0.05m. Velocities were collected on the marsh surface and in the creeks using two Nortek Acoustic Doppler Velocimeters (ADV) and one Nortek[tm] Acoustic Doppler Current Profiler (ADCP) (Figure. 10). The ADVs both sampled at 4 Hz and the

Figure 9: Placing a tide gauge within a stilling well in a marsh creek.

Figure 10: ADV positioned on the marsh surface

instruments were positioned for point measurement at 0.1m above the bed. The velocities collected by the ADVs had an accuracy of ±1 mm/s. ADV1 was moved into a creek next to tide gauge 1 (TG-1) after a day of data collection on the surface. The ADCP sampled one profile every 30 seconds, and measured up to 6.2 meters of the water column in 0.5 m bins. This instrument was used to record depth average velocity in a tidal creek with an accuracy of ±0.005 m/s.

Vegetation samples were taken at several locations on the marsh using a quadrat method to measure heights and stem diameters. This informed the selection of manning's n roughness coefficients. Vegetation characteristics on the marsh surface varied between high and low marsh areas. Low marsh had heights of 0.07 to 0.17 m and stem diameters of 0.001 to 0.005 m. All instruments were placed in low marsh areas and within marsh creeks. There was dead vegetation from the previous season in marsh areas as the growing season was just beginning.

There were no significant meteorological events during data collection period. Between May 18th to 20th, 12.4 mm of precipitation was recorded at the Kentville weather station (KENTVILLE CDA CS) nearest to the study area. This rain event was not recorded in the results as water flows only occurred with tides. Winds were minor and temperatures ranged between 4.9 and 22.2°C.

3.3.3 Validation

For validation data collected during an overtopping event would have been ideal to use but this type of event did not occur during this study period; nor were there any

historical flood events mapped. Instead, the observed data was compared with simulations using various grid resolutions, configurations and parameter values. The simulation was driven by a WebTide time series for May 18th to the 20th 2011, using all available tidal constituents (DuPont et al., 2005). The WebTides prediction for the maximum elevation of tides was 7.67m CGVD28 and the maximums recorded at the gauges ranged between 7.8m and 7.95m CGVD28. The goal was to see if the high tide water level could be simulated within the accuracy of the boundary condition (DuPont et al., 2005). To test the accuracy of model configurations in simulating a storm surge event, a 1.8m storm surge was added to the boundary condition data and used to test various configurations.

3.3.3.1 Attempted Model Configurations

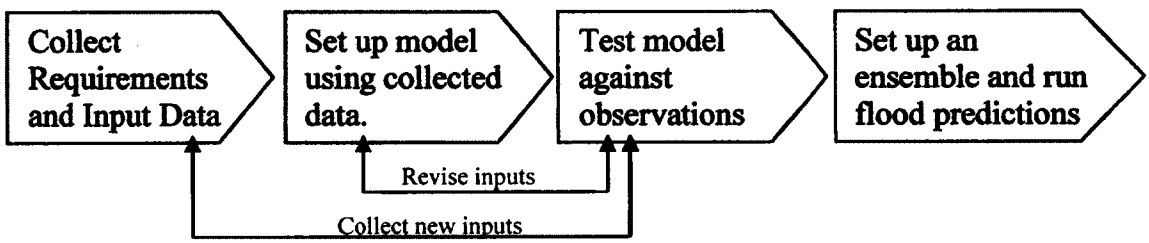

Figure 11: Model Configuration Testing Process

Sensitivity to changing parameters was investigated in an iterative process (Figure 11). It was found that grid resolution, the orientation of the inflow boundary condition, and surface roughness within the channel of the Avon River had significant effects on the fit of the results to the observed data. It was also found that increasing grid resolution

does not always result in increasingly realistic model predictions as unrealistic solutions were produced even on high resolution domains. The complexities of the terrain and very high flow volumes also limited options as linking and nested 2D grids of various resolutions did not produce realistic solutions. Additional details regarding the setup of the TUFLOW simulations can be found in Appendix. A.

3.3.3.1 a) Single 2D Domains (3, 5, 10, 30m Cell Size)

The first experiments dealt with a single 2D domain representing the study area. All runs except those with the 3m cell size configuration produced realistic solutions. Alterations to the 3m grid were made to smooth the terrain in an attempt to prevent steep slopes which can cause the model to produce unrealistic solutions; however this was unsuccessful. The orientation of the boundary condition proved to be critical, for all cell size cases, as if it was not perpendicular to flow, the model simulated spurious flow patterns which led to errors in velocities and instabilities (Syme, 1991).

Instrument	5m Grid	10m Grid	30m Grid
ADCP	0.318	0.390	0.409
ADV1 - Surface	0.040	0.039	0.057
ADV1 - Creek	0.292	0.298	0.310
ADV2 - Surface	0.041	0.043	0.055

Table 1: *Root Mean Square Error of computed velocities compared to observed velocities at different instruments from different grid resolutions.*

The 5, 10 and 30 m grids were first tested and it was found that all these grid resolutions were able to replicate the high tide water level within the accuracy of the boundary condition. However, significant differences were found in the prediction of velocities and drainage. The lowest resolution 30 m grid showed the greatest errors as it most significantly under predicted velocities and inundation times (Table 1; Figure 12). This

was due to the poor representation of validation locations at 30m resolution. The 10m grid produced results similar to the 5m grid but the representation of creeks was still too coarse (Figure 12 and 13). The literature review indicated that a cell size of 5m or less would be required for urban inundation modelling and the 5m grid proved to be the best choice out of the various single grid configurations.

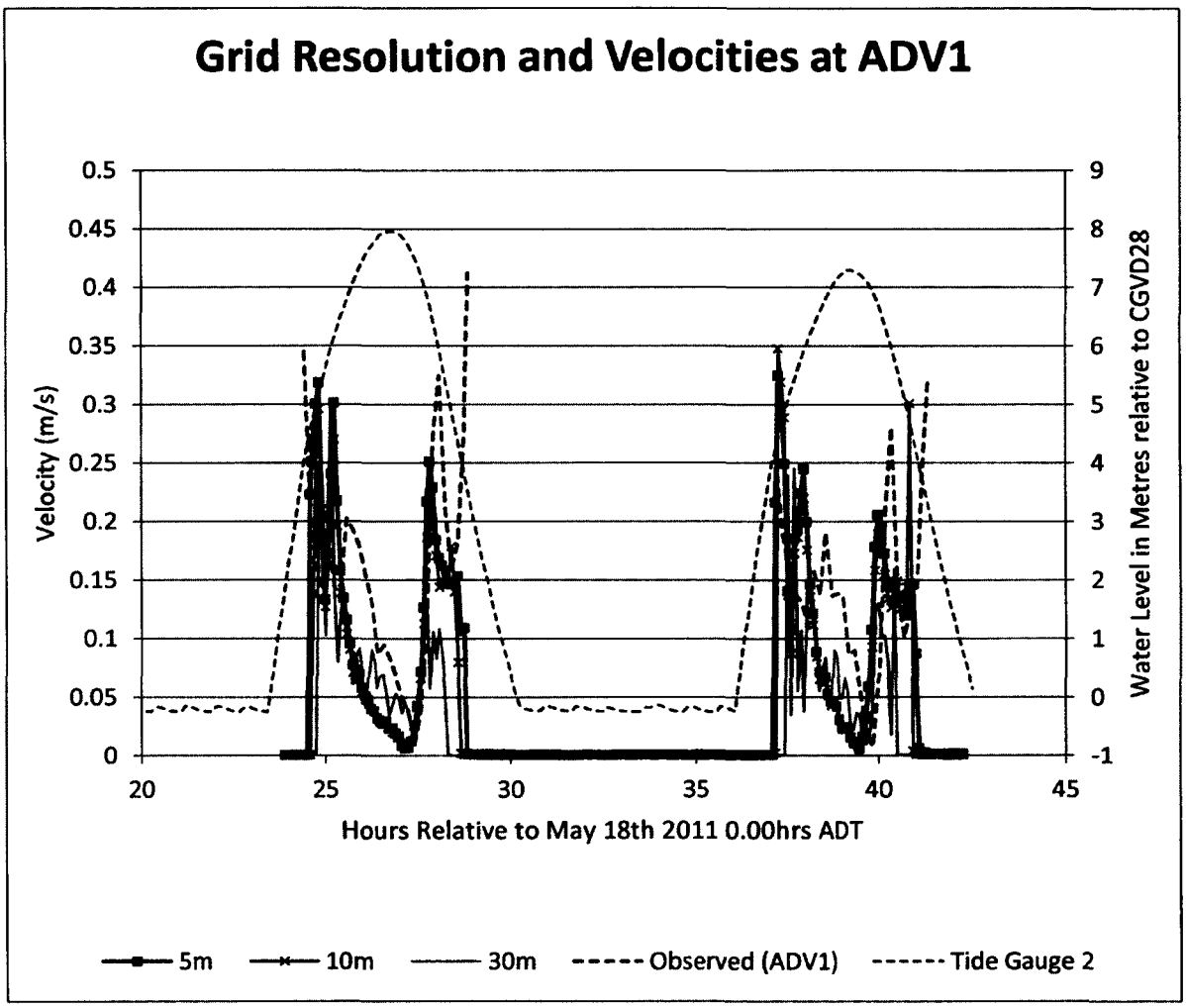

Figure 12: Velocities at ADV1 at different grid resolutions

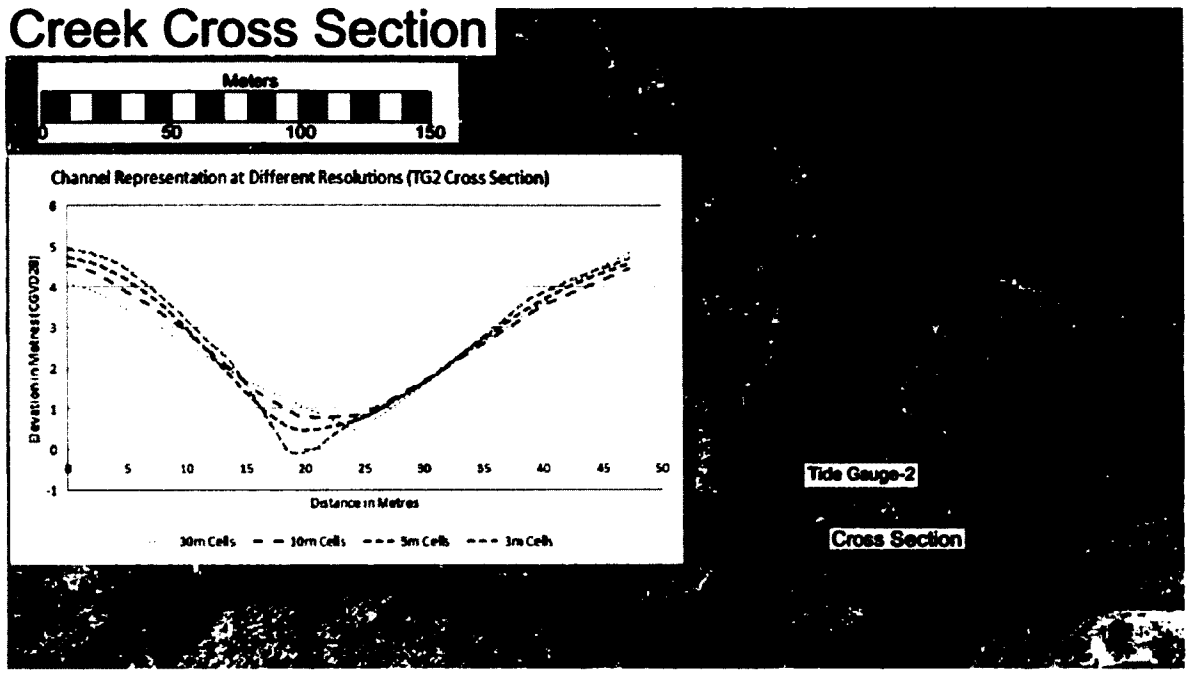

Figure 13: Creek representation at different resolutions. At lower resolution, the thalweg is shown as having a higher elevation.

3.3.3.1 b) Nested/Linked (10/5/2m) 2D Domains

TUFLOW is capable of linking multiple 2D domains. In this configuration, user defined boundaries between domains transfer water at nodes between different domains. In the previous section, it was found that decreasing the domain cell size had positive effects on results as channels were more adequately represented (3 m cell size case notwithstanding). A single 2m grid was too computationally prohibitive to run on available hardware and the grid generation software used (SMS 11.0 64-bit) was unable to interpolate a grid with the required number of elements. By nesting and linking grids of different cell sizes, it was had hoped that results would be improved while maintaining a reasonable run-time for the simulations.

Figure 14 shows the configuration that was used. A major difficulty with this configuration was the required set-up time as each boundary between grids needed to be perpendicular to the flow direction and situated across an area of minimal elevation change. The elevations in each grid needed to be altered so that the transition between domains would be smooth. Both of these conditions are limitations for using a model consisting of nested grids in this environment. A validation simulation producing realistic results was run; however it was found that the results across boundaries were showing spurious areas of wetting and drying and that the velocity pattern predictions near the boundary were unrealistic (Figure 15).

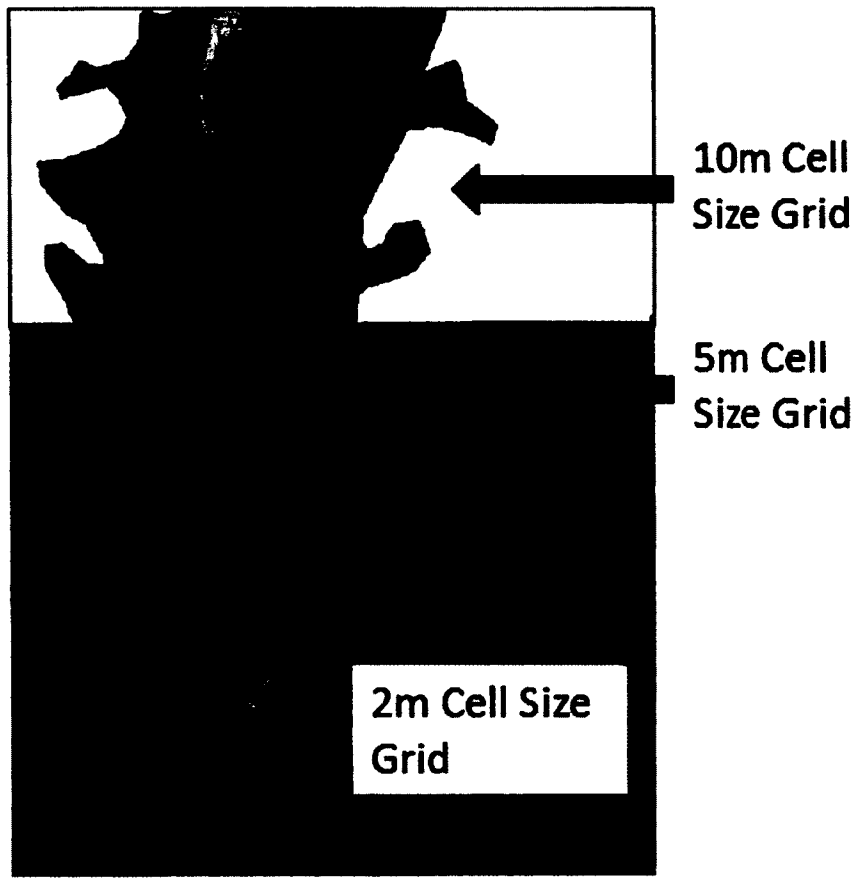

Figure 14: 2D/2D Grid Link Configuration. Brown lines are individual grid boundaries

The nested configuration produced unrealistic results for runs with the 2m storm surge. Falconer et al, (2007) state that in areas where there are rapid transitions in flow types or supercritical flows, the shallow water equations solved with the ADI-scheme used by TUFLOW produce discontinuous solutions that lead to poor performance. Hydraulic engineers at BMT-WBM indicated to us that TUFLOW does include a method of handling transitions to supercritical flow that compensates for the shortcomings in the ADI scheme (BMT-WBM Personal Communication, 2011).

The 5m single domain simulation provided better results in all but the 2m grid area and was able to produce realistic solutions for both validation and storm surge runs.

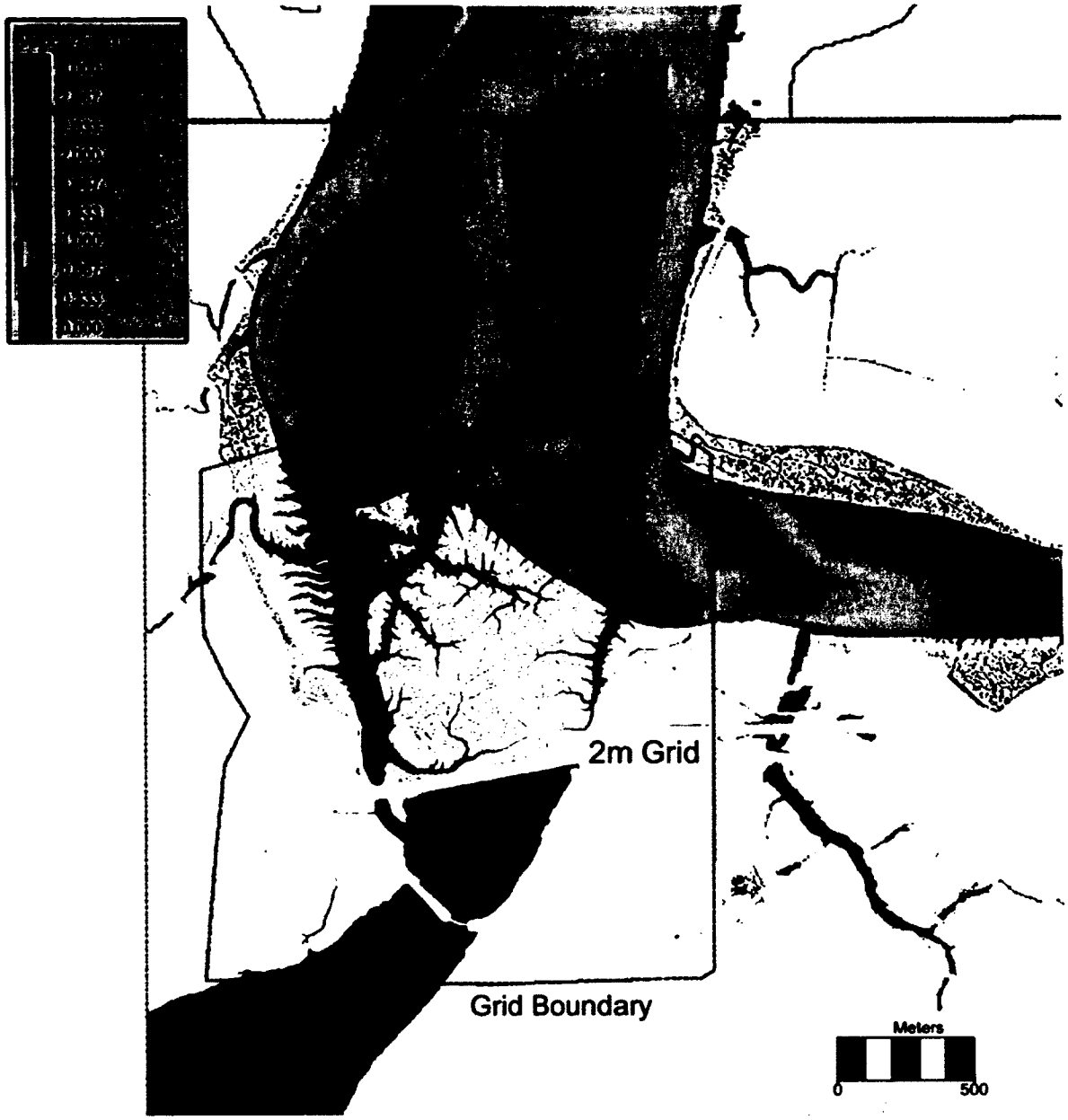

Figure 15: Validation velocity results for nested grid configuration showing unrealistic flow patterns at grid boundaries.

3.3.3.1 c) Nested 1D Channel in 5m cell size 2D Domain.

In order to cut down on the run time of the 5m grid size simulation, a configuration was created whereas a section of the grid across the St.Croix River was replaced with a 1D channel (Figure 16). In this approach, 30264 computational nodes were replaced with 29 cross sections. The linking between 1D channels and multiple 2D grids is similar and is subject to the same limitations. A section of the river, which was relatively straight and contained minimal intertidal areas and creeks where lateral flows would be significant, was replaced. Cross-sections were created from the 2m LiDAR terrain data, which somewhat mitigated the issues with loss of detail associated with the 5m grid. However, linking the domains proved to be a problem. The simulation of dyke overtopping in the storm surge scenario was also compromised as linking locations were along nodes that did not always correspond to location of water run-up and overtopping.

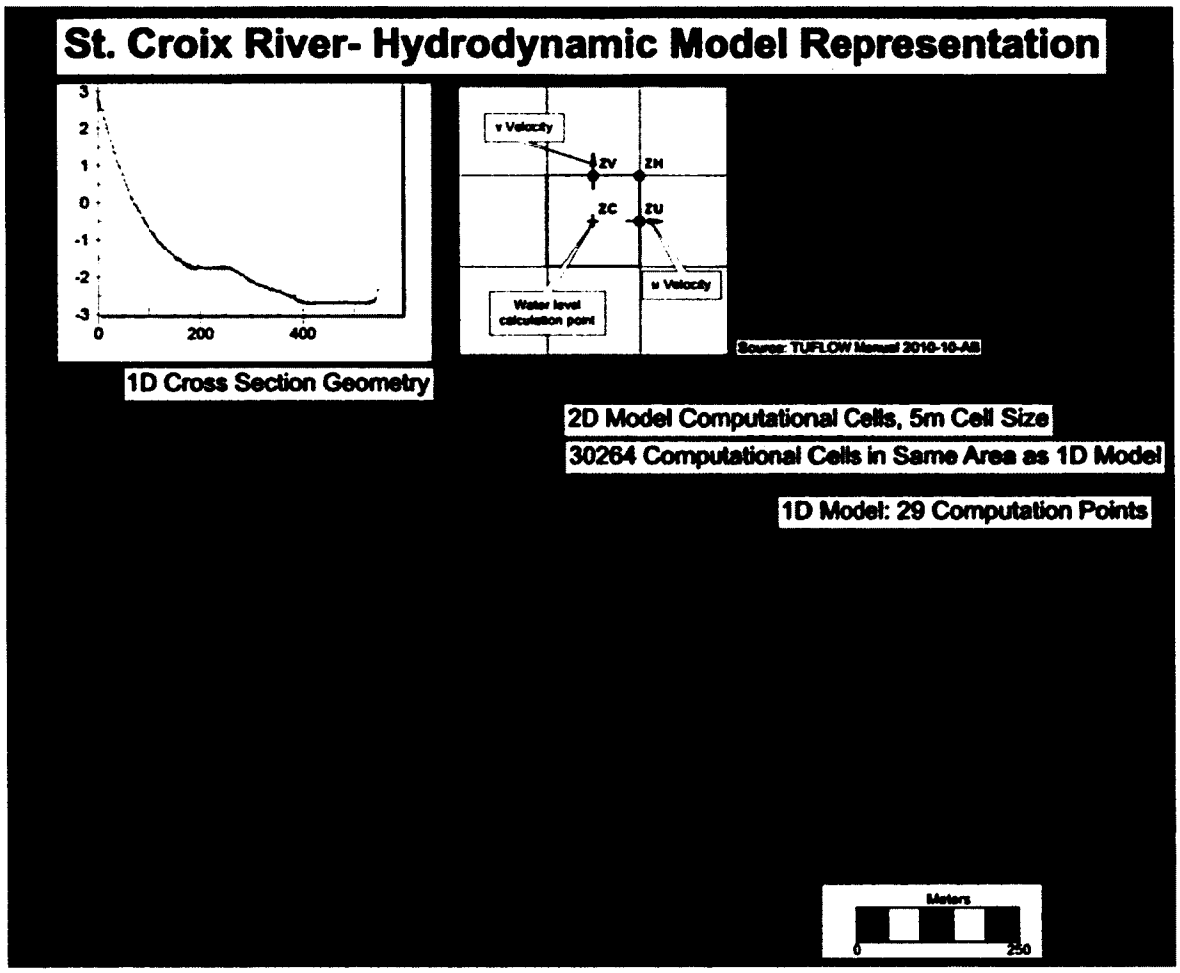

Figure 16: 1D channel nested within 2D grid. The channel is defined by cross section arcs. The edges of the cross sections are joined to the 2D grid. Within the cross sections, the 2D grid is inactive. The line joining the cross sections through the center is the thalweg of the channel.

3.3.3.2 Validation Results

After testing different configurations, a single 5m domain was found to be the best overall set-up. Validation using this configuration showed that phase errors due to the boundary condition time series and elevation errors due to the interpolated representation of the surface caused the largest errors in the simulated elevation and velocity results.

The boundary condition (Figure A.3) of the TUFLOW model was on the edge of reliable data from WebTides (areas that do not fully dry during low tide) and when the WebTides time series used to run the model was advanced twenty minutes, the phase error was reduced. However the phase difference varied between tidal cycles.

Figures 17 to 19 show validation results from the various tide gauges. It was found that the error in estimating the high tide level ranged between 5 to 30 cm (always an under prediction). This is consistent with the approximately 20 cm under prediction of amplitude reported by DuPont et al., (2005) for WebTides in the Minas Basin. The surveyed level of the tide gauge (taken with a survey grade GPS) was -0.44 m (CGVD28) while in the 5 m grid generated with SMS the elevation of the same location was 1.07 m (CGVD28). This is due to water returns in the LiDAR used for creating the computational grid and the loss of detail when high resolution LiDAR grid (1 m) was resampled to 5 m for creating the grid (Appendix. A). Note that neither the observed nor the predicted values decrease to a completely dry level; this is because of shallow water flow within the channel during low tide and shallow water that was not drained in the simulation.

Figures 20 to 23 show observed vs. simulated velocity values from the two ADVs (5 minute mean values) and the ADCP. The phase difference seen in the elevation values is also present here as the peaks are somewhat offset. ADV observations were taken at a point near the bottom of the marsh so it is expected that they would be less than depth averaged simulated values from TUFLOW. Such is the case for ADV values from the marsh surface where simulated values are always larger than observed (Figures 21, 22).

Within the marsh creek, the predicted velocities for tidal inflow are greater in the simulation while observed outflows are greater.

Results from the ADCP are depth averaged and are therefore a better indicator of simulation performance (Figure 23). A similar pattern to the marsh creek ADV results is seen as TUFLOW is under predicting the outflow velocity; however inflow velocities show a closer correspondence. Additionally, ADV and marsh creek ADCP results both show a spike in velocity as water level drops below 2m while the model shows a drop of velocity to 0 (Figures 20,23). This indicates that the marsh drains more quickly in the model representation than in observations, due to the interpolation of the channel elevations in the grid representation.

Separate surface roughness values were explored for the intertidal and channel zones. It was found that altering the intertidal roughness had a very small effect on simulated values. Changing the channel roughness to higher than the recommended values for a muddy channel in French, (2009) resulted in a change in the symmetry of the tidal curve but no change in amplitude. Therefore it was concluded that using different values within the recommended range does not cause significant differences in model outputs. Also, results are more sensitive to changes in the channel configurations than intertidal parameters.

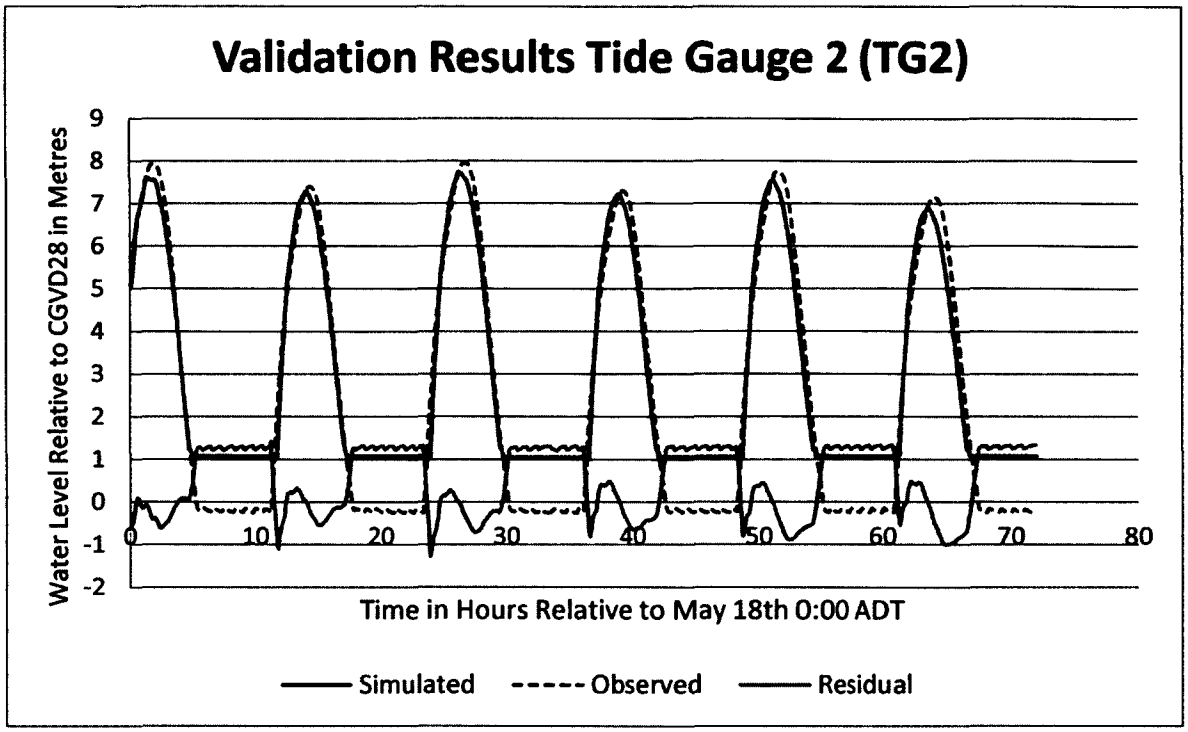

Figure 17: Simulation results for velocities at TG2 with observed levels and residual between observed and predicted values.

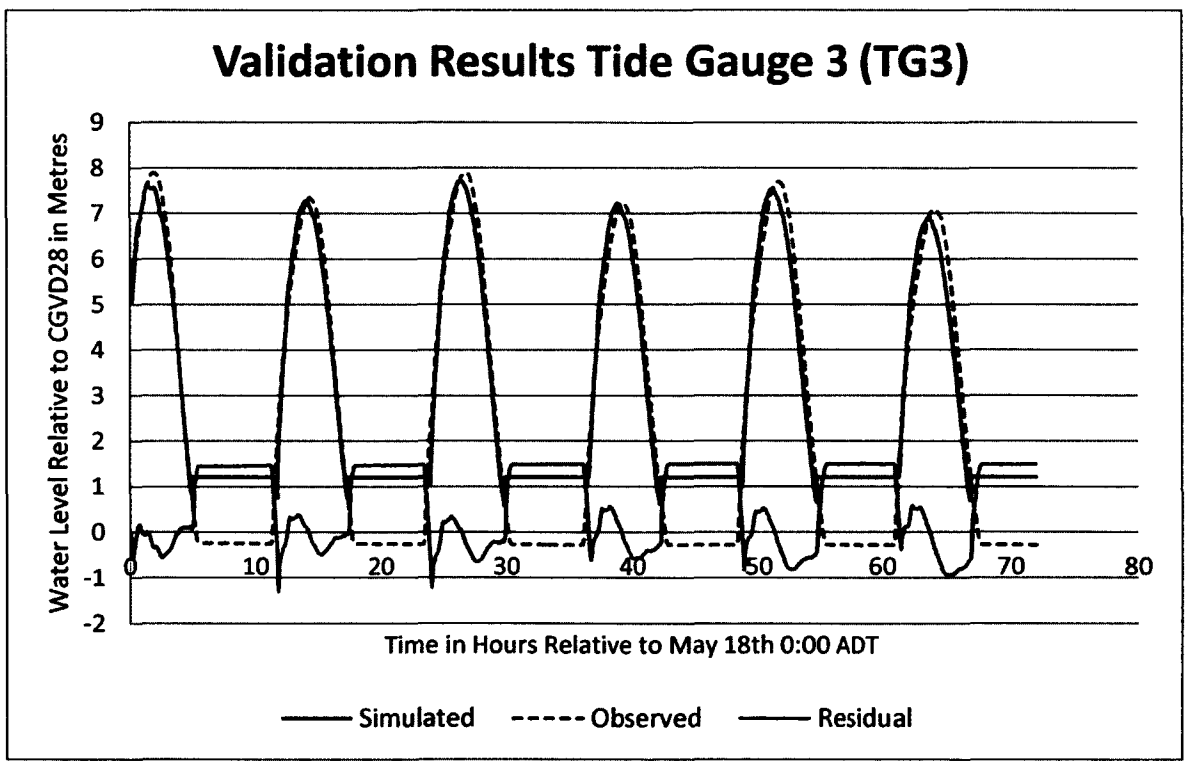

Figure 18: Simulation results for velocities at TG3 with observed levels and residual between observed and predicted values.

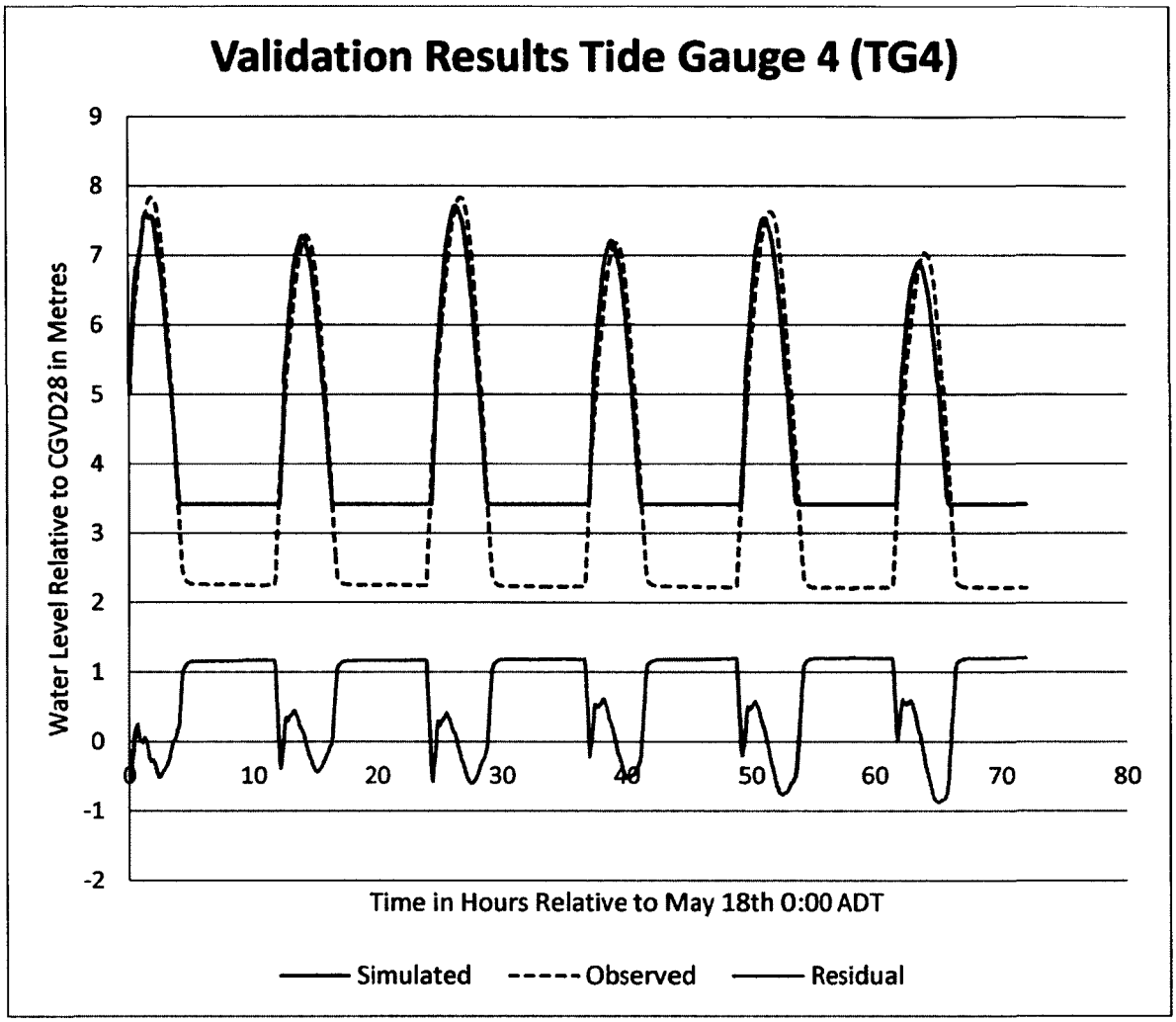

Figure19: Simulation results for velocities at TG4 with observed levels and residual between observed and predicted values

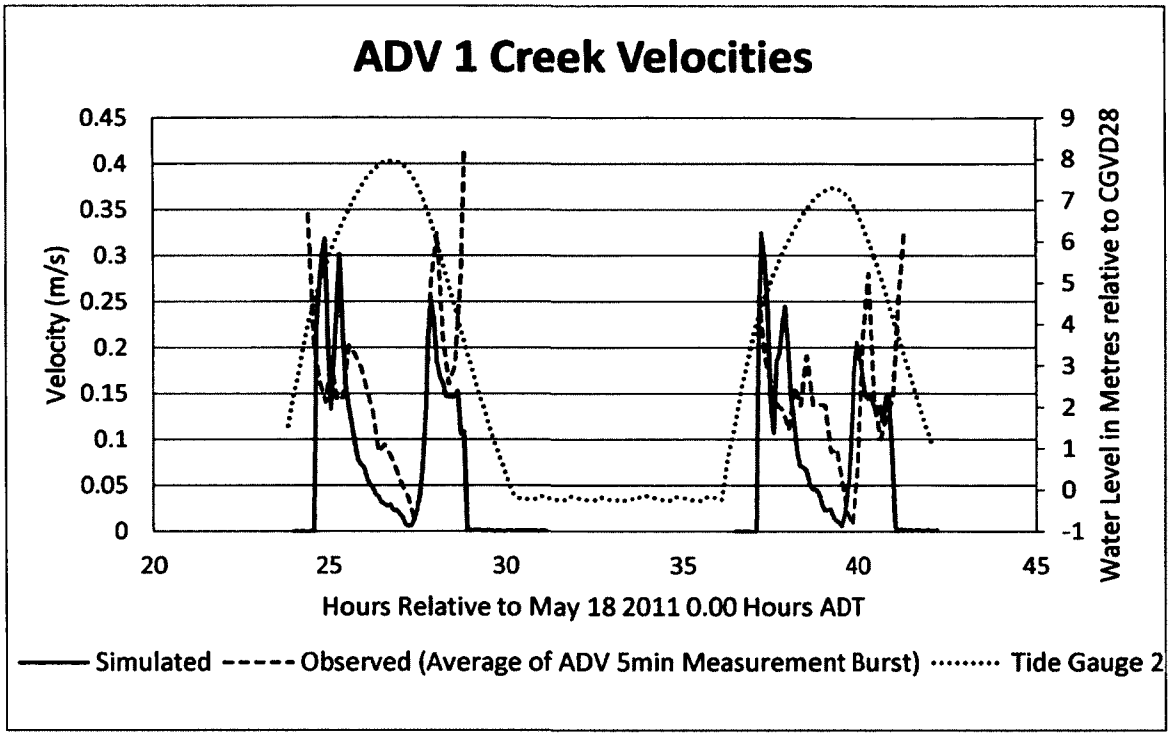

Figure 20: Simulation results for creek velocities at ADV1(TG1 location) with observed velocities and water levels

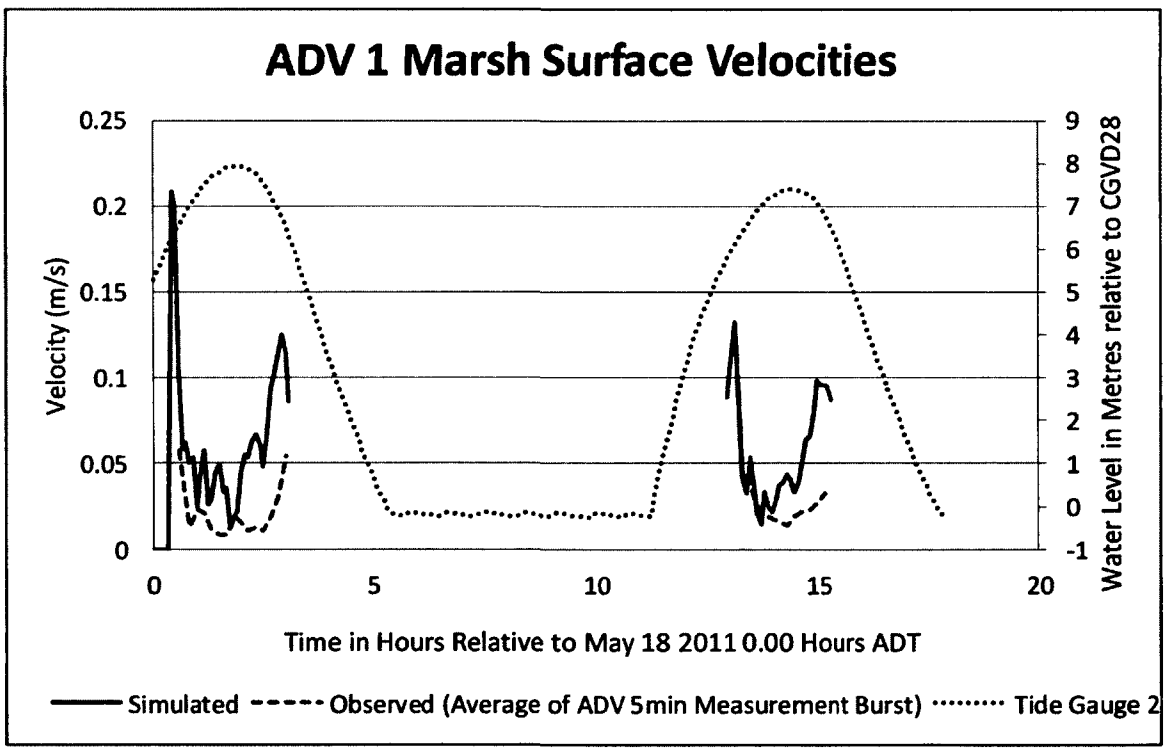

Figure 21: Simulation results for surface velocities at ADV1 with observed velocities and water levels

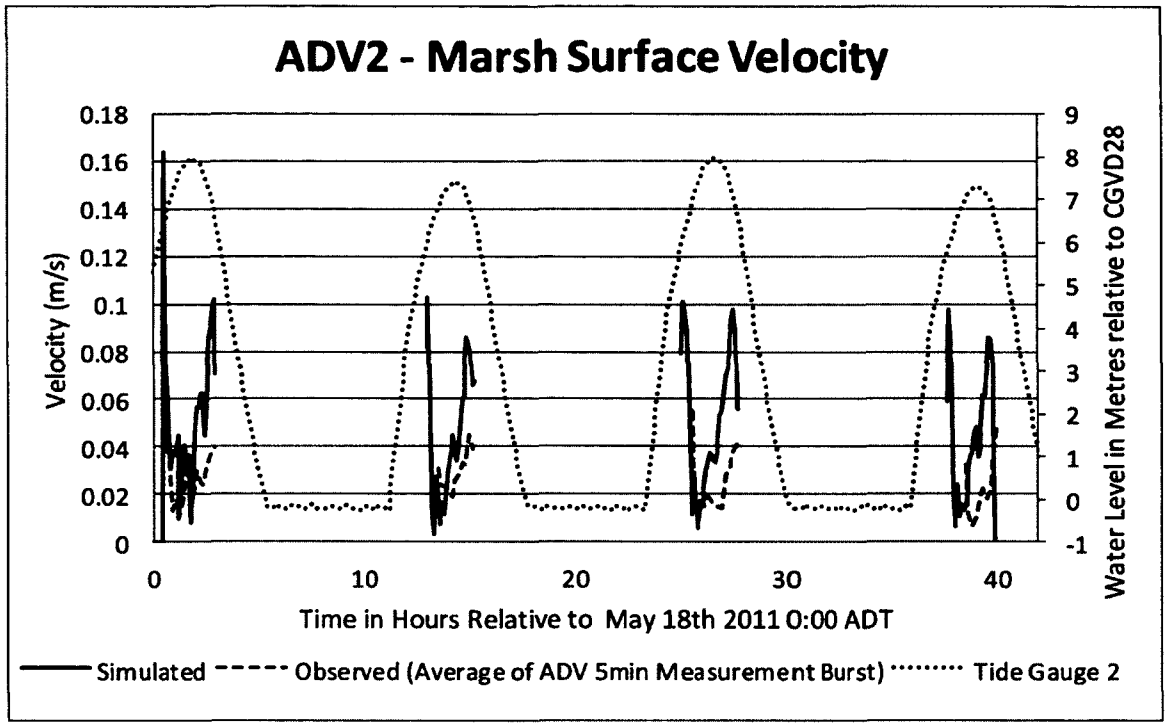

Figure 22: Simulation results for surface velocities at ADV2 with observed velocities and water levels

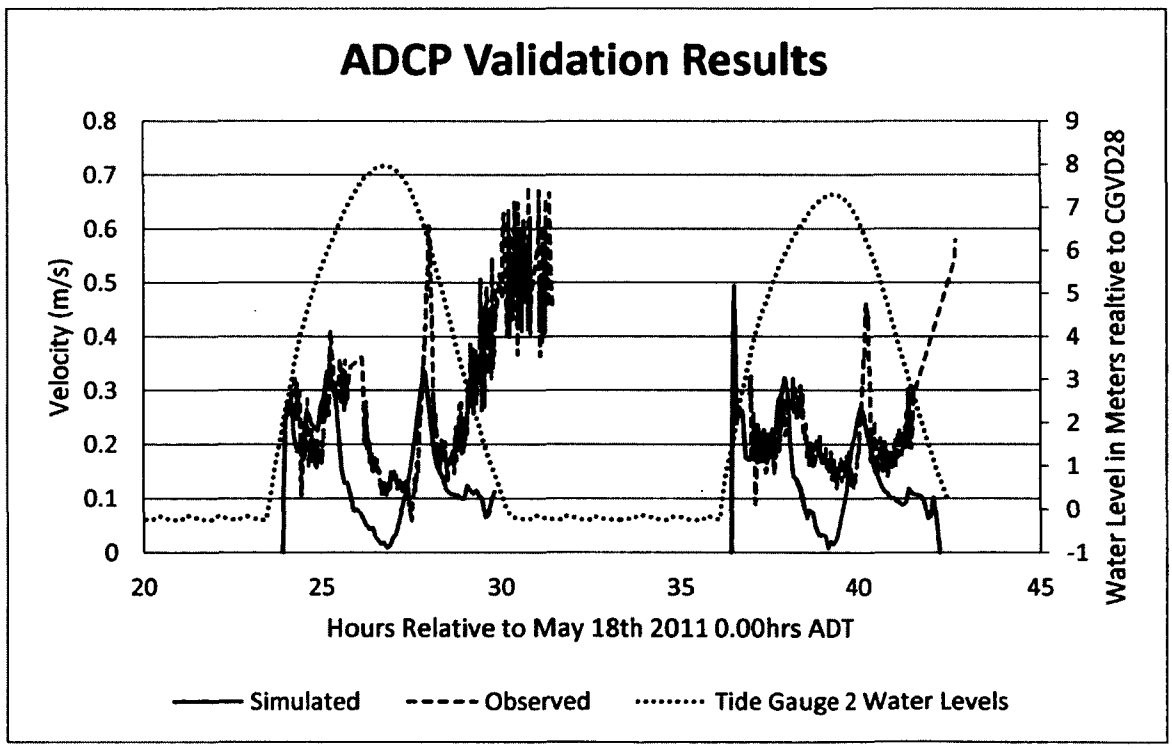

Figure 23: Simulation results for creek velocities at ADCP with observed velocities and water levels

3.3.4 Final Model Configuration and Simulation Set-Up

The validation stage assisted with finding shortcomings, omissions and errors in various TUFLOW configurations. Since the 5 m grid resolution configuration proved to be the most accurate; an ensemble of simulations using this grid configuration was created. Tables 2, 3 and 4 show the final boundary conditions, parameters and initial conditions used to set up the simulations. Appendix A describes the process of building the model in more detail.

The final ensemble of simulations consisted of 14 different scenarios (Table 5). Historical data for a large storm was not available so a set of simulations was created to investigate storm surges coinciding with a higher high water large tide (HHWLT) based on water levels in Daigle and Richards, (2011). To create the simulations an inflow boundary condition was set up. This consisted of a normal spring tide from a WebTides prediction at -64.132° W, 45.03839° N (WGS84) for March 16, 2011 augmented with 0.79 m sea level rise; which brought it up to an approximately 8.1 m HHWLT (Greenberg et al, in press) (Figure 24). Storm surges, corresponding with the high tide, were then added on top of the HHWLT curve on the third simulated high tide. The maximum water levels began with a HHWLT (labelled as HT81) and, in 0.2 m increments, increased to a 2.2 m storm surge (10.3m maximum water level, HT103). This yielded 12 storm surge scenarios and two special scenarios for a dyke breach and blockage of the aboiteaux.

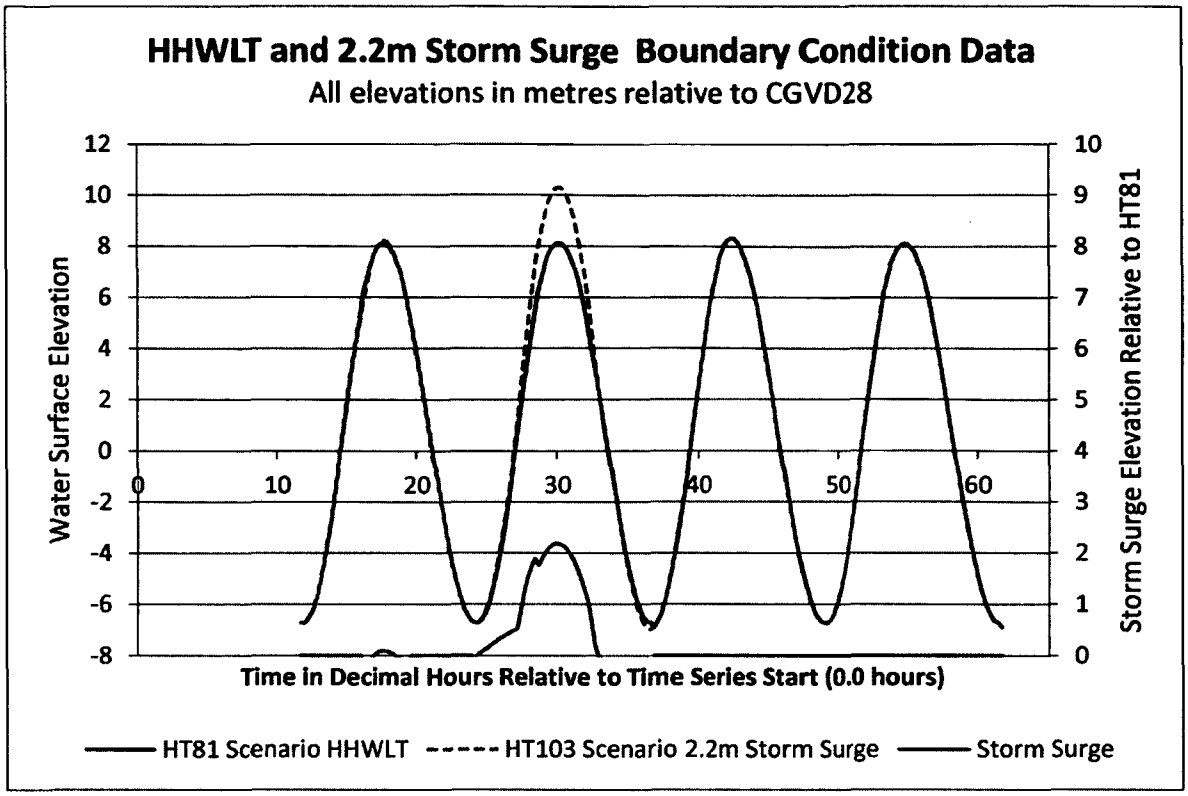

Figure 24: Boundary condition time series examples. All scenarios (Table 5) are based on the HHWLT curve which is named "HT81". The model was run from 11.67 to 61.67 hours of the time series for four tidal cycles. Times are in decimal hours relative to the start of the time series.

These simulations contain uncertainties, especially during a large storm event. Debris buildup blocks drainage features and protection structures. A simulation was run to test what may happen if the aboiteaux draining the Tregothic marsh were partially blocked by debris or ice. Also investigated were changes in flood extent and drainage that may occur if there was a dyke breach during the storm surge event.

Simulation outputs were water levels, depths, velocities, and velocity depth product related hazard metrics. Output from the model was written in 5 minute intervals to an extensible model data format (XMDF) file. Additional details are provided in Appendix A.

The major constraints were the model run time and numerical stability issues relating to the magnitude of the storm surges which were simulated and the complexity of the intertidal terrain. A 49.5 hour simulation took between 18-23 hours (larger floods with more wetting and drying took longer to simulate) at a 5m cell size.

The following sources of data were used to set up the model:

Boundary Conditions:

1. Water Surface Elevation Time Series
2. Storm Surge

Parameters:

1. Terrain Elevations and Bathymetry
2. Surface Roughness
3. Dyke and Culvert Elevations
4. Culverts and Aboiteaux
5. Cell Size
6. Windsor Tide Gate
7. Buildings
8. Timestep

Initial Conditions:

1. Lake Pisiquid Water Level.
2. Channel and intertidal initial Water Level

Boundary Condition	Source
1. Water Surface Elevation Time Series	WebTide Prediction Model (DuPont et al., 2005) HHWLT Tide (8.1m based on chart datum Hantsport CHS Tide Station 4140, 2002 see Webster et al, (2011)).
2. Storm Surge (added to HHWLT curve)	Range of values from 0.2m to 2.2m , Greenberg et al., in press; Daigle and Richards, 2011. For consideration of larger storms such as the Saxby Gale Webster et al., 2011 was consulted.

Table 2: Final Boundary Conditions

Parameters	Source
1. Terrain Elevations and Bathymetry	LiDAR DEM 1m spatial resolution, 0.15-0.30m vertical accuracy see Webster et al., 2011. This was taken at low-tide when the Avon/St.Croix Rivers in April 2007 when the study area had negligible amounts of water so the LiDAR is assumed to represent the bottom of the channel. Some sensitivity testing was done to determine the effect of LiDAR data with significant amounts of water returns. Lake Pisiquid did contain approximately 4m of water but there was no high resolution bathymetry available so the bottom was interpolated using TUFLOW geometry modifications.
2. Surface Roughness	GIS layers used to specify Manning's n coefficient for each cell. Based on aerial images and field visits. Values from Chow, (1959); French, (2009), Wamsley et al, (2010). See Figure 25. Value of 0.05 was used as a default for inland areas and for salt-marsh vegetation (French, 2009). Sensitivity testing showed that inland roughness values lower than 0.1 and not in a channel did not make an appreciable difference in flood

	characteristics.
3. Dyke and Channel Elevations	GIS data used to modify cell elevations for dykes based on RTK GPS surveys. Each dyke segment is based on survey elevations taken every 15m (50 feet) along the top of the dyke.
4. Culverts and Aboiteaux	See Section 3.3.2.1 and Appendix A. Manning's n values were assigned to culverts based on material type and condition (good condition plastic= 0.012 to poor condition steel/ rough concrete 0.02).
5. Cell Size	There was experimentation with increasing the resolution as much as possible, especially in marsh and urban areas. Started with 30m as the coarsest, 3m as the finest. 5m was used. Pender and Neelz, suggest a ~5m cell size or finer is appropriate for representing urban areas.
6. Windsor Tide Gate	van Proosdij, et al., 2009 provided specifications on the Windsor Tide Gate.
7. Buildings	Edited NS 1:10,000 database building polygons as well as LiDAR DSM height values. See Figure 26 for grid before modifications, Figure 27 for grid after modifications
8. Timestep	½ the cell size is suggested but depends on courant number and stability which is affected by the maximum velocities and the configuration of the software. Advice on the appropriate timestep was obtained from TUFLOW hydraulic engineer Phillip Ryan of between 1.25 and 1.5 seconds. 1.5 seconds was used The sensitivity of the model was also tested to changing timesteps against the validation data and with the maximum storm surge simulations. It was found that lowering the timestep under 1.5 seconds

	had very little effect on velocities (0.01m/s difference at the most), depths and errors.

Table 3: Final Parameters

Initial Condition	Source
1. Lake Pisiquid Water Level.	Lake Pisiquid initial condition bankful elevation of 5.18m from Ken Carroll Personal Communication.
2. Channel and Intertidal Water Level.	Initial water level of -6.7m (lowest level in WebTides prediction) resulted in a mostly dry starting domain.

Table 4: Final Initial Conditions

Simulation Name	Storm Surge Level metres	Peak water level metres (CGVD28)	Peak water level metres (Chart Datum)
HT81 (HHWLT)	0.0	8.1	15.33
HT83	0.2	8.3	15.53
HT85	0.4	8.5	15.73
HT87	0.6	8.7	15.93
HT89	0.8	8.9	16.13
HT91	1.0	9.1	16.33
HT93	1.2	9.3	16.53
HT95	1.4	9.5	16.73
HT97	1.6	9.7	16.93
HT99	1.8	9.9	17.13
HT101	2.0	10.1	17.33
HT103	2.2	10.3	17.53
Dyke Breach	2.2	10.3	17.53
Aboiteau Blockage	2.2	10.3	17.53

Table 5: All simulation scenario maximum water levels and storm surge. Chart datum is -7.23 metres relative to CGVD28 at Hantsport.

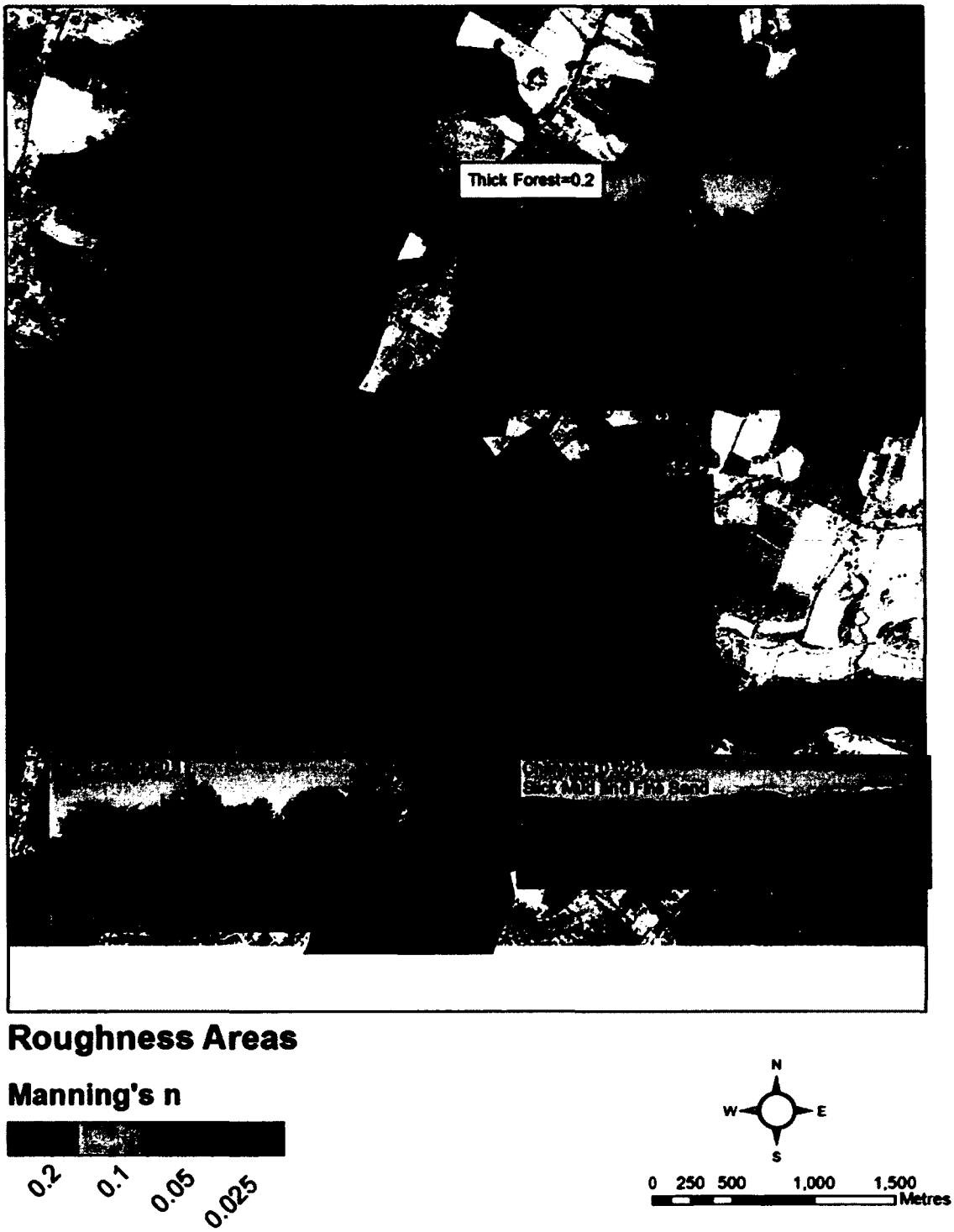

Figure 25: Distributed Surface Roughness Values for Simulation Runs.

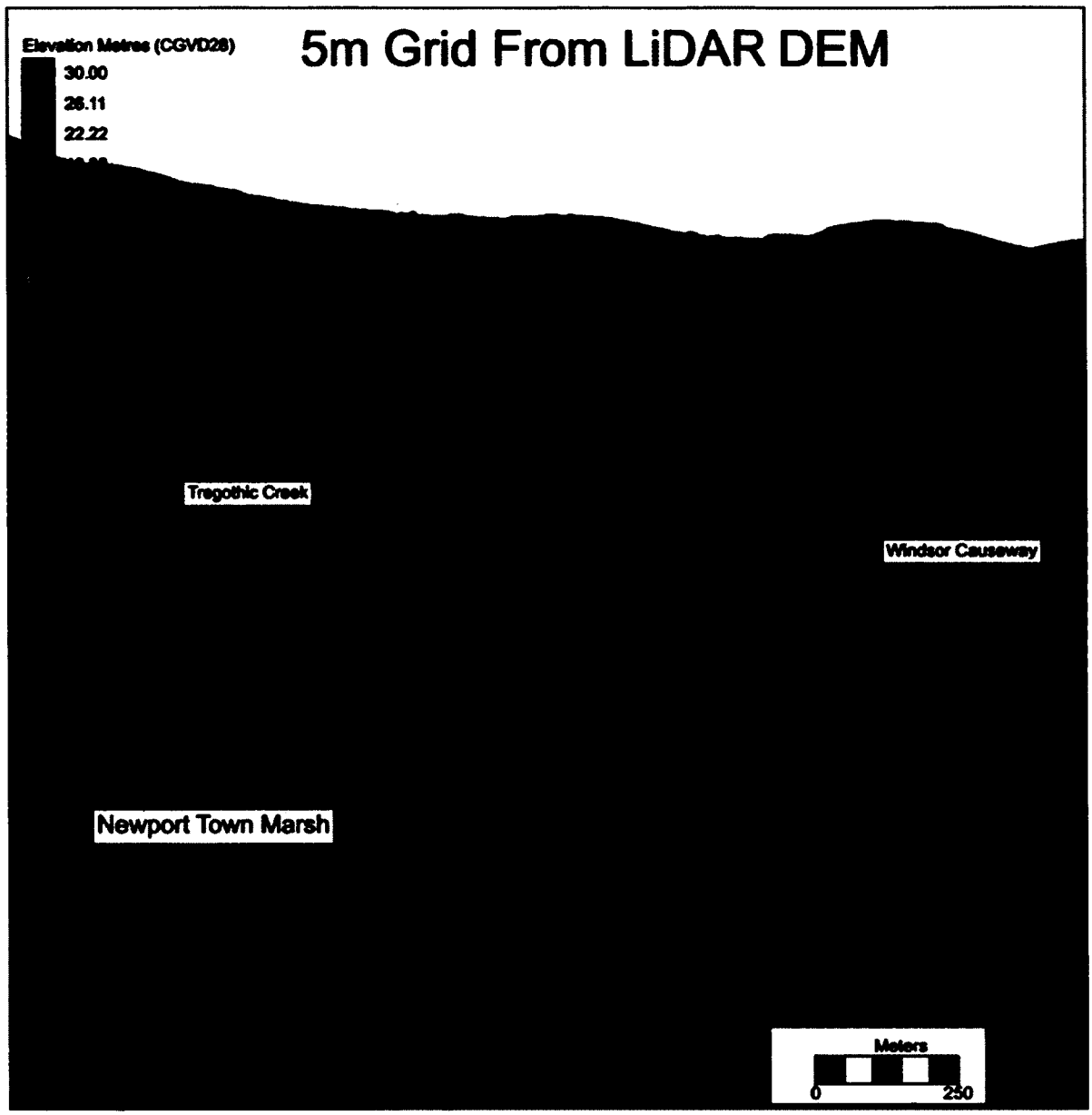

Figure 26: Hillshade of TUFLOW model domain with no modifications.

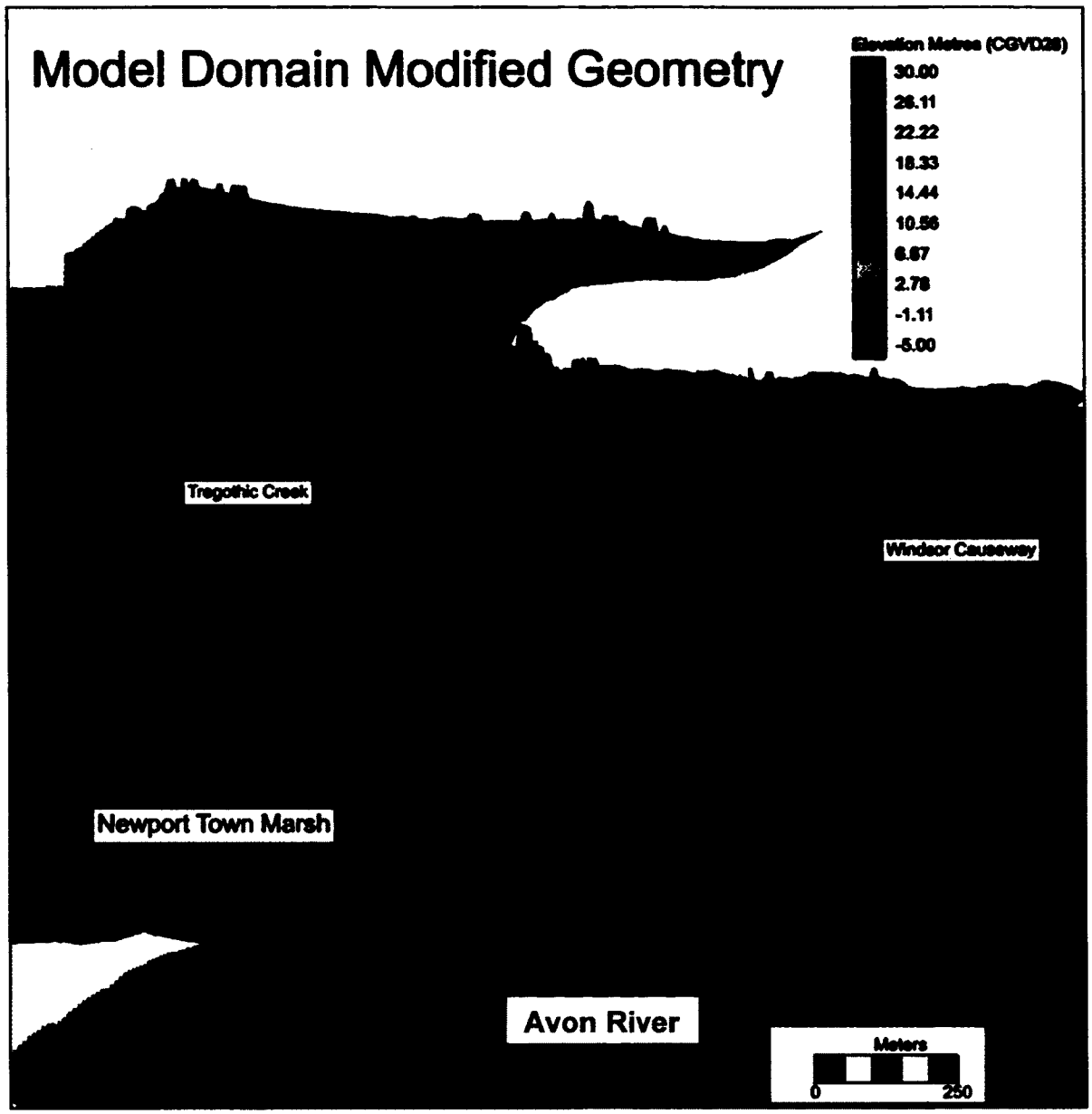

Figure 27: Hillshade of TUFLOW Model Domain with Buildings and Dykes added as a Geometry Modification.

3.3.5 Assumptions and Limitations

This study has several assumptions and limitations in terms of the choices that were made during the modelling process and those implicit to the model and data that was used.

- TUFLOW is a 2D depth averaged model meaning that the vertical velocity gradient is ignored. Hydrostatic equilibrium (upwards pressure from fluid cancels out downwards pressure from atmosphere). This is only valid on mild slopes.
- Surface roughness is represented by the empirically derived Manning's n coefficient with single values for areas (Figure 24).
- Fluid moves from boundaries as a long wave (wave length is greater than depth) and short-period surface gravity waves are negligible which is valid as the fetch length is limited (van Proosdij, 2009).
- There are some 'water returns' in the LiDAR, meaning that the elevations of the bottom of some channels are actually the water surface. However, this data was recorded at low tide when there was very little water in the channel.
- LiDAR can only record the heights of surface features and needed to be post-processed with SMS to incorporate below ground features such as culverts and overpasses (Webster et al, 2011).
- Each computational cell has homogenous conditions in terms of assigned parameters.
- The bed is assumed to be non-mobile; which is known not to be true. Meaning that the morphology is constantly changing so surface data for marshes and bathymetry is quickly out of date (van Proosdij et al, 2009). It is however unlikely that very significant change to channels would take place over the course of the scenarios investigated here.
- Grid must be in a Cartesian coordinate system and metric units are used.
- The grid size was limited by the computational time required for higher resolution models and also the ability of SMS to interpolate computational grids from millions of points (SMS was unable to do this for resolutions smaller than 3m for the entire study area).
- Limitations of hydrodynamic models using the Shallow Water Equations, in areas with steep slopes and large amounts of wetting and drying (Pender and Neelz, 2011). The large intertidal areas, dykes, and inland infrastructure all caused rapid changes in flow types which comprised the accuracy of TUFLOW results..
- There are no data related to large tidal curves in the study area, there are also no storm simulations that may be used to generate more realistic storm surge curves.
- Buildings are represented as solid features possibly underestimate flood extent (Chen, 2007).

3.4 Data Management

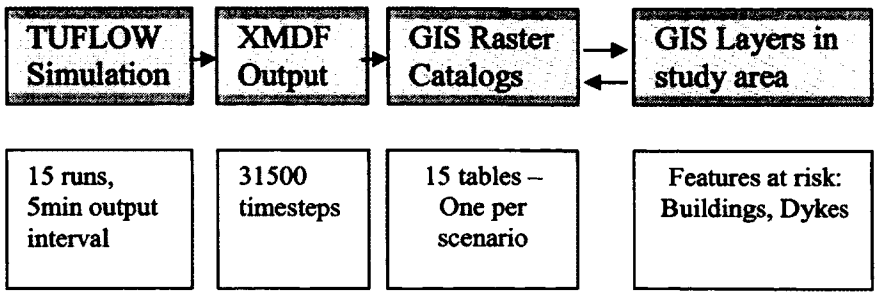

Figure 28: Data Management Workflow

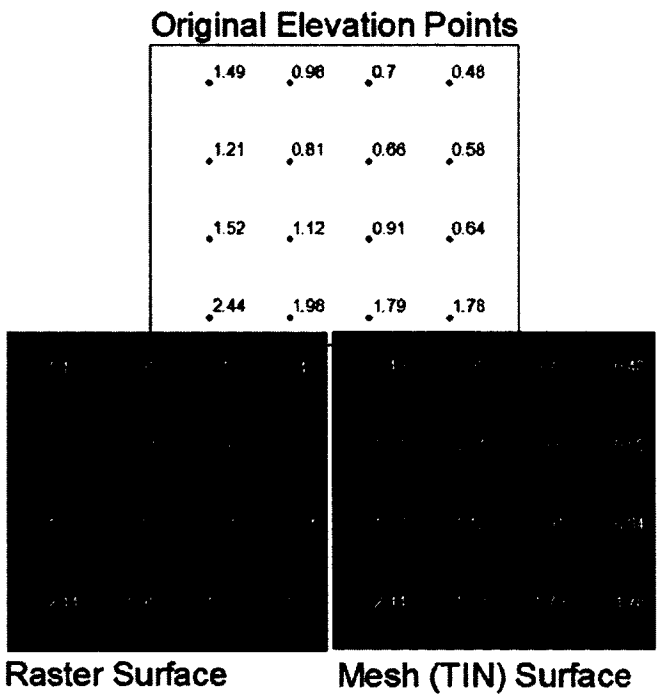

Figure 29: Raster vs. Mesh Representation of a surface generated from elevation points

Outputs from TUFLOW were in a XMDF format, this is a mesh based data model native to the Surface Water Modelling System and not readable by GIS software packages. The Department of Agriculture in Nova Scotia uses ArcGIS software for spatial data management so results needed to be transferred into a compatible format

(Figure 28). TUFLOW software comes with utilities for transferring model results into an ASCII raster format from a mesh, see Figure 29. All data were referenced to a Cartesian coordinate system (NAD83 UTM Zone 20N) with coordinates in metres as Eastings and Northings. The vertical datum was CGVD28 and all height values were in metres. It should be noted that using a single 2D Cartesian grid made it easy to transfer results to a raster format since each cell in the model could correspond with a cell in the output raster. This would be much more difficult to do with an unstructured mesh with non-square areas.

Due to the large quantity of model outputs, a GIS is essential for dealing with these data (Zerger & Wealands, 2004). The output consisted of 31,500 individual raster files each with a 2.5m cell size (1/2 the computational grid cell size) consisting of over 4 million cells (about half of which contained no data) (Appendix A). Placing these rasters in a raster catalog enabled the reduction in the size of the output datasets to 1/4 their size in XMDF format. A raster catalog also allowed attachment attributes to the data which made it possible to make relational joins with other datasets. Figure 30 shows an entity relationship diagram of the outputs and exposed features of interest, namely dyke points and building polygons. The spatial raster data in the catalogs were related to spatial features in other datasets through non-spatial tables which contain the raster values for each building or dyke point in each dataset. For example, for the 9.1m maximum water level scenario (HT91) raster catalog; there are 445 individual entries for water level and each corresponds to an output from TUFLOW. At each dyke point, there is potentially a value for each time step of output if the dyke point is overtopped. This is a one-to-many

relationship because each entry in the raster catalog may have many dyke points associated with it.

Ultimately, organizing the data in a database allows queries to summarize the datasets in order to retrieve relevant information that would be useful or managers or emergency officials. For example, it is possible to summarize the total time each building was at risk by finding the catalog items associated with each building.

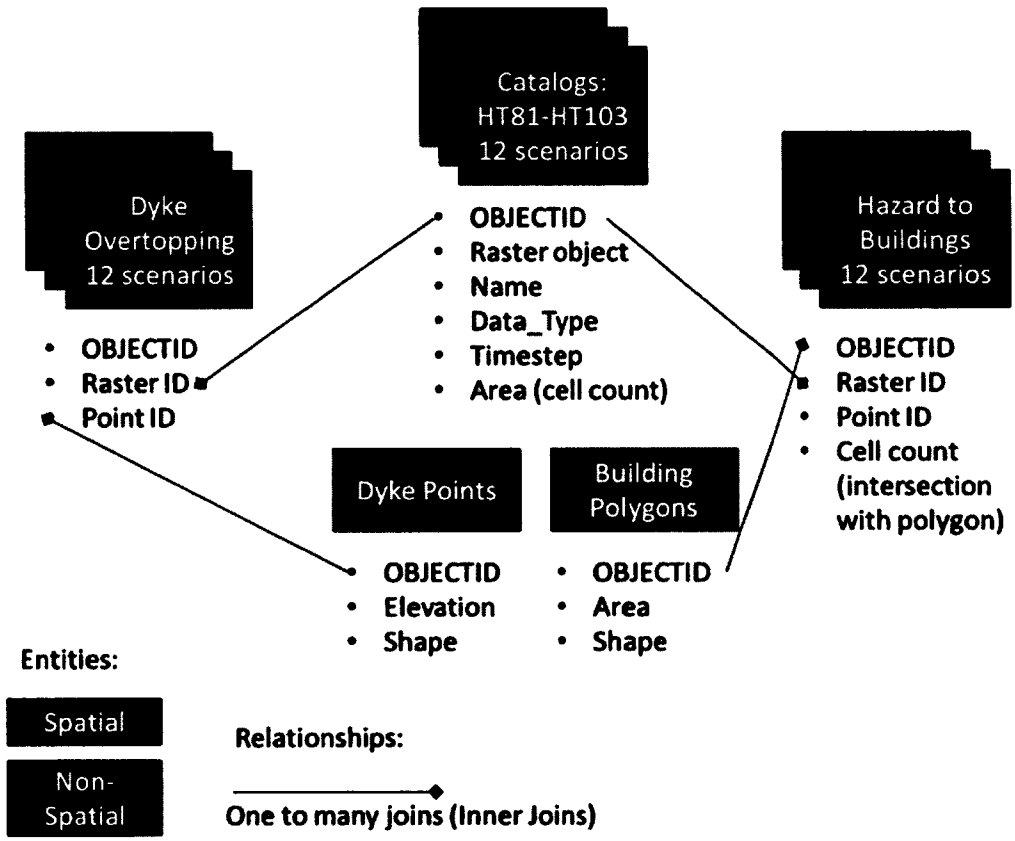

Figure 30: Final data organization entity relationship (ERD). This shows how simulation results were linked to the locations of buildings and dykes in the study area.

CHAPTER 4: Results

Results from the 14 simulations were divided into three groups based on the number of buildings exposed to flooding (Figure 31). These divisions show the water levels at which flooding affects primarily agricultural areas (group 1), industrial, commercial and limited numbers of residential buildings (group 2) and the dense downtown core of Windsor (group 3). These divisions are not apparent if flood extent results alone are examined. Building locations are based on a building polygon dataset from the Nova Scotia Geomatics Center.

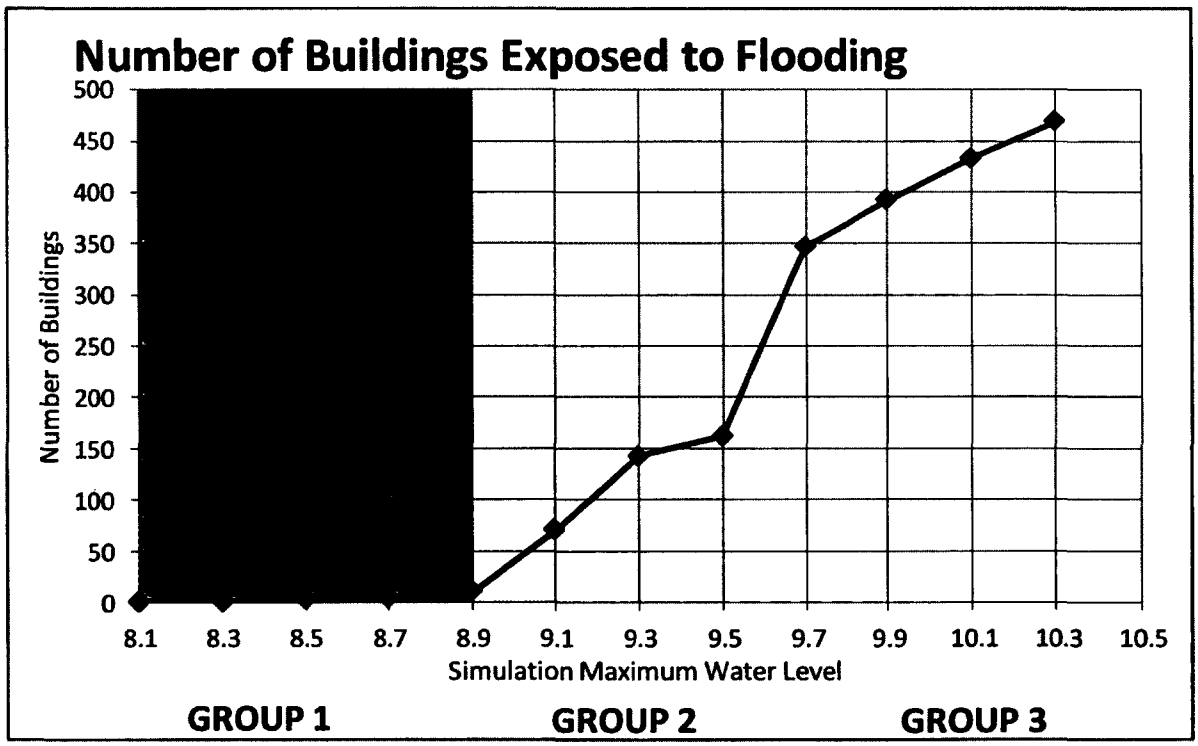

Figure 31: Number of buildings exposed to flooding by simulation maximum water level

4.1 Speed and Extent of Flooding

This section discusses the particular characteristics of flooding in the study area in terms of where water will go and how fast it will get there. Differences between ensemble results are discussed and compared with existing areas of flood related development constraints (incorporated marsh body boundaries).

4.1.1. Flood Extent

Figure 32 shows the maximum flood extent over the dyke by simulation. These are inland areas that are protected by dykes and exclude water in the Avon River channel and Lake Pisiquid. The channel (HHWLT extent) was delineated using a lake flood algorithm (Figure 1). During a simulation, maximum water level is output as a composite

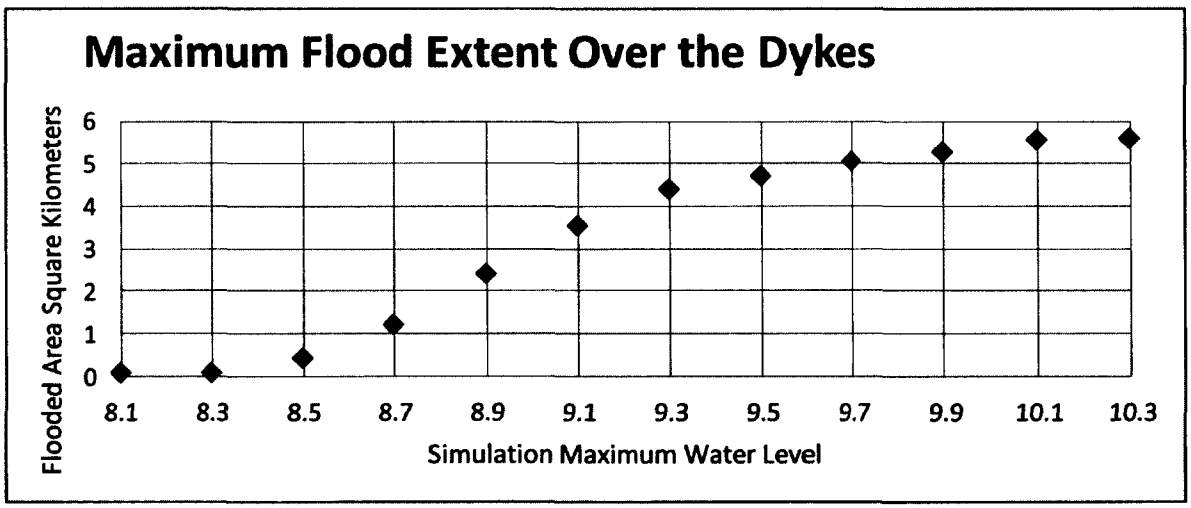

Figure 32: Maximum flood extent in dykelands by simulation maximum water level

of the highest water levels for each cell across all time steps in the simulation.

For simulations in group one (8.1, 8.3, 8.5, 8.7, 8.9m maximum water levels) flooding tends to be restricted to agricultural areas and lands without buildings, almost all within established marsh bodies (Figure 33). On the Tregothic and Elderkin marsh bodies, the extent of flooding is controlled by the Highway 101 and the rail beds, neither of which were overtopped and both acted as obstructions. Culverts under the rail line and Highway 101 carried flow under the highway from Elderkin marsh into the Tregothic marsh. These culverts were assumed to be unblocked. A 0.8m storm surge overtopped the dyke immediately west of the Tregothic Creek aboiteaux; this exposed some buildings to flooding. On the Newport Town Marsh, there are fewer man-made obstructions to flow and flood waters initially flowed through irrigation channels in the farmland. However, a 0.8m storm surge (8.9m maximum water level) was not confined to the channels and spreads across the farmland affecting a much greater area. Flooding reported in the HHWLT and 0.2m storm surge simulations was due to shallow (<0.2m) overtopping of some dyke segments.

In group two (9.1, 9.3, 9.5m maximum water levels), flooding was mostly confined to the incorporated marsh bodies but also extended into populated areas and affected major infrastructure (Figure 34). The greatest difference in extent between group 1 and 2 simulations occurred in the Tregothic Marsh. Water is conveyed under the highway through overpasses and culverts to flood areas in the Windsor Industrial Park as well areas of Falmouth between Highways 1 and 101. Overtopping of Highway 101 occurred in two locations during the 1.2m surge (9.3m maximum water level) simulation whereas

the causeway and Highway 101 near the Town of Windsor (Exit 6) and Elderkin Marsh (Exit 7) were overtopped in the 1.4m surge simulation (9.5m maximum water level). Near Exit 6, simulated flooding extended beyond the established marsh boundaries and into areas with homes and businesses. Both the 1 and 1.2m surge simulations were blocked by the rail bed on the Tregothic marsh, this rail bed was predicted to be overtopped in the 1.4m simulation. This was significant, because it opens up a floodway into the more densely populated areas of the town. In the 1.2 and 1.4m simulations the rail line is overtopped near the southern edge of the domain opening a floodway to suburban areas. In Newport Town and Elderkin marsh bodies, flooding was contained by higher elevation areas and extents did not differ significantly between surge scenarios. In the Newport Town Marsh, the road was overtopped near the eastern end of the model domain. In this area, water flooded beyond the marsh body boundary and outside of the simulation domain. Most of the dykes are overtopped in group 2 versus less than half in group 1 (Table 5).

In group three (9.7, 9.9, 10.1, 10.3m maximum water levels) flooding fully overtopped the causeway and extended into the Town of Windsor and parts of Falmouth (Figure 35). This group represented the worst case scenarios of possible storm surges with elevations upwards of 1.8m on top of the HHWLT. An event of this magnitude is comparable to the Saxby Gale. Most of the difference between this group of simulations and the previous occurred in the area of Lake Pisiquid around the Town of Windsor and Falmouth. As King St. was overtopped, water exited the established marsh boundaries and a flow path would be opened to Lake Pisiquid through the Town of Windsor (Figure 35). There is not

much difference in the extent of flooding through the town as it appears to be constrained by two higher elevation areas to the north and the south. In the 1.8 to 2.2 m surge simulations, Highway 1was overtopped, allowing water into an area which appears to be mostly forested. As can be seen in Figure 32, flood extents begin to peak as total area of flooding reaches 5.0 km^2. There is comparatively little difference in flood extent between a 2.0 m and 2.2 m storm surge (10.1 and 10.3 m maximum water level respectively). Overtopping locations along Highway 101 in the Tregothic Marsh were similar to those seen in the previous group of simulations. The most significant differences were the complete overtopping of the causeway and additional highway overtopping on the Falmouth side near exit 6. With the exception of the area near Falmouth and the causeway, flood extents in the Elderkin and Newport Town marsh bodies were very similar to the previous simulation group.

Scenario (Maximum Water Level)	Buildings Exposed	Dyke Segments Overtopped	Max Flood Extent Over Dyke (sq.km)
8.1	0	1	0.07
8.3	0	1	0.07
8.5	2	5	0.42
8.7	4	11	1.18
8.9	10	184	2.40
9.1	70	485	3.53
9.3	142	501	4.39
9.5	162	510	4.69
9.7	347	514	5.04
9.9	392	514	5.27
10.1	433	514	5.56
10.3	469	514	5.58

Table 6: Simulation Results for Dyke Overtopping and Building Exposure. Dyke segments are 15.24 m (50 feet). Excludes Avon and St. Croix main channel and Lake Pisiquid.

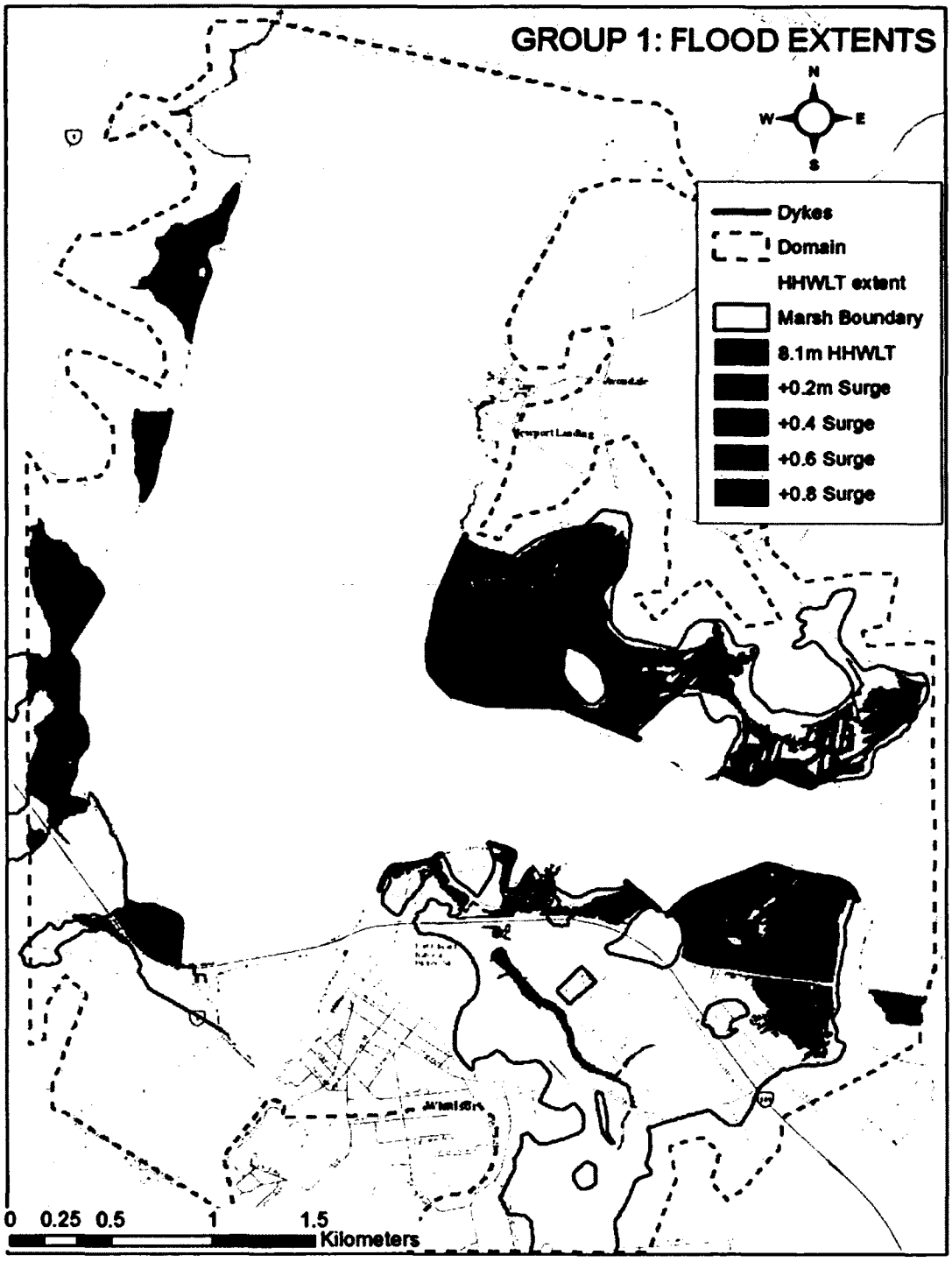

Figure 33: Group 1 Maximum Flood Extents. Incorporated marsh boundaries are shown in red.

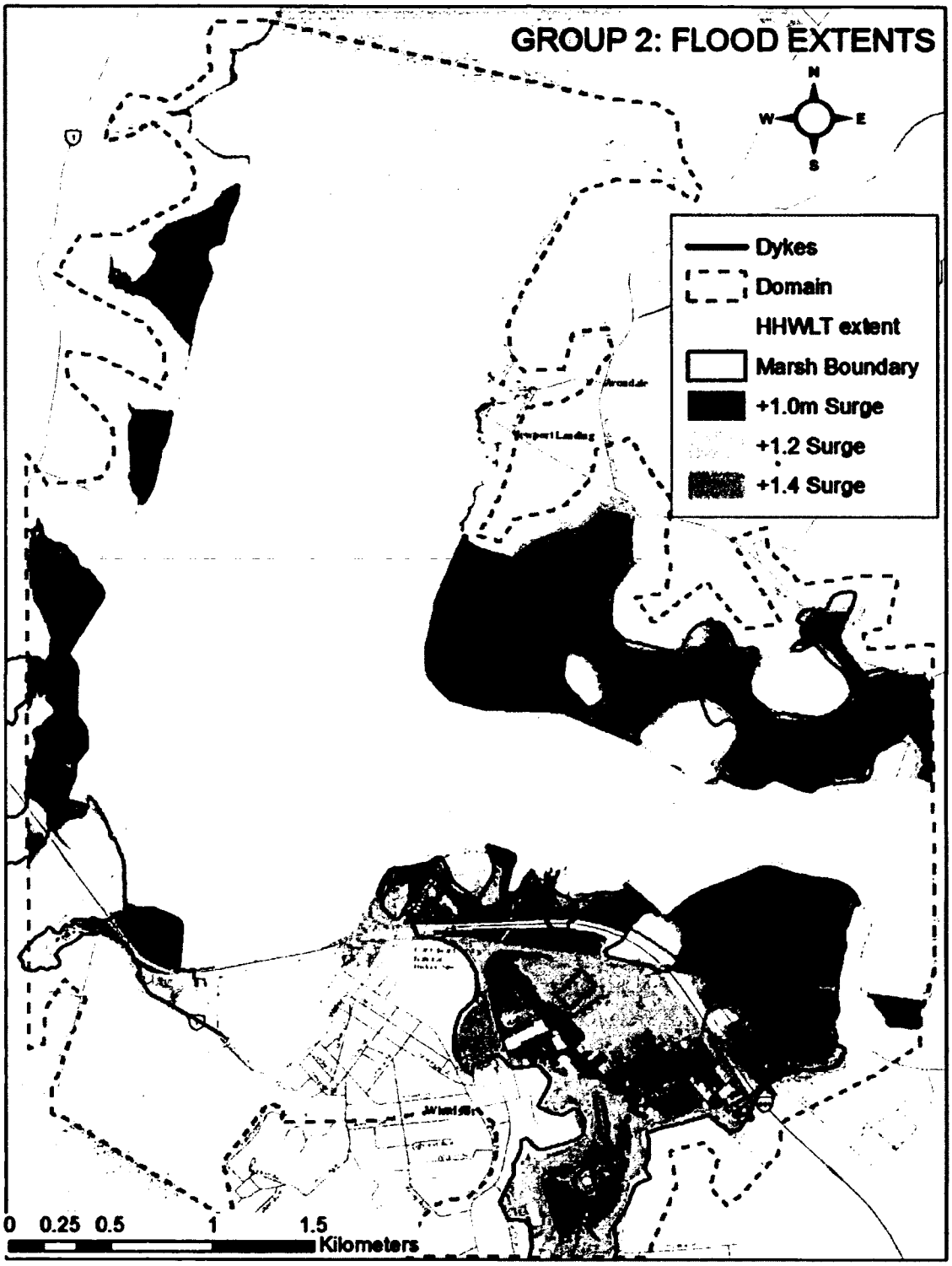

Figure 34: Group 2 Maximum Flood Extents. Incorporated marsh boundaries are shown in red.

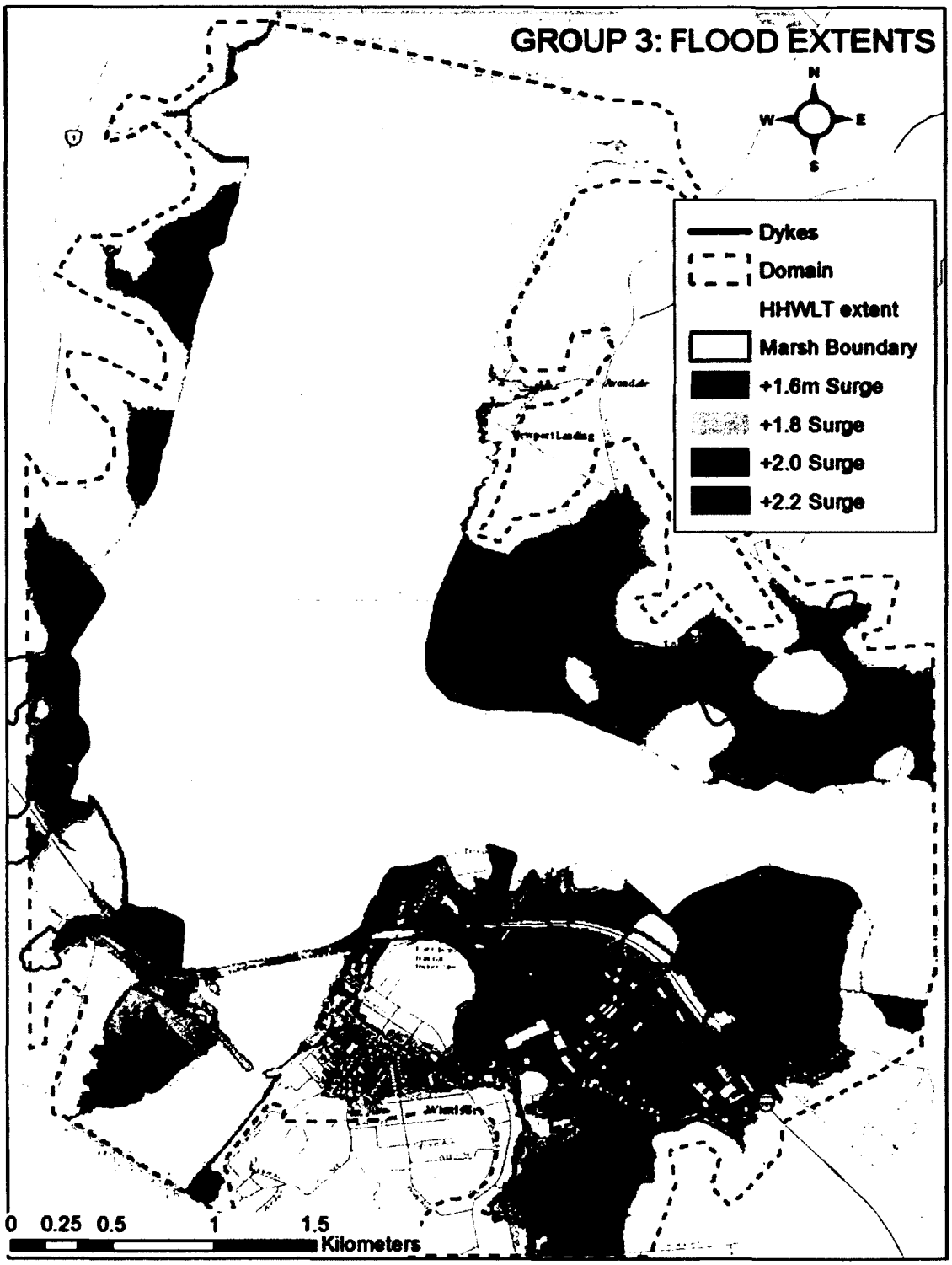

Figure 35: Group 3 Maximum Flood Extents. Incorporated marsh boundaries are shown in red.

4.1.2 Speed of Flood Onset and Drainage

Figure 36 shows the time it takes for water to reach a maximum level in different parts of the Tregothic Marsh. Times are reported in decimal hours relative to the start of the boundary condition time series (see Figure 24). The overtopping of dykes occurs

Figure 36: Time to Maximum Water Level relative to simulation start

around 29 (29:00) hours and continues until about 31.5 (31:30) hours but the maximum water levels on the inside of the highway are not reached until 32 to 33 hours and flooding does not spread across the rail bed until 34 hours, about 2.5 hours after dyke overtopping has stopped and the tide is receding. Speed of onset is different across the area depending on man-made and natural obstructions. However, the onset in the simulations is confined to a single tidal cycle and drainage begins with low tide.

Figures 37-39 show the flood extent vs. time based on 5 minute outputs from the simulation in raster catalogs (see sections 3.1.3 and 3.2). The general pattern across all simulations is rapid inundation (1-3 hours to peak extent) during the high tide storm surge and then a gradual drainage until the end of the simulation. However, the maximum extent does not indicate that flooding stops spreading (Figure 37). There are increases in flooded area during high tides after the initial flood. This is because water backs up behind the aboiteaux structures and floods previously drained areas. The shape of the tidal curve (water level time series) has important drainage implications as it is asymmetrical whereas it takes longer for the tide to exit the estuary than it does to flood (Dupont et al, 2005). It is during low tide that flood water would drain from the area, so the time it takes for the tide to exit controls the amount of time for drainage. Soil infiltration and evaporation values were not considered in the simulations but it is known that soils in dykelands are heavy clay which impedes drainage. Some conclusions can be drawn about the drainage rate. For group 1, much of the water seems to be trapped and draining very slowly. The fields in the dykelands are sloped as to route water into drainage ditches but the drainage rate through the aboiteaux may be very slow. This has

implications for areas with high runoff coefficients (such as paved areas) as water would remain trapped and may need to be drained artificially. In group 2 and 3 simulations, drainage through the aboiteaux is occurring; however, reaching the flood extents shown in group 1 would likely take several days (a rough estimate is 3-5 days) provided there is no blockage or failure of the culverts/aboiteaux. These drainage rates are comparable to the Truro dykelands after a flood (Ken Carroll, Personal Communication, 2011).

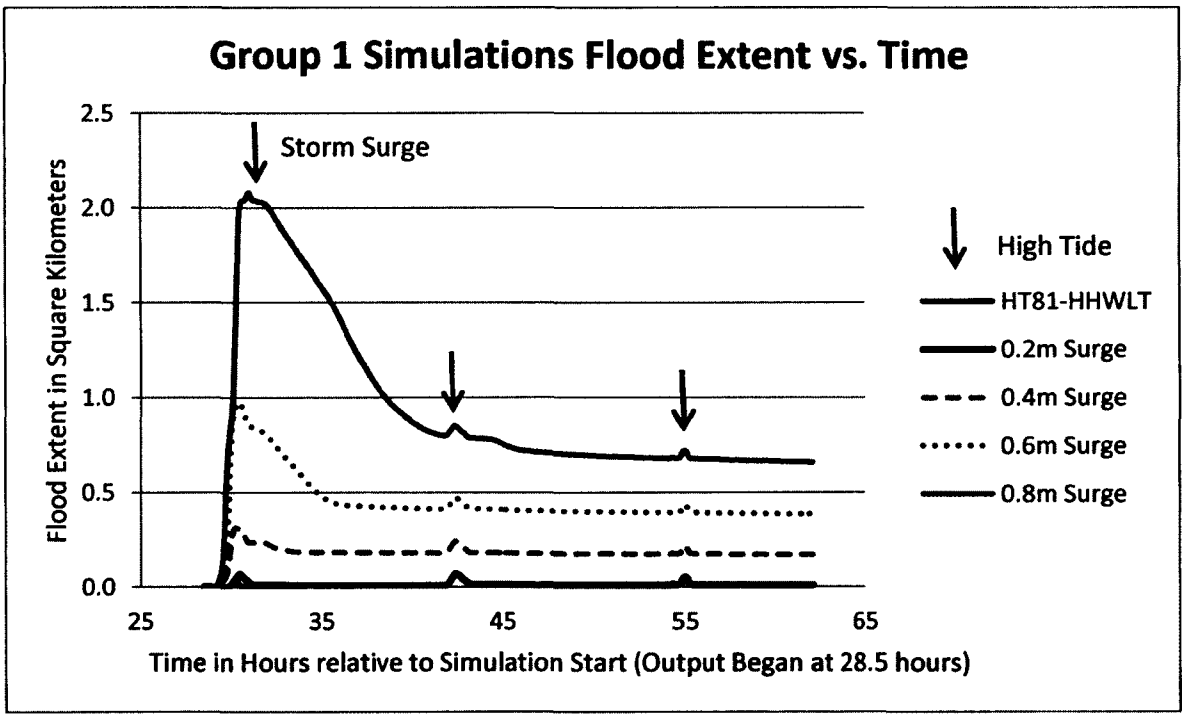

Figure 37: Flood extent over the dyke for group 1 simulations

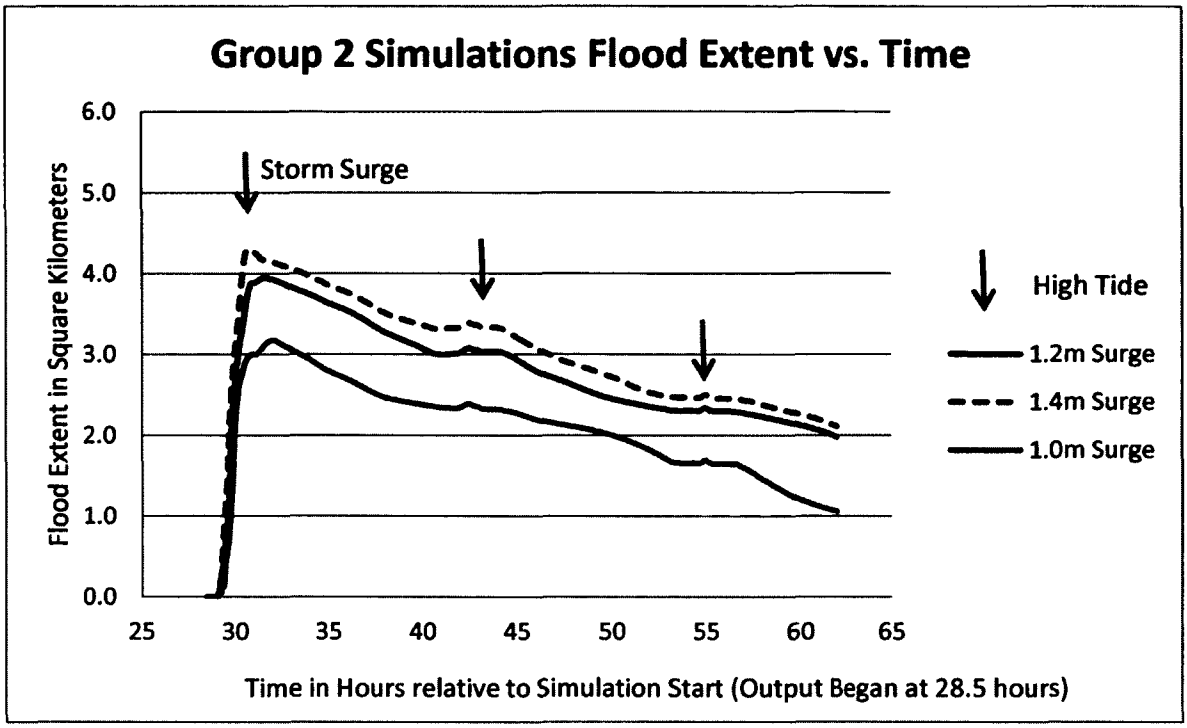

Figure 38: Flood extent over the dyke for group 2 simulations

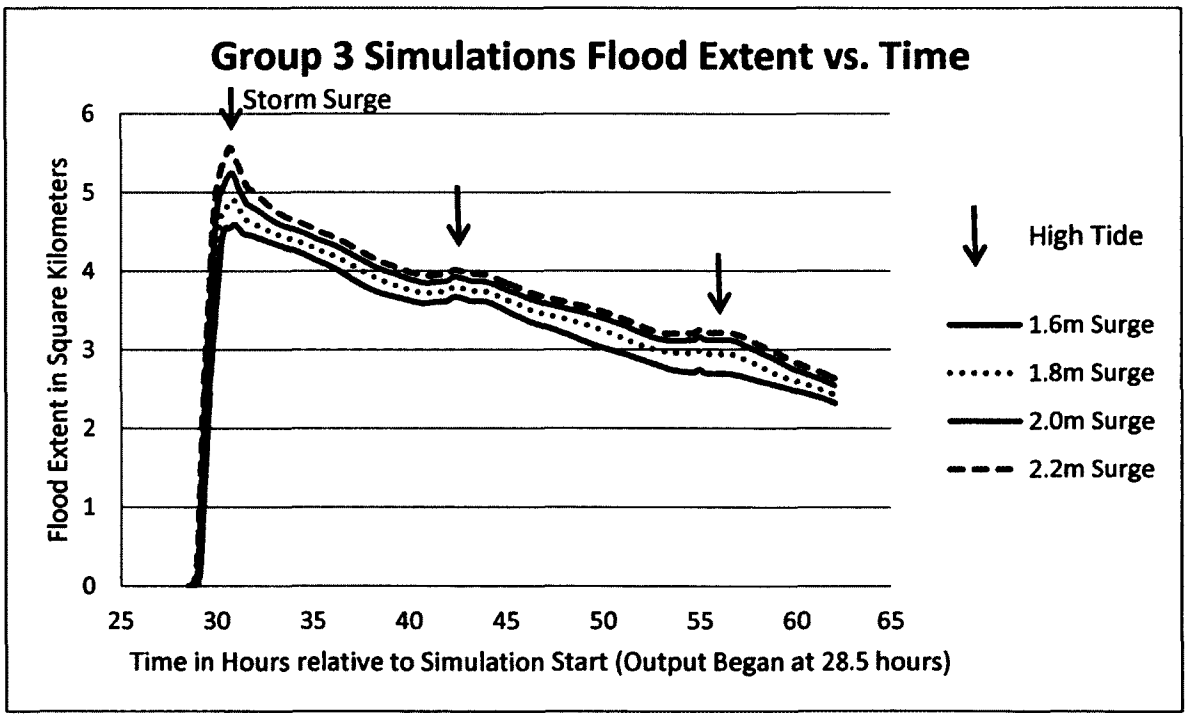

Figure 39: Flood extent over the dyke for group 3 simulations

4.2 Depths/Water Levels

TUFLOW was set up with a wet/dry depth of 0.01m, meaning that any cell with a water depth of 1cm would be considered flooded. It is important to discover which areas have flood depths representing higher levels of hazard as greater depths are known to cause greater damage to buildings and harm to people (Xia et al., 2011; HR Wallingford et al., 2006; Scawthorn et al., 2006).

Table 7 shows the proportion of maximum water depth of flooded area over the dykes. As the maximum water level rises, and more dyke segments overtop, the proportion of high (>2m) depth flood areas increases.

Scenario (Maximum Water Level)	Area of Maximum Depth <1m	1-2m	>2m
8.1m	99.7%	0.3%	0%
8.3m (+0.2m Surge)	99.1%	0.9%	0%
8.5m (+0.4m)	95.78%	2.47%	1.75%
8.7m (+0.6m)	75.27%	21.72%	3.01%
8.9m (+0.8m)	72.02%	11.73%	16.25%
9.1m (+1.0m)	23.94%	35.03%	40.77%
9.3m (+1.2m)	19.13%	19.30%	61.41%
9.5m (+1.4m)	14.19%	22.86%	62.76%
9.7m (+1.6m)	12.57%	19.07%	68.15%
9.9m (+1.8m)	11.83%	14.08%	73.77%
10.1m (+2.0m)	12.65%	11.45%	75.68%
10.3m (+2.2m)	9.72%	13.04%	77.12%

Table 7: Proportion of Water Depth Over Dyke.

Group 1 simulations are of low depth flooding in primarily agricultural areas (<1m). The low depths are not necessarily areas of low hazard, as there are combinations of velocity and depth that are hazardous to cars and people within this range (see section 4.4). Highway 101 separates areas of deep flooding on the seaward side from medium to low

depths of flooding (Figure 40). Between the maximum water levels of 8.9, 9.1 and 9.3m there are large increases in high flood depth areas. This is largely due to agricultural lands and creeks filling up with water (Figure 41). Depths of flooding above 2m are considered to be extremely hazardous to most people (HR Wallingford et al., 2006; Xia et al., 2011). After the 9.3m (1.2m storm surge) scenario, the water depth on the landward side of Highway 101 begins to rise to hazardous levels. At 10.3m (2.2m storm surge), the majority of Tregothic Marsh and the inundated areas of the Town of Windsor have flooding of over 2m depth (Figure 42).

As the flood wave travels across the terrain, water level decays due to roughness and obstacles such as roads and buildings. Figure 43 shows the distribution of maximum flooding values per building on the surface of the Tregothic Marsh and the Town of Windsor. It can be seen that most of the maximum flood depths are between 1 and 3m with a maximum mean depth of flooding (around buildings) of 4.37m and mean depth of 1.37m (Figure 43).

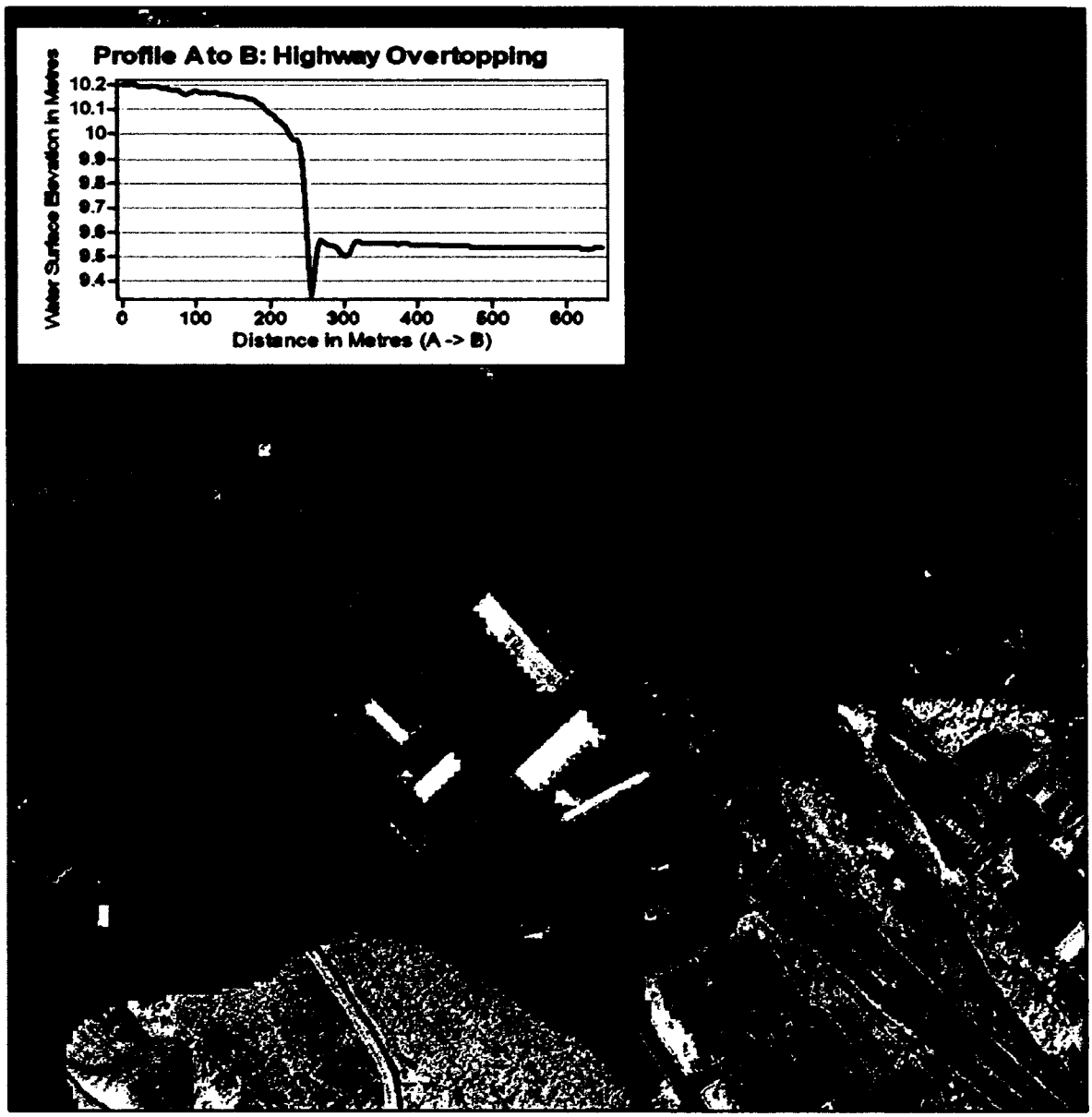

Figure 40: Effect of Highway 101 on flood depths. Green areas are flooded.

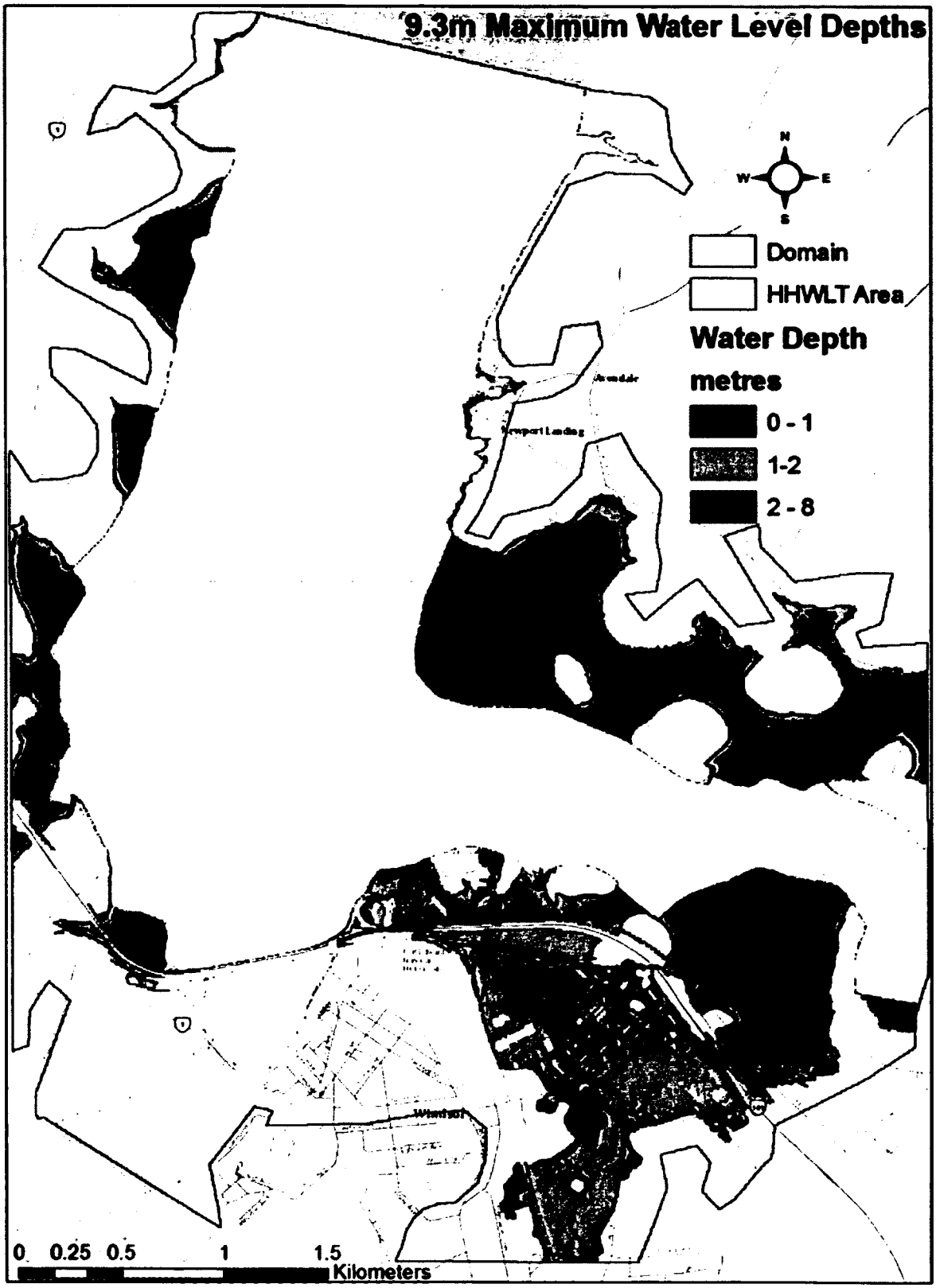

Figure 41: 9.3m Scenario (1.0m storm surge) maximum water depth

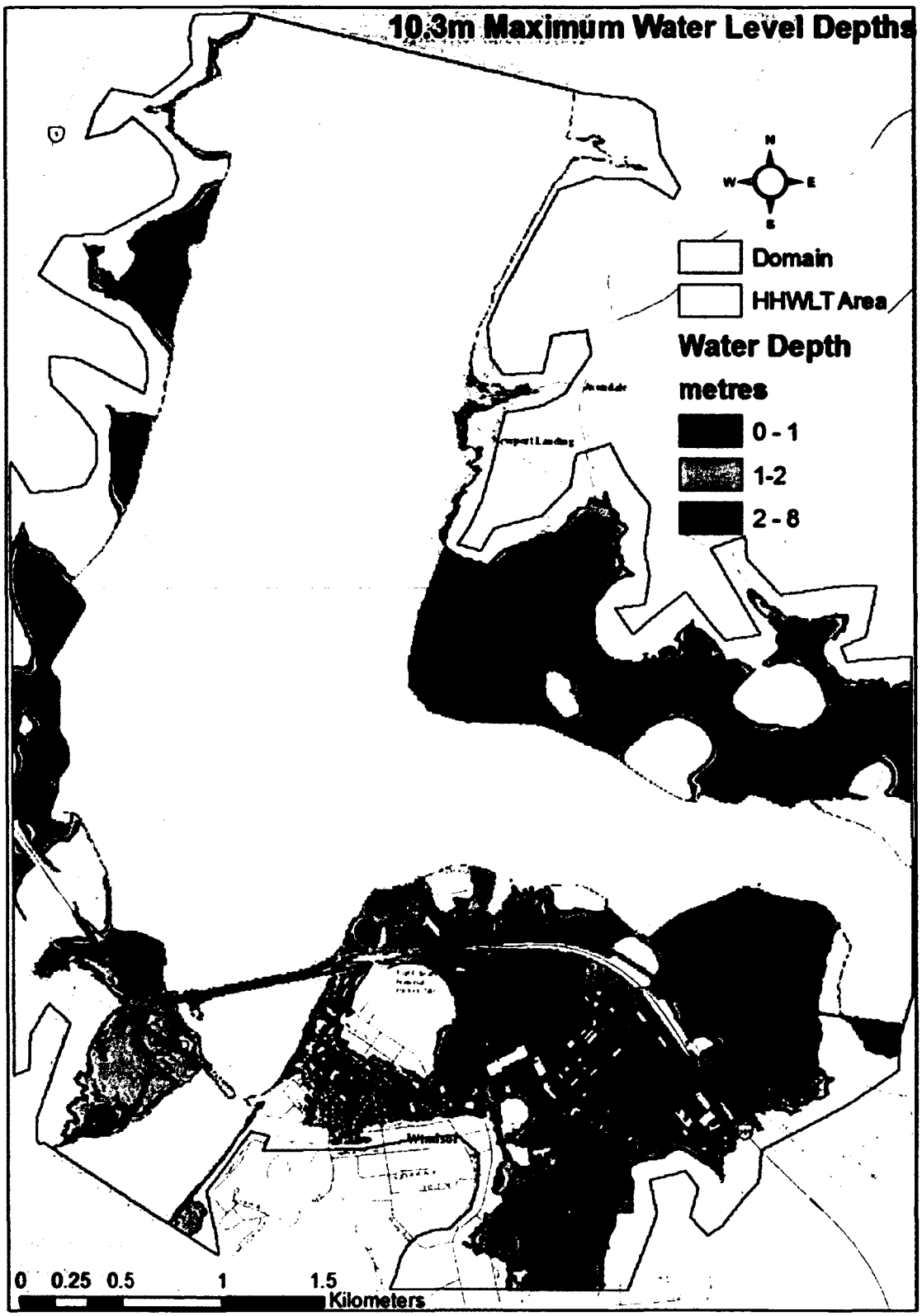

Figure 42: 10.3m maximum water level (2.2m storm surge) scenario maximum depths

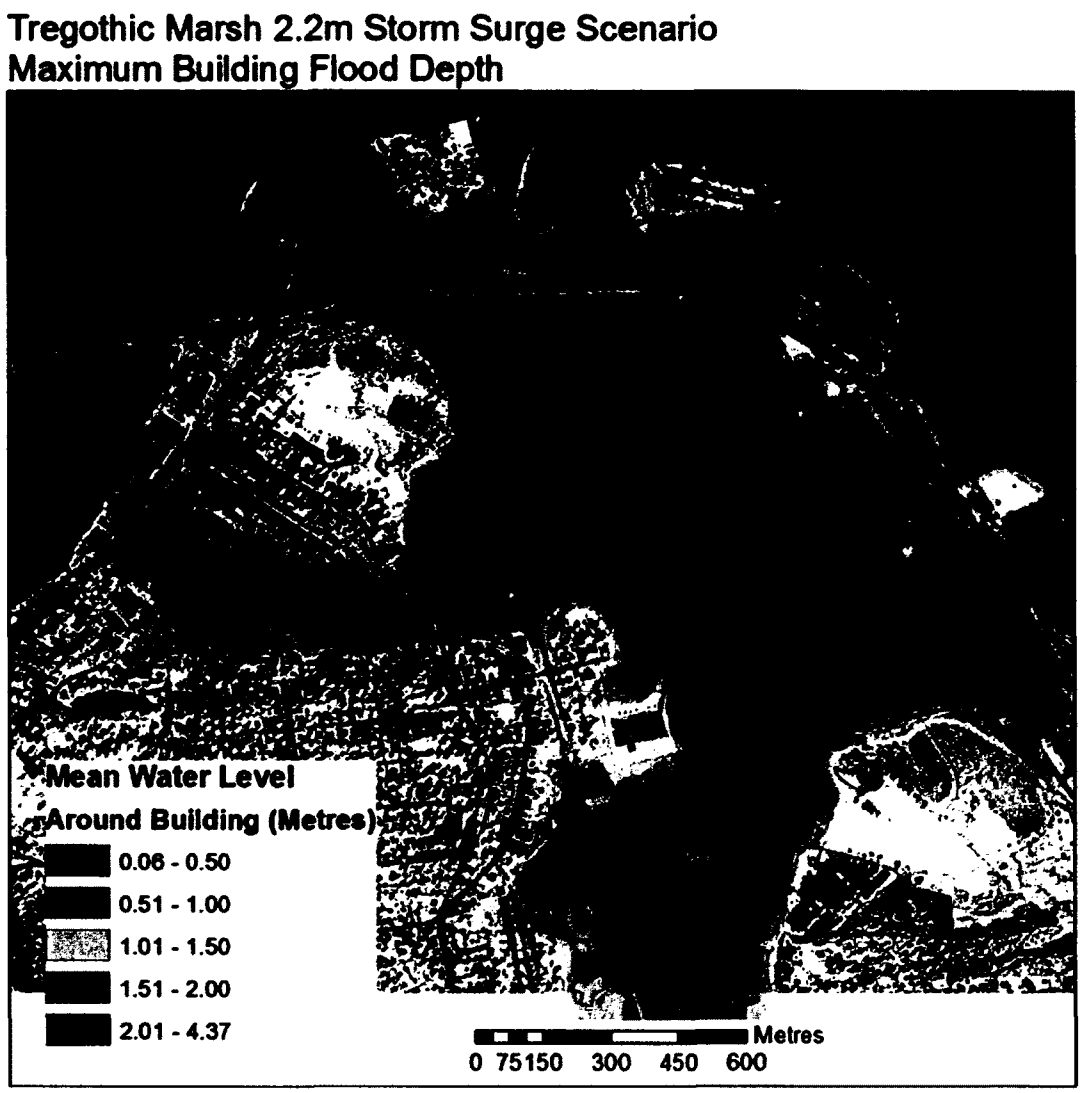

Figure 43: Distribution of Building Flood Depths 10.3m maximum water level 2.2m storm surge scenario

4.3 Velocities

There are a number of possible hazards relating to high velocities in the study area (Figure 44). All of these hazards exist with the larger extent (group 3) scenarios as highways and dykes are overtopped and buildings are exposed to flood waters. Group 2 simulations have less urban flooding and road overtopping. But flow still proceeds through creeks and through the overpass at high velocities and volumes. Group 1

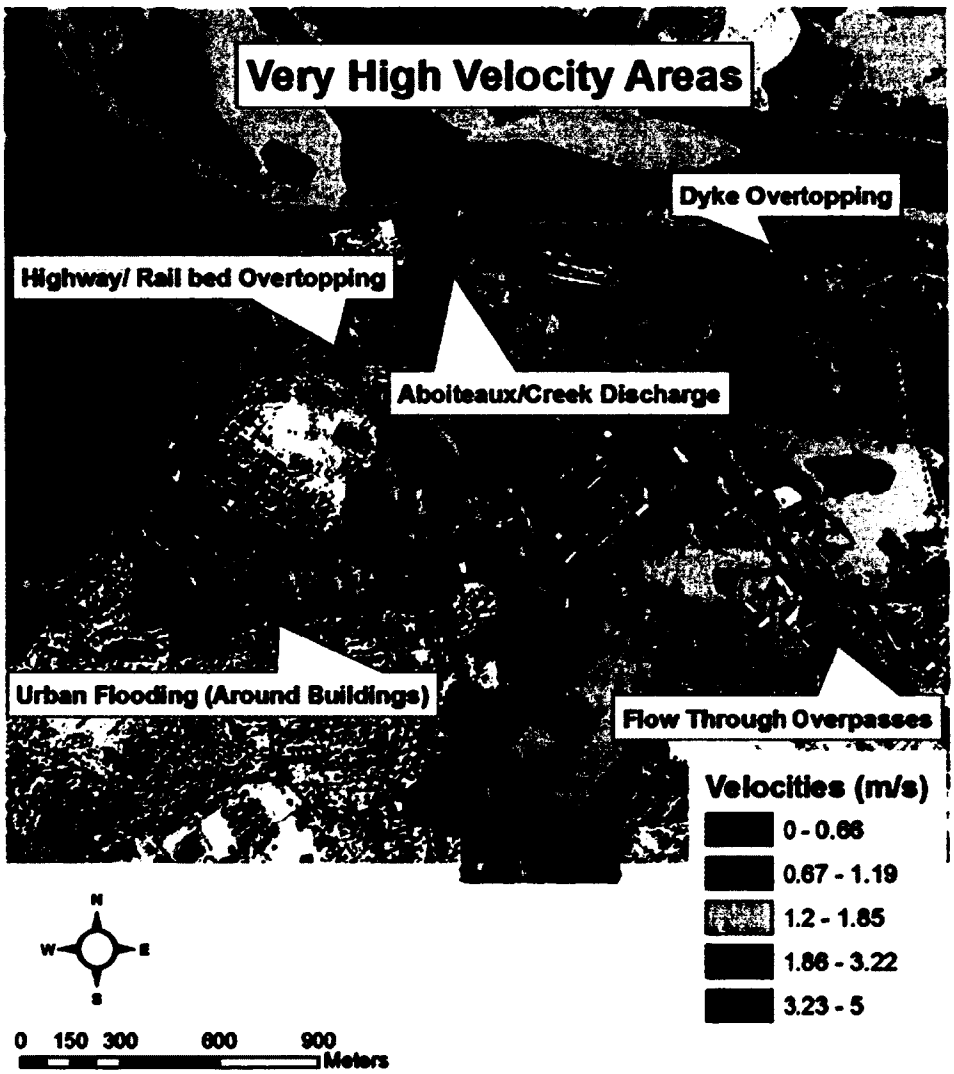

Figure 44: Velocity Hazards 2.2m Storm Surge (10.3m Water Level) Scenario.

simulations do not result in overtopping of roads or flow through overpasses. However, dyke overtopping does occur as does increased flow through culverts, creeks and aboiteaux. These high velocities would induce serious erosion of the dykes which may result in their failure if these velocities are sustained (Ryan Mulligan Personal Communication, 2012).

TUFLOW is able to represent important physical processes, such as flow constriction, which increases velocities through an overpass. As water overtops a dyke, TUFLOW simulates a transition in flow type (subcritical to supercritical flow) through a surge in water velocity on the landward section of the dyke (Figure 45). Lin et al., (2006) and Hunter et al., (2008) showed that it is essential for a model to include this feature for the simulation of dyke overtopping and complex flows. Velocities through urban areas are increased by flows channeled between buildings.

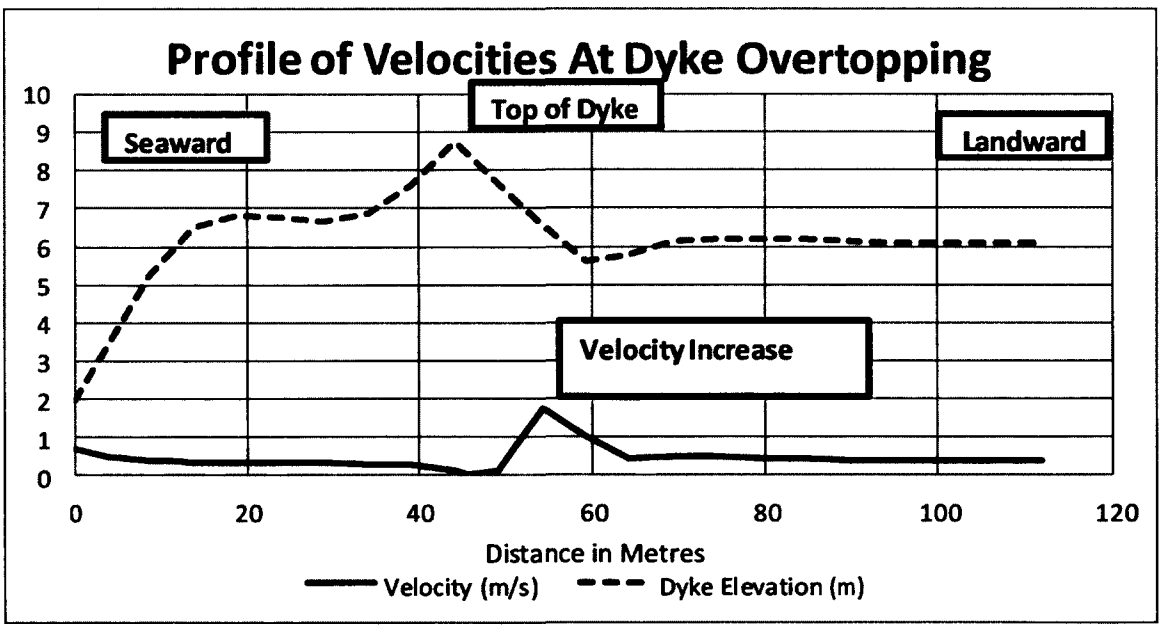

Figure 45: Velocity increase from supercritical flow during dyke overtopping as velocity increases on the landward slope of the dyke and decreases as depth increases on the flat landward areas.

4.4 Velocity Depth Product Hazard.

Datasets have been output showing flood hazard to people based on the methodology presented in HR Wallingford et al., (2006) for all ensemble scenarios. Figure 46 shows the maximum calculated hazard to people in the study area for the 2.2m storm surge scenario. The categories of danger are based on studies which investigated the combinations of velocity and depth which pose a danger to people (HR Wallingford et al., 2006). "Danger for some" indicates danger for children in areas of shallow flowing or deep standing water, "danger for most" outlines areas with deep fast flowing water and "danger for all" delineates fast flowing water that is dangerous for all adults regardless of height and weight (HR Wallingford et al., 2006). It can be seen that at this water level, most of the flooded areas pose a severe danger to people as well as built-up areas within the Town of Windsor. Previous estimates of drainage (section 4.1.2) have shown that dangerous depths of water would persist after the initial flood subsides for possibly days depending on the magnitude of the flood.

Figure 47 shows how the velocity depth product (V x D) may be used to delineate the route most water would take in a flood (floodway). In Figure 47 it can be seen that, by themselves, neither velocity nor depth results reveal a clear floodway, but taken together they show a clear path water may take after overtopping the dyke.

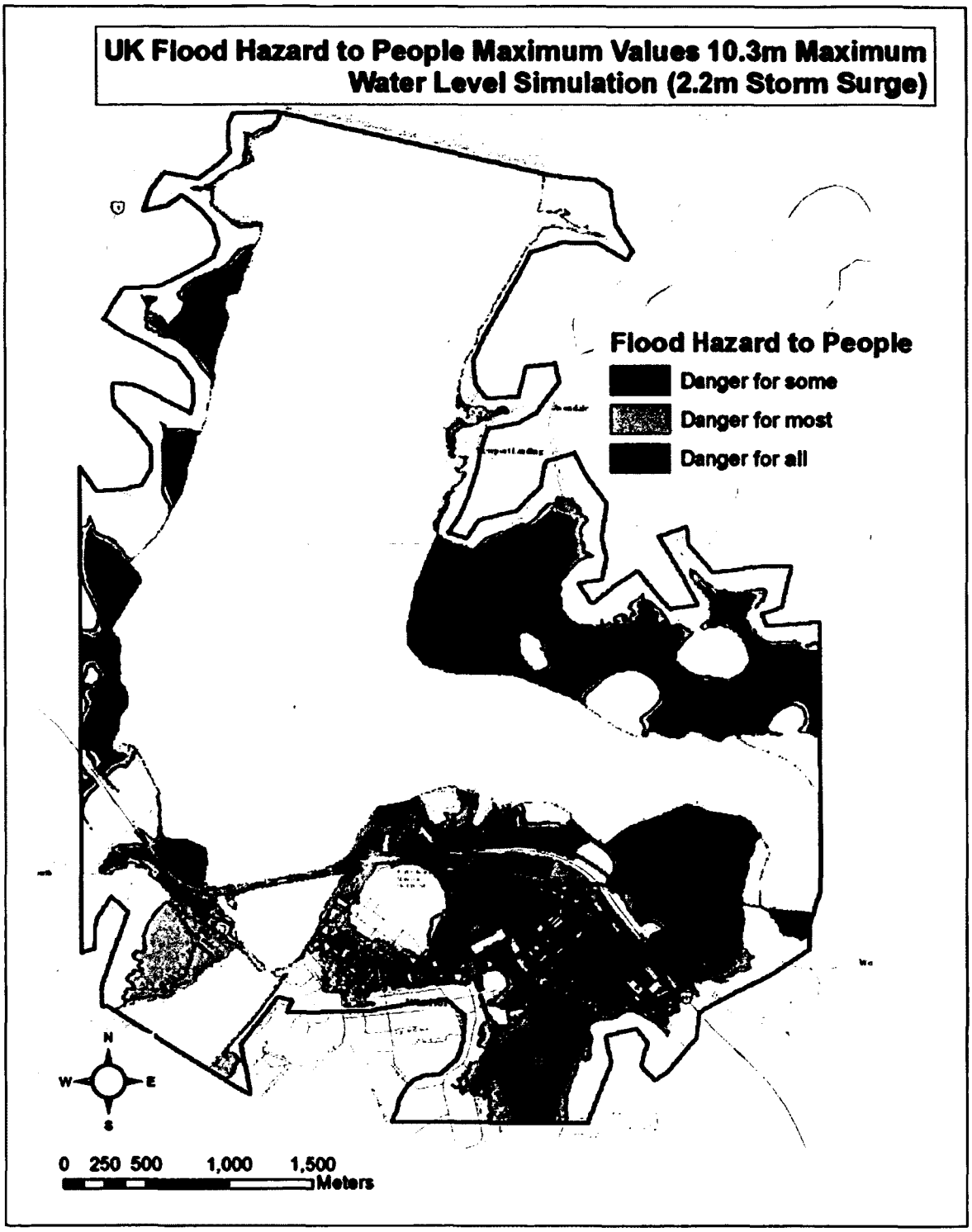

Figure 46: Flood hazard to people based on the criteria in H.R. Wallingford et al., (2006)

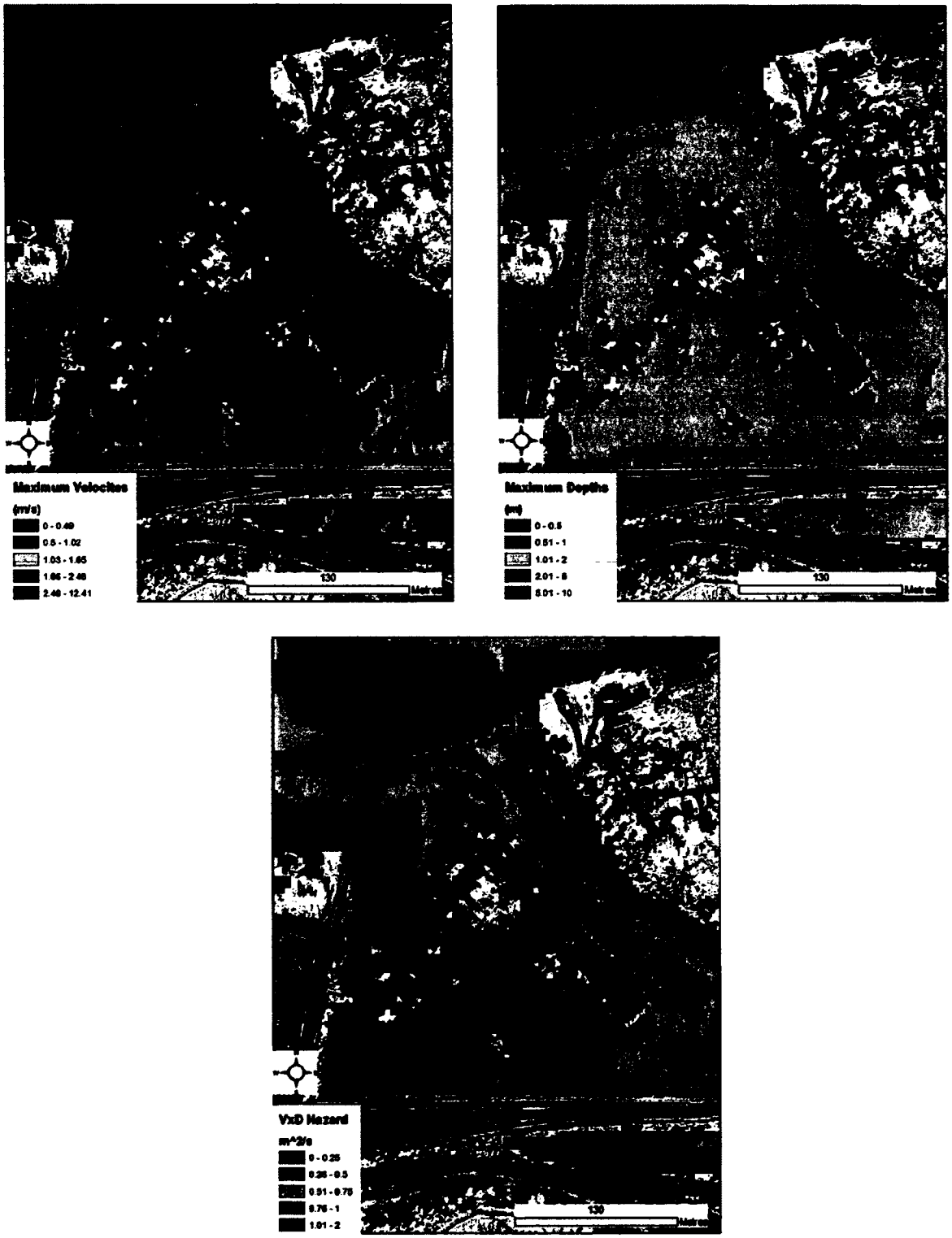

Figure 47: 1.0m Storm Surge (9.1m maximum water level) Simulation Results, Left: Maximum Depth, Center: Maximum Velocity, Right: Velocity Depth Product

4.5 Special Cases

4.5.1 Dyke Breach

Up to now, reported results have been based on the representation of infrastructure elements such as dykes, roads and houses as solid features which do not change throughout a simulation. In the higher water level scenarios, the stresses on man-made barriers increase which in turn raises their chance of failure (Kamphuis, 2010). Without a proper engineering assessment, it is not possible to say how and when during a flood event these features would fail. This thesis deals with changes in the drainage of marsh bodies if a breach were to occur during a 2.2m storm surge (10.3m maximum

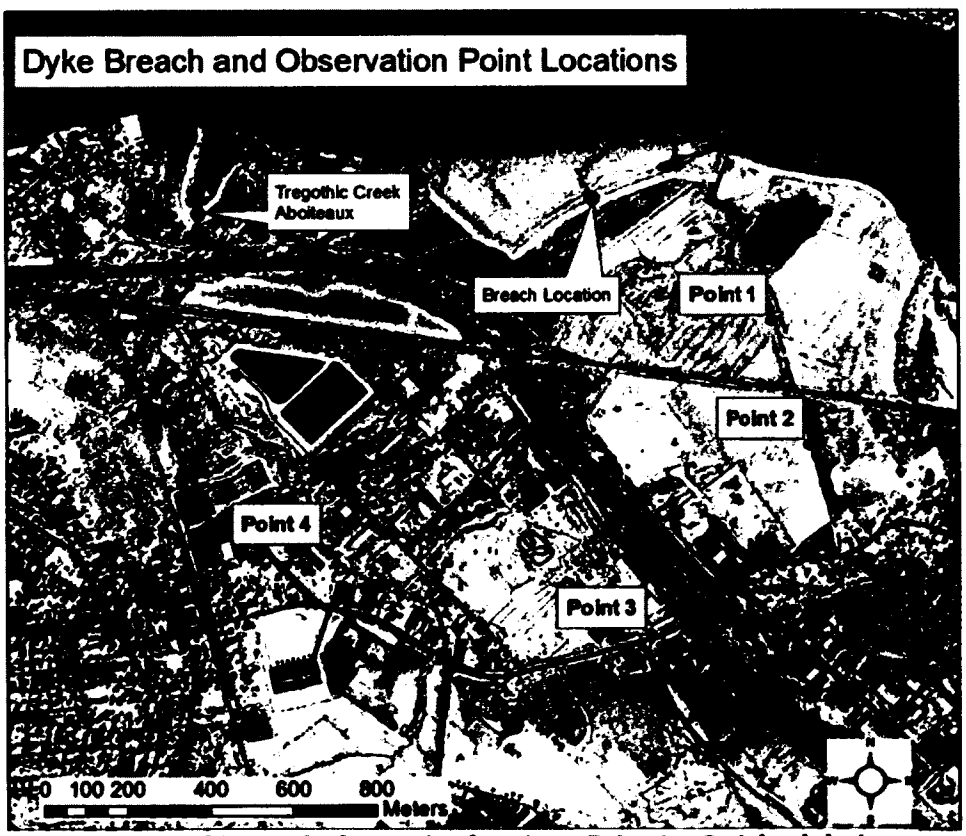

Figure 48: Tregothic marsh observation locations: Point 1 – On inland drainage channel towards aboiteaux. Point 2- On drainage channel landward of rail line. Point 3- Along road by overpass. Point 4- Within Tregothic Creek

water level). A hypothetical breach scenario was set up for a 20m section of a dyke on the Tregothic marsh (Figure 48). Approximately one hour after the flood overtops the dyke, this section is reduced in elevation (to approximate erosion) to that of the high marsh (5.9m) and a channel is created to the existing creek on the marsh surface (Figure 48). This simulation assumes that all other features will be unaltered throughout the flood. Figures 49 to 52 graph the effects of the dyke breach on drainage in different sections of the Tregothic Marsh when compared with the non-breach storm surge scenario (Figure 48 shows the sample points). Initial flood depths are mostly unaffected as the breach occurs as the tide is peaking and dyke overtopping has taken place. The drainage effects are not limited to the eastern section of the marsh, as the drainage of Tregothic creek is also affected. It can be seen that the breach allows additional drainage during low tide thus lowering water levels more quickly throughout the domain. Subsequent high tides flood the marsh surface after the storm surge through the breach, but not enough water enters the marsh to flood much beyond the rail bed (Figure 52). This is assuming that subsequent high tides are higher high water tides which come up to the dyke, smaller tides may only flood the low marsh and water flowing through this breach would only flood areas just inside the dyke. There are a large number of possible dyke breaching scenarios which could occur.

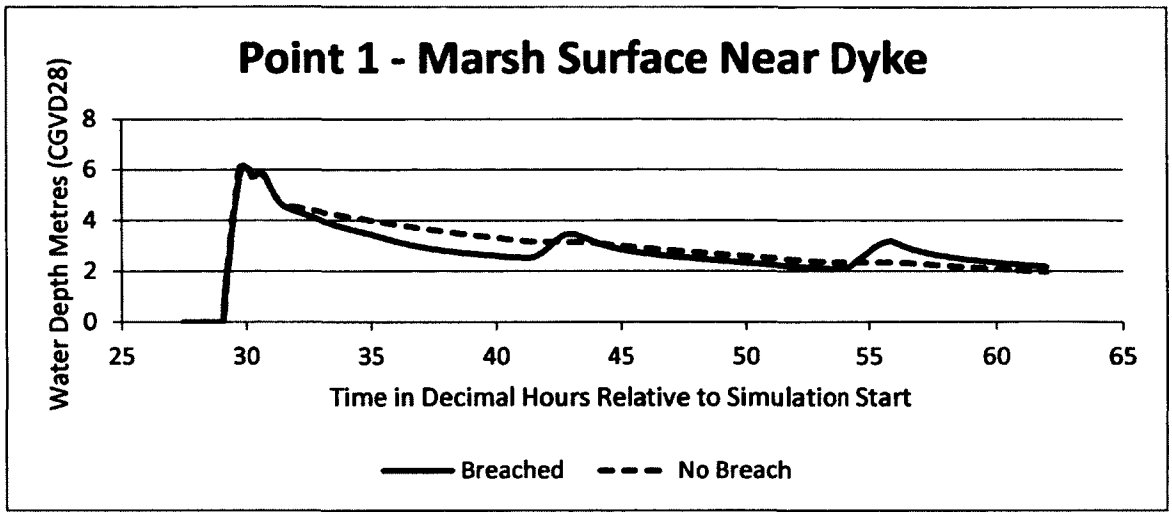

Figure 49: Point 1 simulated water depths through time breached and non-breached scenarios

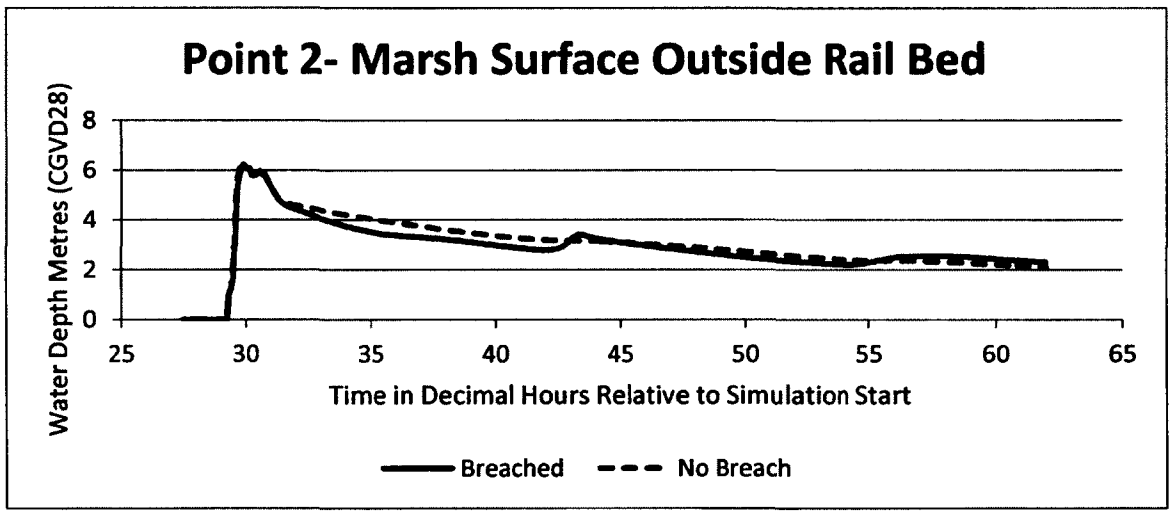

Figure 50: Point 2 simulated water depths through time breached and non-breached scenarios

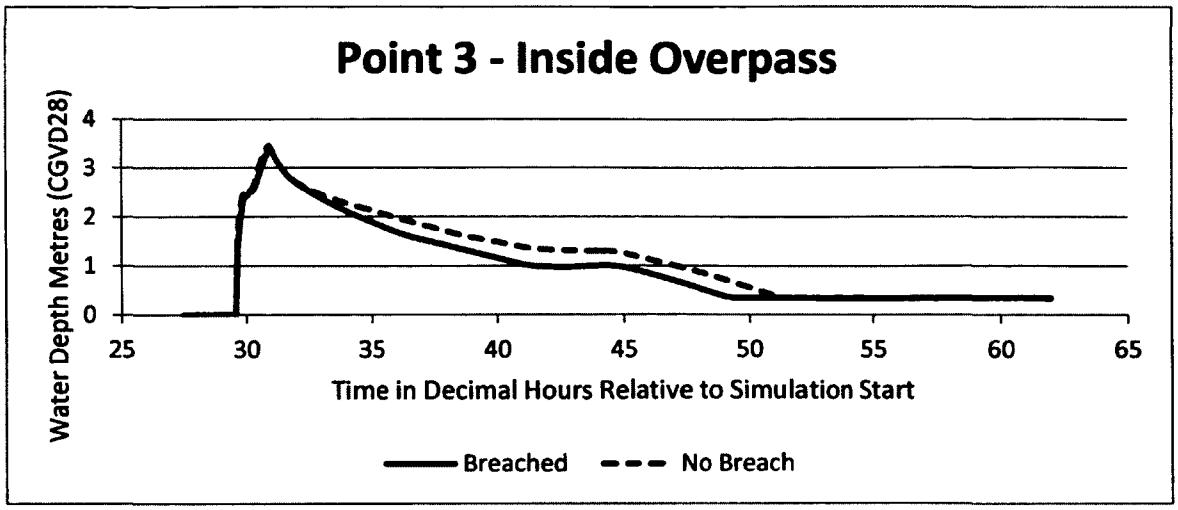

Figure 51: Point 3 simulated water depths through time breached and non-breached scenarios

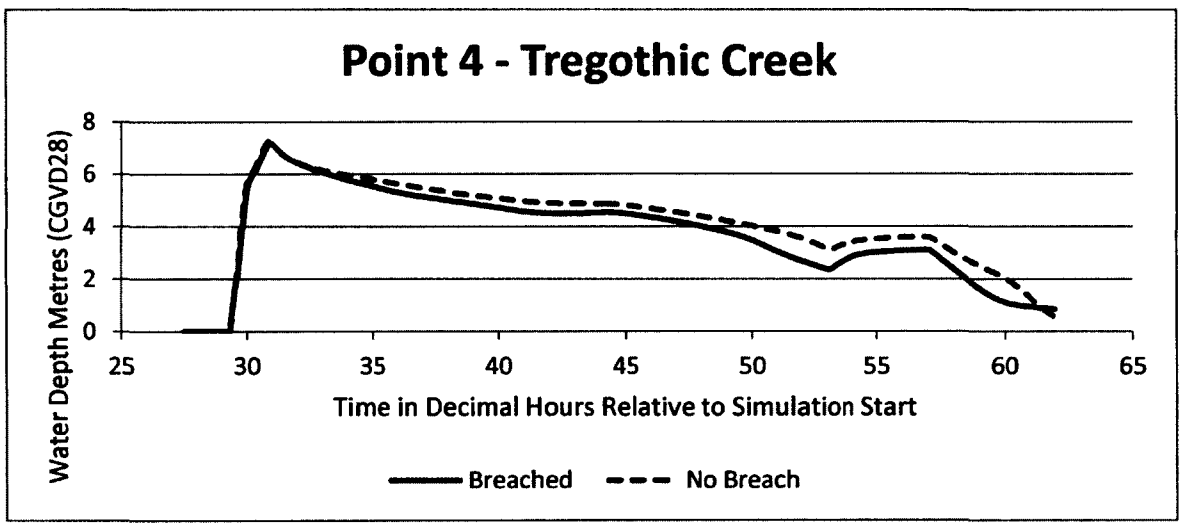

Figure 52: Point 4 simulated water depths through time breached and non-breached scenarios

4.5.2 Partial Blockage

Figure 53 shows the partial blockage of the Tregothic Creek culvert under Wentworth Rd. This example illustrates the type of events which can change hazard predictions, especially in a large storm event where flooding may carry drainage obstructing debris. Also, in the winter; it is common for ice and snow to obstruct culverts and aboiteaux which in itself can cause flooding. This scenario explored what may happen if Tregothic Creek aboiteaux were fully blocked during a 2.2m storm surge (Figure 48). This aboiteaux is the larger of the two outlets in the Tregothic marsh and drains the Tregothic Creek system.

Figures 54 to 57 show that in the event of blockage, drainage rates would be severely reduced and hazardous water levels would remain in flooded areas for much longer periods of time. The smaller aboiteaux seems to be designed to handle much less flow

Figure 53: Tregothic Creek culvert blocked with debris after a large rainfall event. Photo: Michael Fedak, July 2011

than the Tregothic Creek system and even in areas close to this feature, much of the drainage after the initial flood depends on water exiting through the Tregothic Creek system as Figure 54 shows. Inside of the highway, near the overpass both blocked and unblocked drainage happen more quickly (Figure 56). However, below a depth of 0.5m water becomes trapped in this area. Figure 57, in particular, shows the importance of Tregothic Creek for draining an urban area as with blockage, flood waters would remain above 2m while the unblocked aboiteaux results in a drop in depth to below 0.5m.

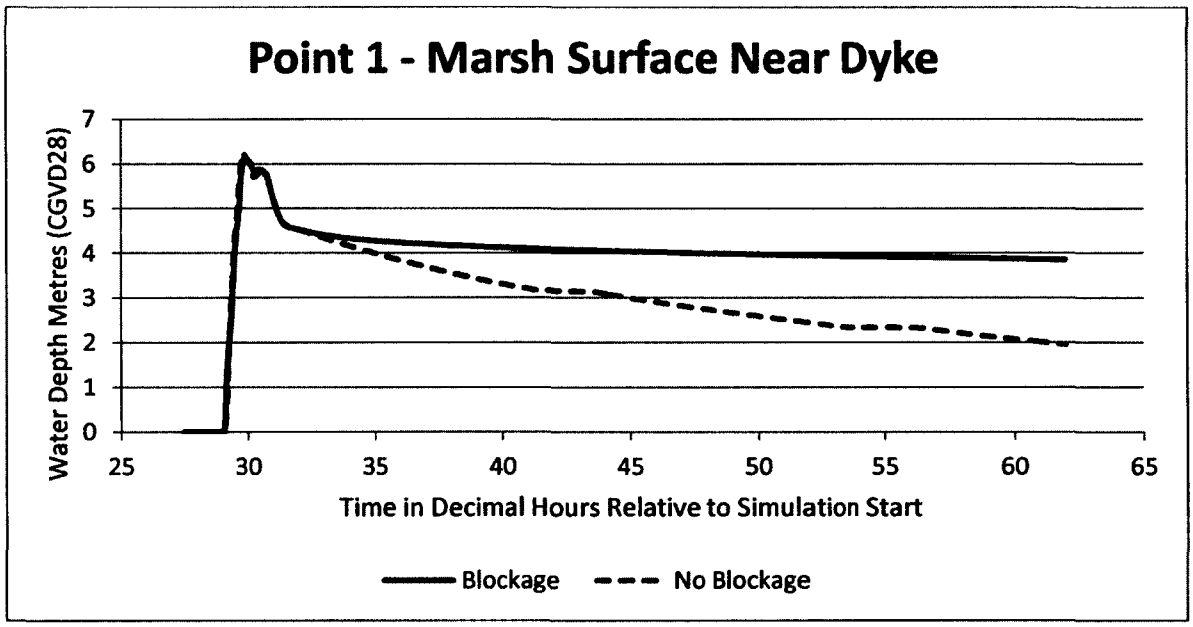

Figure 54: Point 1 Water Depth Results for Partial Blockage Scenario

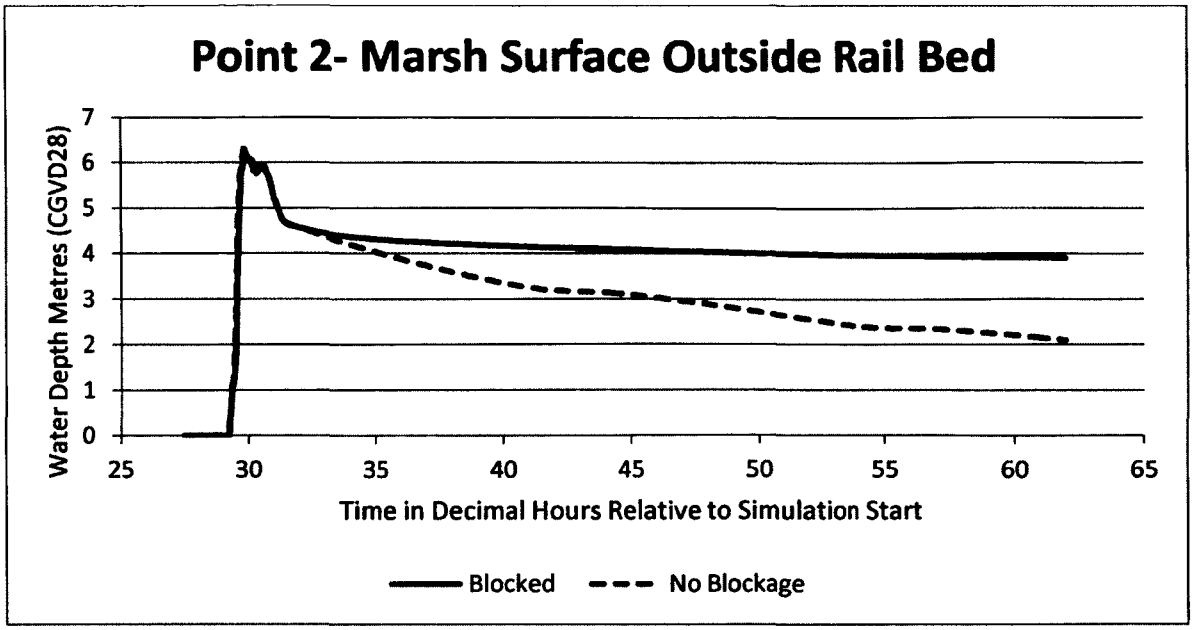

Figure 55: Point 2 Water Depth Results for Partial Blockage Scenario

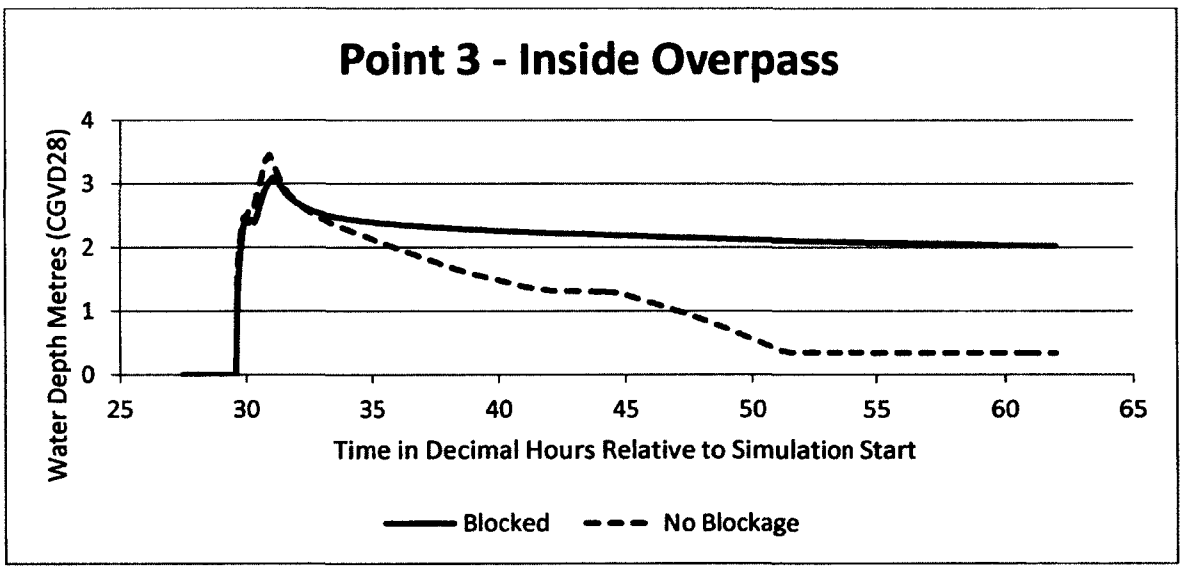

Figure 56: Point 3 Water Depth Results for Partial Blockage Scenario

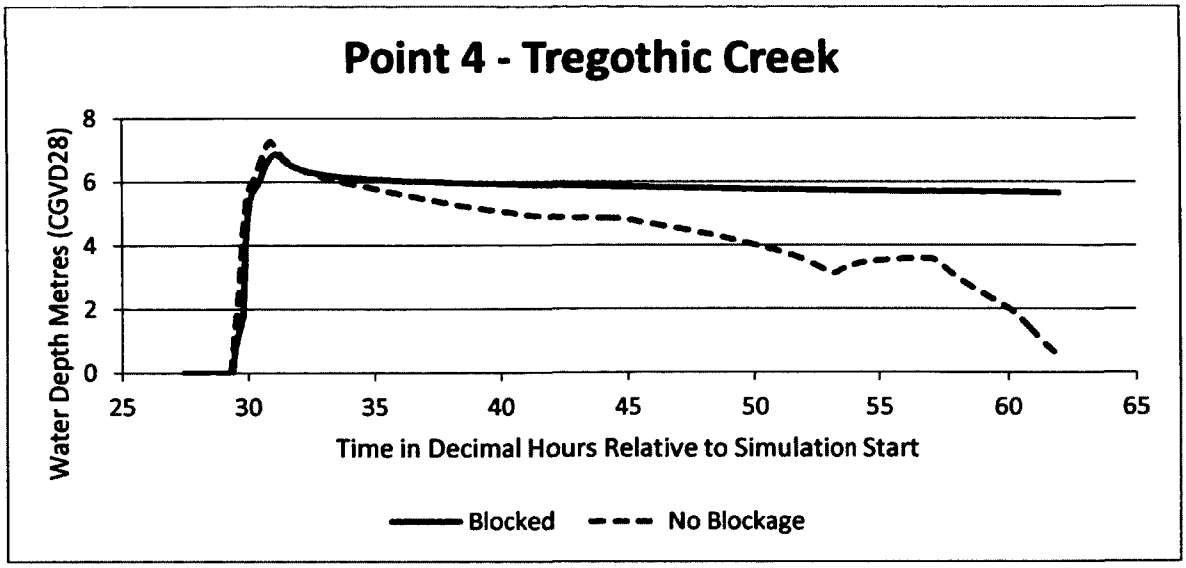

Figure 57: Point 4 Water Depth Results for Partial Blockage Scenario

CHAPTER 5: Discussion

5.1 Natural and Man-made Flood Controls

The results showed that different factors control the flooding of the dykelands depending on the land uses present and the level of the surge. At the highest levels of surge (over 1.6m) the effects of flood defences and infrastructure decline and topography is the primary controller of flood variables. The importance of properly representing the dykes for modelling flows in the Upper Bay of Fundy was alluded to by Dupont et al, (2005). Substantial differences in inundation extents were recorded in all areas due to relatively small increases in water level over the dyke. For example, an increase of 0.20m in storm surge level between 8.9 and 9.1m maximum water levels, increased flood extents by 1.124km^2 (Table 5).

In primarily agricultural marsh bodies (Elderkin and Newport Town Marsh bodies) flooding was controlled by depth of water over the dykes as well as surface roughness, topography and channels. Other studies that have investigated flooding of coastal rural areas noted that topography and roughness were important controllers of flood extent (Bates, et al., 2005; Krupka, 2009). The inertial terms in the Saint Venant equations are considered important here to represent the spreading of the wave across the relatively flat agricultural areas (Lhomme et al, 2008; Krupka, 2009). The effects of inertia are also important in modeling the velocity of flows passing over the dyke and meeting higher elevation areas (Bates, et al, 2006; Hunter, et al, 2008).

The Tregothic marsh body is mostly urbanized. Here, flood extents were controlled by man-made structures and the effects of topography. Bates et al, (2006) alluded to the importance of properly representing small features, such as culverts, in order to predict flooding accurately. The decrease in influence of man-made features and channels with increases in flood depth is reported by Nicholas & Mitchell, (2003). They observed that in shallow floods and in the initial stages of large floods, flows tend to be constrained by existing channels but as depth increases, water spreads according to the floodplain slope. The effects of buildings on flow velocities was observed as flood waters spreading into the town were channelled along roads and between buildings thus increasing velocities (Chen, 2007).

There is an ongoing debate as to the representation of buildings in flood modelling. The misrepresentation of buildings leads to the underestimation of flood extent and velocity (Chen, 2007; Haile, 2005; Kelman, 2002). In this research, buildings were represented as solid features so that velocities between buildings and hazard to people would not be underestimated. However, as Kelman, (2002) and Friedland, (2009) argue, buildings can allow water flow through them or outright fail in a storm event, thus changing flow velocities and introducing additional hazards by creating debris.

In addition to the variables of extent, depth, and velocity examined independently, the velocity depth product approach shows some promise for assessing flood hazard. This approach allows floodway/flood fringe mapping similar to that carried out under the Flood Damage Reduction Program (FDRP) in Truro and mentioned in the Municipal Government Act (MGA) statements of provincial interest.

5.2 Comparison of GIS Based and Hydrodynamic Flood Simulation.

A GIS based planar flood model can only output extents of flooding depths. Maximum depth scenarios were compared between outputs from TUFLOW and flood rasters produced using the 'lake flood' algorithm in SAGA GIS which preserves flow paths (Figure 1). To prepare the DEM for use in SAGA GIS, known culverts and overpasses were incorporated into the LiDAR DEM by lowering DEM elevations to that of the bottom of the feature since LiDAR can only represent surface features. Flood paths are lost without lowering surface elevations to that of underground surfaces (Webster et al, 2011). Finally, extents and depths were obtained and compared in overlapping areas. Figures 58 and 59 show extent results from TUFLOW overlapped with results from SAGA GIS 2.0 (SAGA GIS Development Team, 2011). SAGA was used instead of ArcGIS because it is an actively supported and freely available (open source) software. SAGA GIS contains an easy to use version of the 'lake flood' algorithm, while ArcGIS requires a license which can be costly.

In the 9.1m maximum water level scenario, the SAGA GIS extent is much greater than the TUFLOW extent in the Tregothic marsh body. This is likely because TUFLOW is able to include the effect of flow obstructions (the highway) and surface roughness in its calculations, while the GIS method just finds all connected cells and does not account for volumes of water coming over the dyke. The agreement between TUFLOW and the GIS method is much better in the Newport Town and Elderkin marsh bodies which are mostly farmland with little infrastructure. In Figure 59, the 10.3m maximum water level (2.2m storm surge) output from TUFLOW is compared with the SAGA GIS raster output. The

extents of the two outputs are much more similar than at 9.1m. Nearing this level, TUFLOW flood extents seem to grow much more slowly and flooding was constrained by higher elevation areas.

Figures 60 and 61 show the maximum depths obtained from TUFLOW compared with the maximum depths from SAGA GIS in areas where the two datasets overlap. In Figure 60 the GIS is reporting a greater depth in the Tregothic and Newport Town marsh bodies than TUFLOW. The two are similar within the channel and on the Elderkin Marsh. A 2.2m storm surge seems to be able to flood that marsh body with little to no obstruction from the dykes. The Tregothic and Newport Town results are likely due to the effect of the higher dykes and, in the case of Tregothic, due to the highway acting as an obstruction. In Figure 61 depths between the two results are similar except in the area of the Tregothic marsh landward of Highway 101 where the GIS depth is slightly higher and around Lake Pisiquid. These differences can again be attributed to infrastructure obstructing water flow.

Overall, if the goal of the modelling exercise is to determine potential maximum extents and depths of flooding, the GIS based method seems to work well on small flat marshes bounded by higher ground that will not flood. If the study area were larger, it is likely that even in the 10.3m maximum water level simulation the GIS results would have shown a much greater flood extent. It would have shown the flood continuing to spread south along Tregothic Creek where there are hydraulic structures or infrastructure that may be overtopped. TUFLOW is able to represent the physical processes that control flow and thus offer a more physically based estimate of the flood extent. In terms of potential road

and dyke overtopping locations, both the GIS and hydrodynamic model are able to show areas of low elevation which would potentially be flooded at different water levels. However, because the hydrodynamic model is based on the movement of water volumes, the level of overtopping predicted by the two methods is different. A hydrodynamic model can show areas of more imminent risk. These two modelling techniques may be viewed as complimentary. The GIS based method offering a quick way to delineate potential flow paths which may be used to inform hydrodynamic modelling (provided the DEM is of sufficiently high resolution). Comparison between the two datasets can also show areas where friction and other physical processes are important.

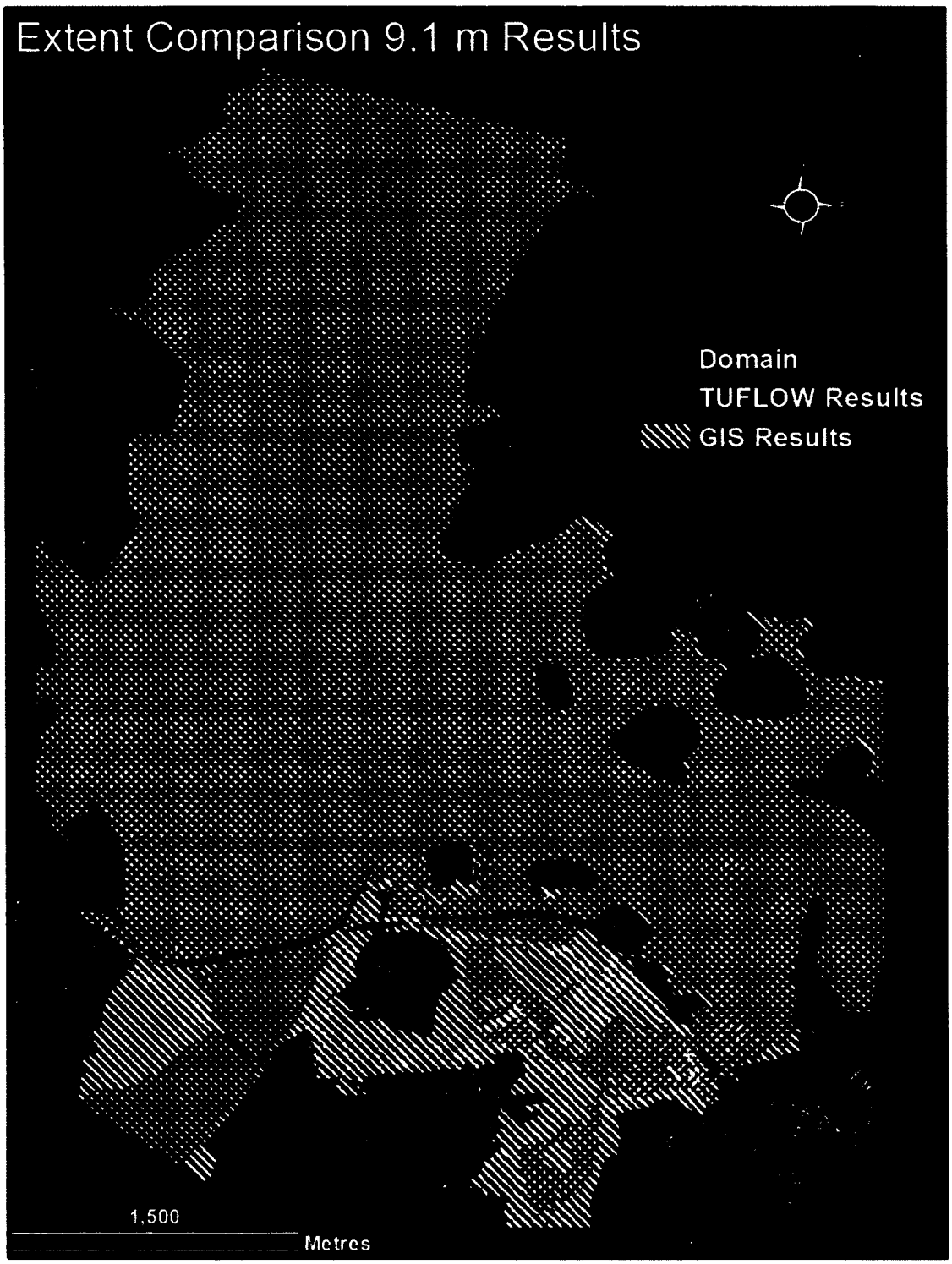

Figure 58: 9.1m Maximum Water Level (1.0m storm surge) Extent Comparison

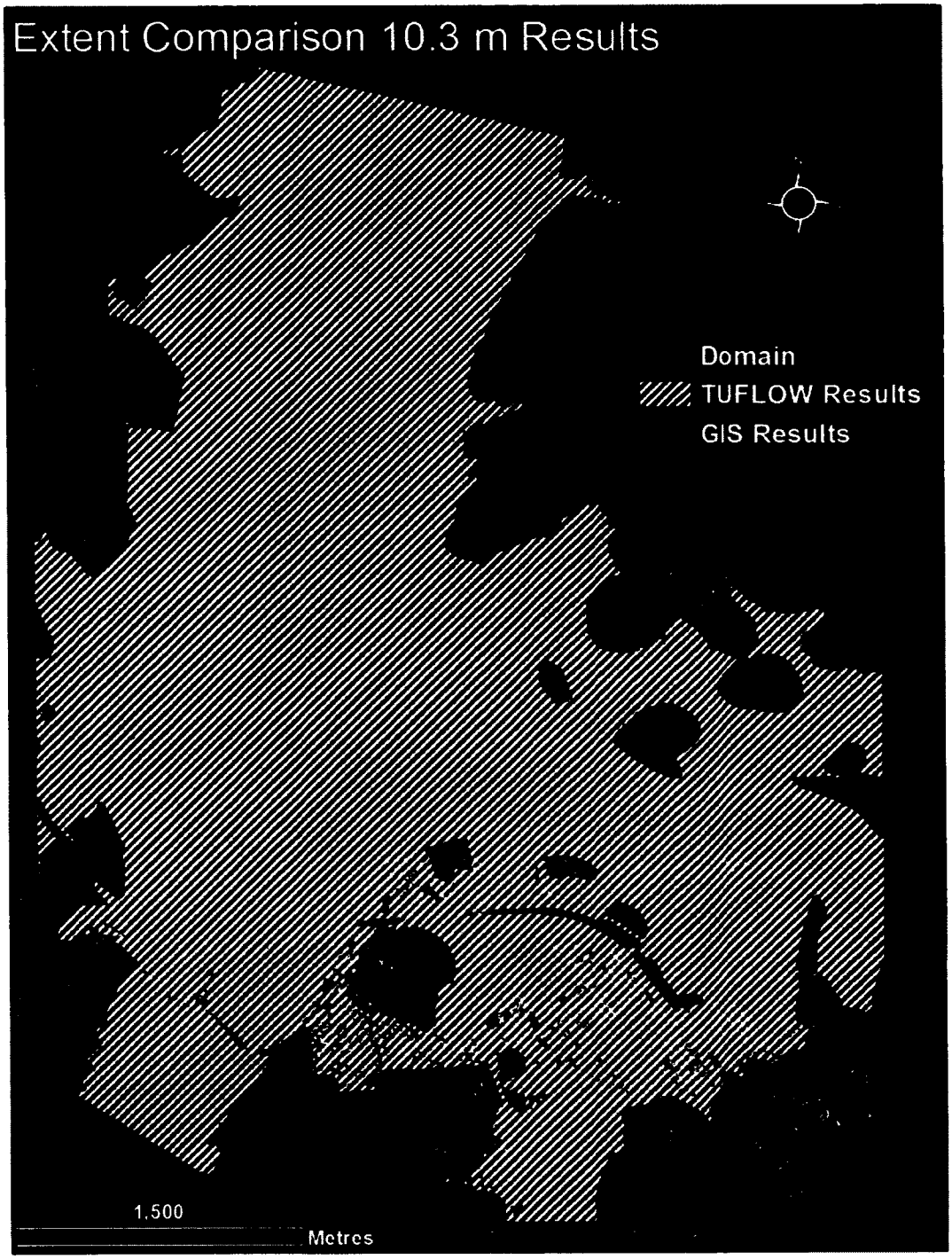

Figure 59: 10.3m Maximum Water Level (2.2m storm surge) Extent Comparison

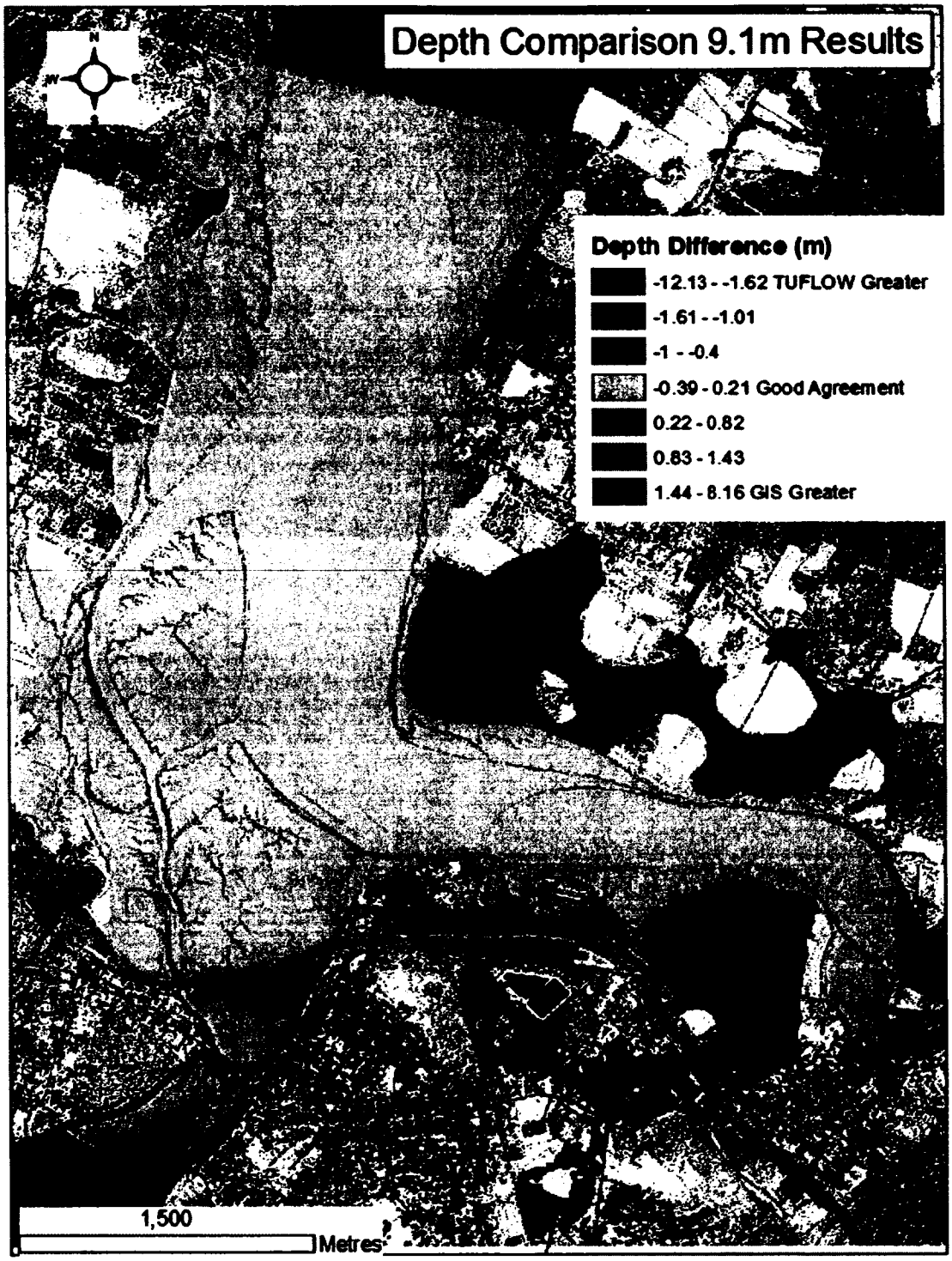

Figure 60: Depth Comparison 9.1m Metre Maximum Water Level (1.0m Storm Surge)

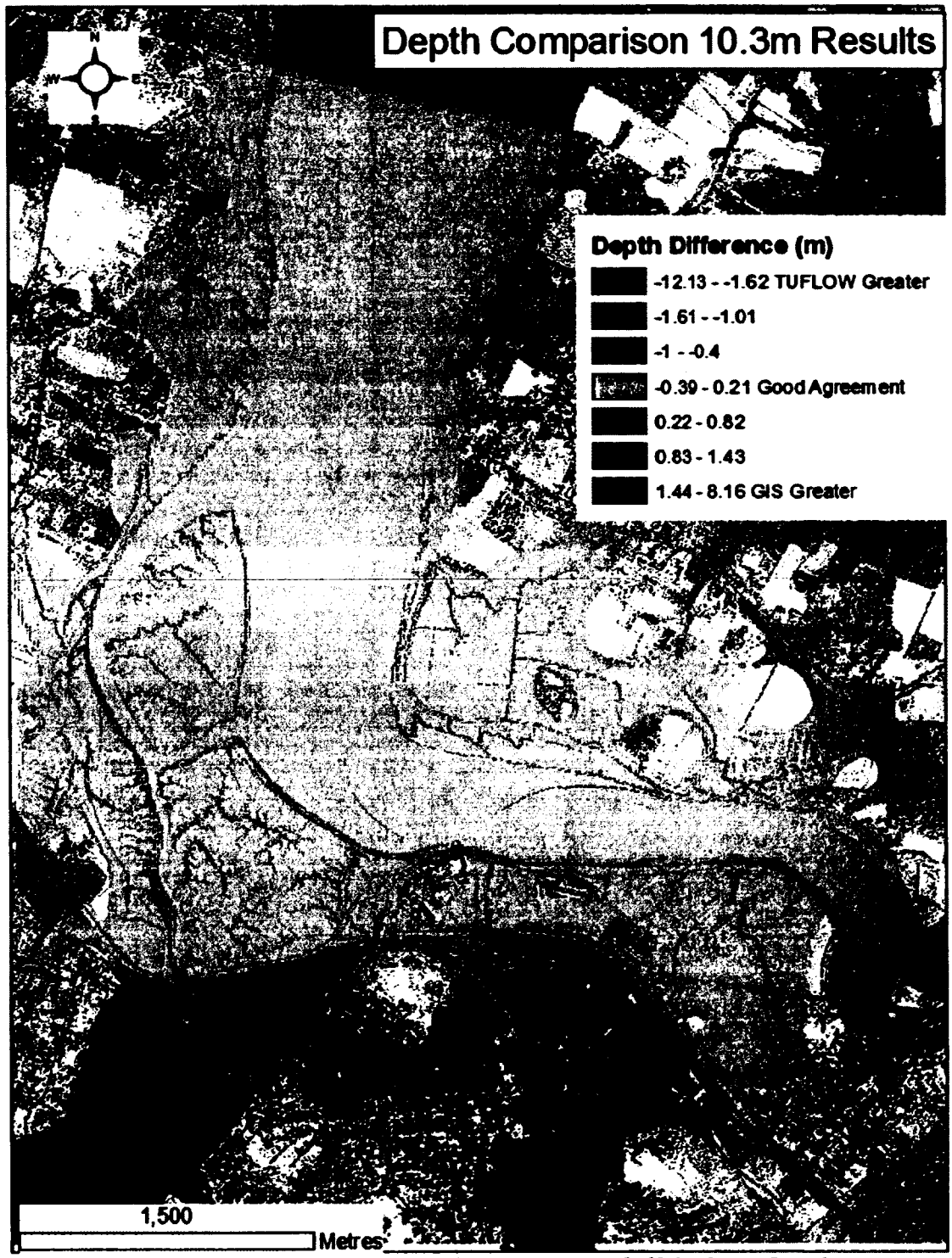

Figure 61: Depth Comparison 10.3m Metre Maximum Water Level (2.2m Storm Surge)

5.3 Sources of Uncertainty and Error

In this section sources of uncertainty in the results are discussed as well the importance of features in controlling the degree of flood hazard. Model sensitivity to changing parameters was tested to see what impact changing parameters would have on final results.

Table 8 shows the source, pathway and receptor components considered in this study. Table 8 is divided into modelled and non-modelled uncertainties. The non-modelled uncertainties were discussed during the preparation of this study and are anticipated to have some importance for determining flood hazard. Future studies may consider these variables.

	Sources	Pathways	Receptors
Modelled	• Sea Level • Storm Surge • Tides • Lake water levels (Lake Pisiquid)	• Differences in flood attenuation due to surface roughness. • Overtopping of dykes and infrastructure. • Floodplain • Channels • Culverts, overpasses, and gates. Including culvert blockages.	• Properties • Infrastructure • Buildings
Non-Modelled	• Rainfall • River/Creek Flow • Wind/short period wind driven waves	• Groundwater Flows • Wave attenuation by plants • Pumping stations and storm sewers. • Dyke breaching and other structural failures • Ice effects • Morphological Changes. • Evaporation/Infiltration values.	• Social vulnerability and resilience • Ecosystems • Development of Floodplains.

Table 8: Modelled and non-modelled uncertainties in the study area.

5.3.1 Source Uncertainties

It is important to acknowledge that the non-modelled aspects of the system introduce uncertainty into the predictions. Given the sensitivity of the predictions to the timing of high tide, there is uncertainty which impacts potential flood extents, velocities and drainage times. The timing of storm surge is also uncertain. A worst-case scenario

was assumed (in terms of maximum water level) where the peak of the storm surge would be timed to coincide with the peak of high tide. It is entirely possible that a storm surge would happen close to high tide and last for several hours which would cause higher than normal water levels that might impede drainage. Greenberg et al, (in press) pointed out that that the average duration of storm surge along the Atlantic coast is 2.2 hours (but may last for up to 12 hours) but the risk due to flooding depends on the storm surge corresponding with the 1 to 2 hours that the tide is near maximum.

Non-modelled effects will have differing impacts on the uncertainties of the predictions. Adding rainfall would increase water levels, and depending on the intensity, cause flooding independent of the overtopping. The Department of Agriculture was particularly concerned with rainfall-caused flooding and associated river/creek discharge based on their experiences in the Town of Truro where there have been multiple flood events caused by water becoming trapped behind a dyke during high tide. Discharge from the St. Croix River was not included in the model due to lack of data and left this as an open boundary condition. However, the discharge in this river is normally negligible compared to the tide (van Proosdij, 2009). The difference between an open and closed boundary condition was tested at the St. Croix River would make on predictions. An open boundary allows water to flow out of the domain, a closed boundary is a barrier against flow. It was found that a fully closed boundary increased maximum water levels 1 to 5 cm, but had very little effect on channel velocities (<0.01 m/s maximum difference) and tidal phase. Short period wind driven waves can cause flooding and overtopping on their own. This is especially true for exposed coastlines (Cariolet, 2010). However, van Proosdij, (2009)

points out that due to the limited fetch length and time during which the tide is high enough to affect the dykes, these waves tend to be small and would not cause significant flooding on their own. However, these waves do put additional stress on dyke structures which may cause them to weaken or potentially breach (van Proosdij, 2012).

The method used to generate the boundary condition ignores the change in tidal dynamics that would occur with sea level rise and due to a storm surge (Pugh, 2004; Cunge, 2003; Greenberg et al, in press). Due to the dykes, flooding in this area is dependent on the amount of time water is overtopping (or breaching) these defences. Overtopping is most likely to occur during high tide; therefore having a good representation of the tidal curve is important.

5.3.2 Pathway Uncertainties

In the results it has been shown that obstructions to flow, topography, and surface roughness control the path, velocity, and timing of inland flooding. Within the main channel of the Avon River, surface roughness was found to be the most important parameter. Sensitivity testing showed that increasing the channel roughness to values in excess of those recommended for muddy channels significantly altered the shape of the tidal curve. Increased roughness in salt marshes had limited effect on flooding extents and depths. In a HHWLT, the marsh surface is covered by over 5 metres of water so in an overtopping event, the marsh surface will be completely covered before any overtopping takes place. The effects of vegetation decrease with depth, and their interaction with water is improperly represented by a single Manning's n value (Moeller, 2006; Mason et al., 2003).

Seasonal changes were discussed as a significant factor in the performance of pathways. In the winter, surfaces are covered with snow and ice blocks which changes flow characteristics. Surface roughness may be reduced over marsh areas as vegetation is sheared off and snow and ice can block culverts and aboiteaux (Davidson-Arnott et al., 2002). Evaporation and infiltration values would change and this would also change drainage characteristics. The model validation was performed in the spring but extreme water levels in the study area may occur throughout the year. Furthermore, ice in the channel would change flow characteristics.

The condition and characteristics of infrastructure are also an uncertainty. It is not known whether a section of dyke, road or rail-bed would breach under certain conditions but the results show that a dyke breach can change water levels and drainage characteristics throughout a marsh body. Culverts and aboiteaux performance is also uncertain as debris is known to obstruct these features; some seem to be in poor condition which would reduce their capacity or lead to failure (Figures 62 and 63). The locations, characteristics, and conditions of all man-made features in marsh bodies are not known. Buildings are also a source of uncertainty as they impact flow depths and velocities by channelling water. There is ongoing debate around the best way of representing buildings because, in flood situations where the water is deep enough to enter a building; the building will stop behaving like a solid obstacle (Haile, 2005; Kelman, 2002; Chen, 2007).

Figure 62: Damaged Culvert under Tregothic Creek
Photo credit: Michael Fedak, July 2011

Figure 63: Culverts under Highway 101 near Falmouth
Photo credit: Michael Fedak, July 2011

5.3.3 Receptor Uncertainties

Future development of marsh bodies will determine what may be exposed to harm. There are multiple development scenarios which may be considered depending on whether or not the dykelands will continue to be protected agricultural land. The locations of buildings prone to flooding are also an uncertainty. Databases are not updated every time new construction happens. The building polygons dataset used in this study also did not contain all of the structures which may be at risk. Furthermore, estimates of damage to these structures are difficult given the effects that unmodelled variables (wind, rain) may have on building failure. However, this modelling has provided velocities, depths and durations of possible flooding, all of which can be used to estimate damage based on depth damage curves or velocity depth product, provided additional information about building structures is collected.

5.3.4 Errors

Errors in this study are primarily in the representation of features in the model domain and in model parameters. Figure 12 shows the issues with the representation of creeks in the model. This introduces error as the velocities and flow rates in a creek are dependent on the wetted area of a creek. If this wetted area is significantly smaller than the real area, the model will output erroneous velocities. Figures 64 and 65 show the different creek types present in the study area. Inland areas protected by dykes tended to have shallow (1 to 3 m deep) man-made drainage channels as in Figure 64, while on the surface of the salt marshes, there are much wider and deeper natural channels which drain inland areas (Figure 65).

The validation stage (Section 3.3.3) tested the results from the model at 5m resolution versus observed water levels. The creeks in the model were represented as shallower features than in reality which caused simulated values to be lower than observed. The importance of the smaller inland creeks would diminish with larger flood depths as they were designed primarily for freshwater drainage. Tregothic Creek is an exception, velocity data was not collected to validate the modelling of this feature.

Figure 64: Inland Constructed Channel
Photo credit: Michael Fedak, 2011

Figure 65: Windsor Salt Marsh Natural Channel
Photo credit: van Proosdij, 2011

Important LiDAR related errors were associated with the presence of water returns. TUFLOW sensitivity testing to see how this might affect results and found that even if the minimum channel bottom elevations in the study area were increased to -1m (they are currently ~-4m) runs matching the validation data in the study area were still achieved. This was likely because all of the data was collected at locations with an elevation of over -1m.

By interpolating the high resolution LiDAR to a lower resolution grid, the locations, terrain slopes, and elevations of features became more generalized. Small but important features, such as culvert entrances, became more difficult to recognize and the elevations of the dykes changed. This was a serious problem for reliable overtopping estimates. To address these errors, the grid was post-processed to raise the elevations of cells representing dykes to the exact surveyed elevation. The elevations of cells with important creeks and culvert inlets were also modified so that slopes and channels leading to culverts would be somewhat more correctly represented. Buildings and overpasses were

added in a similar way but the representation of overpasses does not include the road deck. However, none of the flood depths that were simulated were predicted to reach the road deck of an overpass.

Finally, there are errors associated with the boundary conditions and the numerical solution computed by TUFLOW. Since TUFLOW is a numerical software package, it solves the shallow water equations only approximately, and reports errors as 'mass-balance errors' this refers to the amount of water 'lost' by the simulation at each timestep. These errors tended to be under 0.1%, for example, in absolute terms this means that out of 300,000,000 m^3 of water entering and exiting the model, 300,000m^3 may have been erroneously lost due to the approximations made by TUFLOW. Figure 66 shows that these losses tended to occur in areas with abrupt elevation changes and high flow rates/volumes where it is known that finding an accurate solution to the shallow water equations in these areas is very difficult due to hydraulic jumps (Néelz & Pender, 2009).

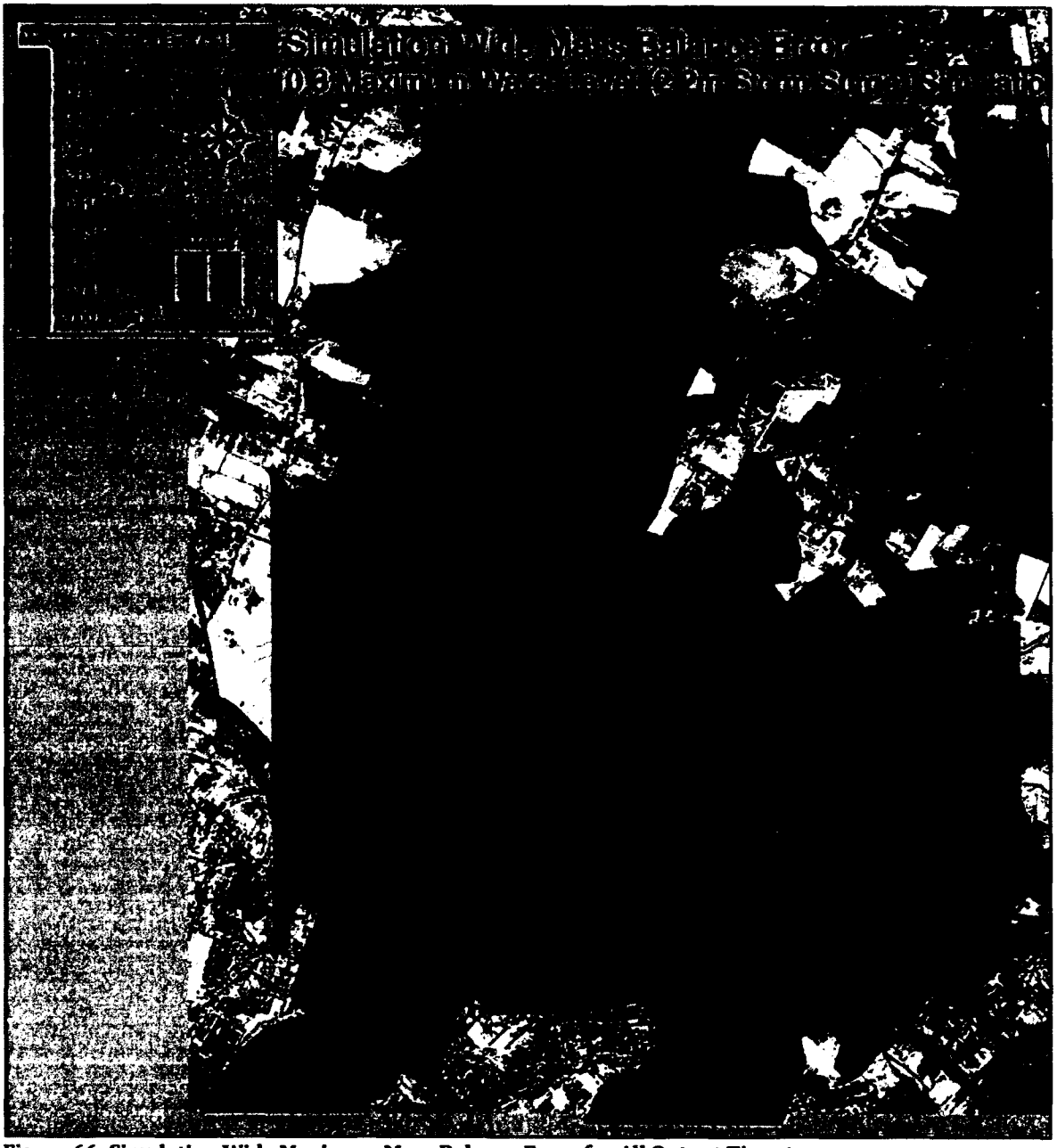

Figure 66: Simulation Wide Maximum Mass Balance Error for All Output Timesteps

5.4 Implications for Climate Change Adaptation

The impacts of climate change will be gradually manifested over the next century. Climate change will cause increasing sea levels. Coastal protection structures will need to be raised to keep up with the water level rise. Time scales over which a deterministic model is valid are shorter than some of the changes decision makers may wish to predict. For instance, the morphology of the channel is constantly changing as sediment is deposited and mudflats and marshes grow. Additionally, development taking place in the marsh bodies changes flow characteristics and flood hazards. Wamsley et al., (2010) attempted to augment their hydrodynamic modelling by using socio-economical and morphological change models to try and determine how their domain would change over a long time period (50 years). Purvis et al., (2008) used a 2D inundation model and an ensemble approach to predict coastal inundation extents for the year 2100 in a section of the macrotidal Severn Estuary in England. Neither of these studies produced 'certain' predictions. The best approach is to try to account for many possible occurrences using an ensemble of simulations and coupled models.

Though the method used in this thesis may not be able to provide certain predictions many years in advance, it should be used as part of an adaptive management approach to deal with flood risks associated with climate change. Over the long term, if data about the system can be kept up to date and the proper analysis tools applied, a SDSS can improve management practices to reduce hazards.

Monitoring changes and re-running simulations with new data gathered when large changes to the floodplain and/or within the channel occur, will keep inundation predictions up to date. Up-to-date information is necessary for decision makers. Fields of hydrodynamic and environmental modelling change rapidly; thus geomatics professionals have to keep up with the technology (Cunge, 1998). Open source modelling and data management solutions, such as the ANUGA inundation model, the PostGIS spatial database, SMS interface make the technologies applied here available to a wider group of people.

5.5 The use of Flood modelling in land-use planning and disaster mitigation

This method can improve the current land use planning controls for flood management by delineating flood hazard based on results from a hydrodynamic model included in a geographic information system. This thesis gives additional information about the categories of flood hazard inside the environmental constraint areas which are currently delineated without degrees of hazard. It also illustrates how flood hazard may be compared with datasets representing vulnerable features in a geographic information system.

Flooding caused by storm surge overtopping dykes in the study area is a real possibility. Due to accelerating sea level rise, the probability of extreme water levels will increase in the Avon River estuary (Daigle & Richards, 2011). At current elevations, the dykes will be overtopped if a 0.4m or greater storm surge coincides with a HHWLT (higher high water large tide at 8.1 m CGVD28). Serious flooding of private buildings and

infrastructure on the Tregothic marsh happens on a 1.0m storm surge coinciding with a HHWLT event. More extreme events (1.6 m - 2.2 m storm surges) will potentially flood the Town of Windsor outside of the current marsh body boundaries. However, these predictions are uncertain due to software and data limitations.

Before flood management steps can be taken beyond the land use controls which exist today; it needs to be determined if the stakeholders see storm surge driven flooding as a risk. If there is no political will to take proactive action to prevent flooding, the resources will not be there to take effective actions. If there is a desire to act on potential flood risks; action would need to be coordinated between multiple provincial and municipal organizations.

ACASA and the draft Nova Scotia Coastal Strategy both indicate there is political will to deal with hazards posed by storm surges and sea level rise related flood hazard. Lack of risk awareness may be a problem stifling hazard management efforts. Relying on structural flood defences can create a false sense of security and apathy among communities, making it difficult to implement other (sometimes cheaper and more effective) measures. Drejza et al, (2011) point out that even though regulations may be implemented, their enforcement may be weak and there may be a lack of awareness of risk throughout the community. They recommend educating people by giving non-technical information about the risks they face and the steps that may be taken to mitigate these risks. Lane et al, (2010) carried out a flood management planning process which directly engaged citizens in the scientific and technical aspects of flood management. They found that by having members of the public (in selected committees) present at

every stage of the flood modelling and planning process; there was increased trust and understanding in communities of the need to implement certain management measures.

Conflicts arise when economic implications are attached to flood risk mapping. The value of farmlands within the marsh bodies is part of the life-savings of local farmers. In the audit of the FDRP, the effect on land values was mentioned in passing as land values in the areas considered in the audit had not dropped or grown more slowly as a result of the hazard mapping (Office of Critical Infrastructure and Emergency Preparedness, 2001).

Major flood management projects in Nova Scotia have historically been carried out through partnerships among the federal, provincial and municipal levels of government. IPCC (2012) recommends that a 'multi-hazard risk management' approach be followed whereby multiple types of hazards are considered and the targeting of a single hazard does not increase vulnerability to other hazards. The Canada National Disaster Mitigation Strategy (NDMS) was created in 2008 to carry out multi-hazard risk management, including flood risk management. It may be possible to coordinate future flood management under the NDMS as a partnership between various agencies and levels of government. Furthermore, municipalities in Nova Scotia are required to submit a Municipal Climate Change Action Plan (MCCAP) by the end of 2013. This document is an opportunity for municipalities to outline climate change hazards and create a plan for adaptation. The plans are a requirement for eligibility to receive funding through the Federal Gas Tax Fund for infrastructure projects which aid community sustainability, including water related infrastructure.

CHAPTER 6: Conclusions

This thesis investigated flooding due to storm surge in the dykelands of a macrotidal estuary. The threat of flooding in this area is controlled by hydrodynamic and morphological processes and structures operating at different temporal and spatial scales. A single storm surge event was simulated for 34 hours to examine predictions for flood and initial drainage patterns. Results were compared with simpler and less time consuming flood extent prediction techniques and found that a hydrodynamic model is necessary for determining flood depths and extents in areas with obstructions comparable in height to the maximum flood level. Although the deterministic modelling technique that was used is limited to a short temporal scale; the use of a properly maintained SDSS can inform the need for future modelling studies. The complexities of flow in extensive intertidal areas and flooding in an urban area necessitate the investigation of processes at large spatial scales (1-5m). High resolution terrain data and information about hydraulic structures is required for this. Tidal and meteorological effects that may cause flooding occur at smaller scales (kilometres vs. meters) are a determining factor in the extent and duration of flooding. These scales need to be linked in order to determine flood hazards in a macrotidal estuary.

6.1 Observations about the Flood Modeling Process

Modeling water flow and coastal hazards due to sea level rise in a macrotidal estuary can be a very complex process requiring significant amounts of input data and expertise. First an inventory of the relevant physical conditions needs to be carried out

and a conceptual model of the coastal system created. Then the specific methods of simulation need to be adapted to fit the area of interest and the physical processes being modeled. Data need to be collected, organized and then placed into the simulation. Results are assembled and analyzed to see if they are consistent with the expected outcomes. The process should be iterative as errors and shortcomings must be identified and parameters adjusted until an acceptable outcome is found.

If acceptable results are produced, the results of these simulations can be extremely valuable to those policy makers and those wishing to gain a better understanding of natural and man-made systems and their responses to different kinds of forcing. Even though the initial effort required for running a simulation model may be large, once the required inputs have been brought together and a framework set up for processing data and results, it becomes easier to run simulations for different scenarios as they may become needed.

6.2 Practical Suggestions for Flood Modelling

A beneficial step for all organizations involved would be to clearly define the problem and the information they would require for making decisions. They need to recognize that the scope of any exercise will need to be limited so tangible problems can be defined and solved. The final information required may not necessitate the use of a physics based hydrodynamic model, but decision makers need to be aware of the type of analysis that different technologies and best practices can provide for flood management used in other locations.

Furthermore, a spatial decision support should be set up for storing all relevant data in formats accessible to all stakeholders. A source, pathway, receptor approach may be considered when setting up this database. This study has demonstrated that alterations to the path of flooding can change the extent and drainage characteristics of the study area. The locations of buildings, infrastructure and hydraulic structures are all important for determining final risk. When alterations are made to areas at risk of flooding, the pathways may change significantly. The sources of flooding will also be changed as sea levels rise and tidal range changes. There would be a need for monitoring significant changes and assessing their impact on risk and therefore reviewing and updating of flood mapping should be part of management strategy. A database would be useful for more than just flood management as much of the infrastructure, such as culverts and storm sewers, should be documented in a database so that any further modelling studies will have this data readily available and stakeholders will have an idea of the location and condition of their assets. It has been shown in this study that the location and condition of drainage features is crucial for determining the spatial extent and duration of a flood event particularly in urban areas. However, there are no validation data available for dyke overtopping and it would be highly beneficial if the date and spatial extents of dyke overtopping were recorded. This database could be automatically updated as new construction happens. Additionally, modelling tools could be used to assess any potential impacts of new development on flood characteristics. The flood results from this model can be stored in a database and used to identify potential hazard to individual buildings and flood extents over time for emergency management.

In this area, the representation of drainage and flood protection features is a determining factor in flood duration and extent. The following are practical recommendations for flood modelling:

- The representation of drainage channels both landward and seaward of the dykes was problematic using a finite difference model with a Cartesian grid. It would be beneficial to use a model with an unstructured grid domain so that detail in the channels could be enhanced and they could be represented more accurately.
- A robust scheme for dealing with shocks due to rapid flow transitions is essential given the complex topography, material types and water volumes.
- Bathymetry data for the main channel and Lake Pisiquid needs to be measured in high resolution.
- Evaporation and infiltration values would also need to be determined as not all the water drains through the aboiteaux structures.
- Inflow and outflow boundary conditions should be used, however it is very difficult to collect data in this area as unconsolidated mudflats and very fine sand can lead to instrument loss and injury to researchers.
- Additional investigation of tidal dynamics in the inner Avon River estuary and how they may change future flood risk.

To conclude this thesis, a quote from Kevin Beven is appropriate as it summarizes some of the major points in this work and puts it into the context of a long term management process which will require constant learning and adaptation:

> The application of distributed hydrologic and hydraulic models can be treated as a form of learning process about places. We should expect that models that up to now seemed to provide acceptable predictions might not prove acceptable in the future. Management based on the predictions of such models should consequently be adaptive (Beven, 2011).

References

Andrews, J. (Ed.). (1993). *Flooding: Canada Water Book.* Ottawa: Canada Communication Group.

Aquaveo LLC. (2007, 07 17). *SMS:Linear Interpolation.* Retrieved from XMS Wiki: http://www.xmswiki.com/xms/SMS:Linear_Interpolation

Aronica, G., Horrit, M., & Bates, P. (2002). Assessing the uncertainty in distributed model predictions using observed binary pattern information within GLUE. *Hydrological Processes*, 2001-2016.

Atlantic Climate Adaptation Solutions Association (ACASA). (2012, March). Retrieved May 2012, from ACASA Website: http://atlanticadaptation.ca/

Baldassarre, D., Schumann, G., & Bates, P. (2009). A methodology for the validation of uncertian flood inundation models. *Journal of Hydrology*, 276-282.

Barnard, P. L., O'Reilly, B., van Ormondt, M., Elias, E., Ruggiero, P., & Erikson, L. H. (2009). *The Framework of a Coastal Hazards Model— A Tool for Predicting the Impact of Severe Storms.* Reston, Virginia: U.S. Geological Survey.

Bartlett, D., & Smith, J. (2005). *GIS for Coastal Zone Management.*

Bates, P. D., Dawson, R. J., Hall, J. W., Horritt, M. S., Nicholls, R. J., Wicks, J., et al. (2005). Simplified two-dimensional numerical modelling of coastal flooding and example applications. *Coastal Engineering, 52*(9), 793-810.

Bates, P., Wilson, M., Horrit, S., Mason, D., Holden, N., & Currie, A. (2006). Reach scale floodplain inundation dynamics observed using airborne synthetic aperture radar imagery: Data analysis and modelling. *Journal of Hydrology*, 306-318.

Bekic, D., Ervine, D. A., & Lardet, P. (2006). A Comparison of One- And Two-Dimensional Model Simulation of the Clyde Estuary, Glasgow. . *Proceedings of the Seventh International Conference on Hydroscience and Engineering* (pp. 1-15). Philadelphia, PA: Drexel University.

Bernier, N. (2005). *Annual and Seasonal Extreme Sea Levels in the Northwest Atlantic: Hindcasts Over the Last 40 Years and Projections fot the Next Century (Ph.D Thesis).* Halifax, Canada: Dalhousie University.

Beven, K. (2009). *Environmental Modelling: An Uncertain Future.* New York: Routledge.

Beven, K. (2011). Distributed Models and Uncertainty in Flood Risk Management. In G. Pender, & H. Faulkner (Eds.), *Flood risk science and management* (pp. 291-307). Blackwell.

Beven, K., Leedal, D., Neal, J., Bates, P., Keef, C., Hunter, N., et al. (2011, September 9). *Good Practice Guidelines for Flood Risk Mapping.* Retrieved November 14, 2011, from FRMRC Dissemination Event - 'Flash' Presentations: http://www.floodrisk.org.uk/images/stories/Dissemination/050911_beven.pdf

Bird, E. (2000). *Coastal Geomorphology: An Introduction.* Chichester: John Wiley & Sons.

Blackburn, C., Wallace, S., & Vimalaratnam, V. (2012). Stormwater Flooding in Bankstown - The Hidden Threat, A Consistent Approach to Managing the Risk . *52nd Floodplain Management Association Conference.* Batesman Bay: http://www.floods.org.au/Batemans-Bay-2012/stormwater-flooding-in-bankstown-the-hidden-threat-a-consistent-approach-to-managing-the-risk.html.

Bleakney, J. S. (2004). *Sods, Soils, and Spades.* Montreal and Kingston: McGill-Queen's University Press.

Brömmelstroet, T. (2009). The relevance of research in planning support systems: a response to Janssen et al. *Environment and Planning B: Planning and Design*, 4-7.

Brown, J., Spencer, T., & Moeller, I. (2007). Modelling storm surge flooding with particular reference to modelling uncertainties . *Water Resources Research*, 1-22.

Browning, D. (2011). *Internal Report.* Nova Scotia Department of Agriculture.

Cariolet, J.-M. (2010). Use of high water marks and eyewitness accounts to delineate flooded coastal areas: The Case of Storm Johanna (10 March 2008) in Brittany, France. *Ocean & Coastal Management* , 679-690.

Carter, R., & Woodroffe, C. (1994). *Coastal Evolution: Late Quarternary Shorline Morphodynamics.* Cambridge: Cambridge University Press.

Cesur, D. (2007). GIS as an information technology framework for water modelling. *Journal of Hydroinformatics*, 123-134.

Chen, P. (2007). *Flood Impact Assessment using Hydrodynamic Modelling in Bangkok, Thailand (Master's Thesis).* Enschede, The Netherlands: International Institute for Geo-Information Science and Earth Observation.

Cheung, K., Phadke, A., Wei, Y., Rojas, R., Douyere, M., & Martino, C. (2003). Modeling of storm-induced coastal flooding for emergency management. *Ocean Engineering*, 1353-1386.

Chinnarasri, C., Tingsanchali, T., Weesakul, S., & Wongwises, S. (2003). Flow Patterns and Damage of Dike Overtopping. *International Journal of Sediment Research*, 301-309.

Chow, V. (1959). *Open Channel Hydraulics.* New York: McGraw-Hill.

Cunge, J. (1998). From Hydraulics to Hydroinformatics. *Keynote Lecture ICHE.*

Cunge, J. (2003). Of Data and Models. *Journal of Hydroinformatics*, 75-98.

Daigle, R., & Richards, R. (2011). Retrieved 03 20, 2012, from The Atlantic Climate Adaptation Solutions Association: http://atlanticadaptation.ca/acasa/sites/discoveryspace.upei.ca.acasa/files/Climate%20Change%20Scenarios%20NS%20and%20PEI%20-%20Final.pdf

Davidge, A., & Gladki, J. (2010). *Model Standard of Practice for Climate Change Planning.* Canadian Institute of Planners.

Davidson-Arnott, R., van Proosdij, D., Ollerhead, J., & Schostak, L. (2002). Hydrodynamics and sedimentation in salt marshes: examples from a macrotidal marsh, Bay of Fundy. *Geomorphology*, 209-231.

De Kok, J., & H.G., Wind. (2003). Design and application of decision-support systems for integrated water mangement: lessons to be learnt. *Hydrology, Oceans and Atmosphere*, 571-578.

de Kok, J., Kofalk, S., Berlekamp, J., Hahn, B., & Herman, W. (2009). From Design to Application of a Decision-support System for Integrated River-basin Management. *Water Resource Management* , 1781-1811.

de Vriend, H., Capobianco, M., Chesher, T., de Swart, H., Latteux, B., & Stive, M. (1993). Approaches to long term modelling of coastal morphology: a review. *Coastal Engineering*, 225-269.

Desplanque, C., & Mossman, D. (1999). Storm Tides of the Fundy. *Geographical Review*, 23-33.

Desplanque, C., & Mossman, D. (2004). Tides and their seminal impact on the geology, geography, history and socio-economics of the Bay of Fundy, Eastern Canada. *Atlantic Geology* , 1-30.

Drejza, S., Bernatchez, P., & Dugas, C. (2011). Effectiveness of land management measures to reduce coastal georisks, eastern Québec, Canada. *Ocean & Coastal Mangement*, 290-301.

Dupont, F., Hannah, C. G., & Greenberg, D. (2005). Modelling the Sea Level in the Upper Bay of Fundy . *Atmosphere-Ocean*, 33-47.

Dyer, K. (1997). *Estuaries: A Physical Introduction.* New York: John Wiley & Sons.

ESPACE. (2006). *ESPACE - European Spatial Planning: Adapting to Climatic Events.* Retrieved September 20, 2011, from TE2100 - Inundation Modelling: TUFLOW: http://www.espace-project.org/part1/publications/reading/espace/Espace%20Piloting_TUFLOW.htm

Falconer, R., Liang, D., & Lin, B. (2007). Simulation of rapidly varying flow using an efficient TVD-MacCormack scheme. *International Journal for Numerical Methods in Fluids*, 811-826.

French, J. (2009). Critical perspectives on the evaluation and optimization of complex numerical models of estuary hydrodynamics and sediment dynamics. *Surface Processes and Landform*, 174-189.

French, J. R. (2003). Airborne LiDAR in support of geomorphological and hydrodynamic modelling. *Earth Surface Processes and Landforms* , 221-235.

Friedland, C. J. (2009). *Residential Building Damage From Hurricane Storm Surge: Proposed Methodologies to Describe, Assess and Model Building Damage.* PhD Dissertation: Louisiana State University Department of Civil and Environmental Engineering.

Gold Coast City Council. (2012). *Gold Coast City Sustainable Flood Management Strategy.* Gold Coast City, Australia.

Granger, K. (2003). Quantifying Storm Tide Risk in Cairns . *Natural Hazards*, 165-185.

GRASS Development Team. (n.d.). GRASS 6.4 Users Manual. Retrieved from http://grass.osgeo.org/grass64/manuals/html64_user/

Greenberg, D., Blanchard, W., Smith, B., & Barrow, E. (In Press). Climate Change, Mean Sea Level and High Tides in the Bay of Fundy.

Haile, T. (2005). *Integrating Hydrodynamic Models and High Resolution DEM (LIDAR) For Flood Modelling (Masters Thesis).* Enschede, The Netherlands: International Institute for Geo-information Science and Earth Observation.

Hardisty, J. (2007). *Estuaries: Monitoring and Modelling the Physical System.* Malden, M.A.: Blackwell.

Haslett, S. (2009). *Coastal Systems.* New York: Routledge.

Haung, Y. (2005). *Appropriate Modeling For Integrated Flood Risk Assessment (PhD Dissertation).* . The Netherlands: University of Twente.

Hearn, C. (2008). *The Dynamics of Coastal Models.* New York: Cambridge University Press.

Hinkelmann, R. (2005). *Efficient numerical methods and information-processing techniques for modelling hydro and environmental systems.* New York: Springer.

HR Wallingford; Flood Hazard Research Centre, Middlesex University; Risk & Policy Analysts Ltd. (2006). *R&D OUTPUTS: FLOOD RISKS TO PEOPLE: Phase 2.* London : Department for Environment, Food and Rural Affairs: Flood Management Division.

Hu, K., Ding, P., Wang, Z., & Yang, S. (2009). A 2D/3D hydrodynamic and sediment transport model for the Yangtze Estuary, China. *Journal of Marine Systems*, 114-136.

Hunter, N. M., Bates, P. D., Neelz, S., Pender, G., Villanueva, I., & Wright, N. G. (2008). Benchmarking 2D hydraulic models for urban flooding. *Proceedings of the Institution of Civil Engineers*, 13-30.

Huxley, C. D. (2004). *TUFLOW Testing and Validation (Honours Thesis).* Queensland, Australia: Griffith University School of Environmental Engineering.

IPCC. (2012). *Summary for Policymakers. In: Managing the Risks of Extreme Events and Disasters to Advance Climate Change Adaptation.* . Cambridge, UK, and New York, NY, USA: Cambridge University Press.

Irish, J., Resio, D., & Cialone, M. (2009) a. A surge response function approach to coastal hazard assessment - part 1: basic concepts. *Natural Hazards*, 163-182.

Irish, J., Resio, D., & Cialone, M. (2009) b. A surge response function approach to coastal hazard assessment. Part 2: quantification of spatial attributes of reponse functions. *Natural Hazards*, 183-205.

Janssen, R., & T.J., S. (2009). Making progress towards effective spatial decision support: a response from Janssen and Stewart. *Environment and Planning B: Planning and Design*, 8-11.

Jones, O., Petersen, O., & Kofoed-Hansen, H. (2007). Modelling of complex coastal environments: some considerations for best practice. *Coastal Engineering*, 717-733.

Kamphuis, J. (2010). *Introduction to Coastal Engineering and Management* (2nd ed., Vol. 30). Advanced Series on Ocean Engineering : World Scientific Press.

Kelman, I. (2002). *Physical Flood Vulnerability of Residential Properties in Coastal, Eastern England.* UK: University of Cambridge.

Kreibich, H., Piroth, K., Seifert, I., Maiwald, H., Kunert, U., Schwarz, J., et al. (2009). Is flow velocity a significant parameter in flood damage modelling? *Natural Hazards and Earth System Sciences*, 1679-1692.

Krupka, M. (2009). *A rapid inundation flood cell model for flood risk analysis.* Heriot-Watt University: Doctoral Thesis.

Lakhan, V. (2005). Coastal Modelling and Simulation. In M. Schwartz (Ed.), *Encyclopedia of Coastal Science* (pp. 266-269). Dordrecht: Springer.

Lakhan, V., & Trenhaile, A. (1989). *Applications in Coastal Modelling.* Amsterdam: Elsevier Science Publishers B.V.

Lane, S. (2005). Roughness –time for a re-evaluation? *Earth Surface Processes and Landforms*, 251-253.

Lane, S., Odoni, N., Landstrom, C., Whatmore, S., Ward, N., & Bradley, S. (2010). Doing Flood Risk Science Differently: An Experiment in Radical Scientifc Method. *Transactions of the Institute of British Geographers*, 15-36.

Lhomme, J., Sayers, P., Gouldby, B., Samuels, P., Willis, M., & Mulet-Marti, J. (2009). Recent development and application of a rapid flood spreading method. In P. Samuels, H. Stephen, W. Allsop, & J. Harrop (Eds.), *Flood Risk Management : Research and Practice* (p. 15). London: Taylor and Francis Group.

Lin, B., Wicks, J., Falconer, R., & Adams, K. (2006). Integrating 1D and 2D hydrodynamic models for flood simulation. *Water Management*, 19-25.

Manson, S. (2007). Challenges in evaluating models of geographic complexity. *Environment and Planning B: Planning and Design*, 245-260.

Mason, D., Cobby, D., Horrit, M., & Bates, P. (2003). Floodplain Friction Parameterisation in Two-Dimensional River Flood Models. *Hydrological Processes*, 1711-1732.

Mason, D., D'Amico, J., & Bates, P. (2009). Calibration of uncertain flood inundation models using remotely sensed water levels. *Journal of Hydrology*, 224-236.

Mason, D., Schumann, G., & Bates, P. (2011). Data Utilization in Flood Inundation Modelling. In G. Pender, & H. Faulkner (Eds.), *Flood risk science and management* (pp. 211-233). Blackwell.

Mirfenderesk, H. (2012). Application of Future Scenario Planning to Flood Risk Management . *52nd Floodplain Management Association Conference Papers.* Batemans Bay, Australia: http://www.floodplainconference.com/papers2012.php.

Moeller, I. (2006). Quantifying saltmarsh vegetation and its effect on wave height dissipation: Results from a UK East Coast Saltmarsh. *Estuarine, Coastal and Shelf Science*, 337-351.

Municipality of the District of West Hants. (2011, September). *Municipality of the District of West Hants Land Use By-Law.* Retrieved March 2012, from

http://www.westhants.ca/index.php?option=com_docman&task=doc_download&gid=457&Itemid=176

National Research Council of the National Academies (NRC) . (2009). *Mapping the Zone: Improving Flood Map Accuracy.* Washington D.C.: The National Academies Press.

Néelz, S., & Pender, G. (2009). *Desktop review of 2D hydraulic modelling packages.* Bristol, UK: Environment Agency.

New South Wales Government. (2005). *Floodplain Development Manual.* Sydney: Department of Infrastructure, Planning and Natural Resources.

Nicholas, A., & Mitchell, C. (2003). Numerical simulation of overbank processes in topographically complex floodplain environments. *Hydrological Processes*, 727-746.

National Ocean and Atmospheric Administration (NOAA). *Tides and Currents: Frequently Asked Questions*. Retrieved July 2012, from http://www.co-ops.nos.noaa.gov/faq2.html#26

Nyerges, T. D. (2007). Constructing a coastal data model for Puget Sound: A classroom experience. *Proceedings of Coastal Zone 07.* Portland, Oregon: Oregon State University.

Nyerges, T., & Jankowski, P. (2010). *Regional and Urban GIS: A Decision Support Approach.* New York: The Guilford Press.

Office of Critical Infrastructure and Emergency Preparedness . (2001). *Managing Flood Risk: Report of an Independent Expert Panel.* Ottawa: Government of Canada.

O'Laughlin, C., & van Proosdij, D. (2012). Influence of Varying Tidal Prism on Hydrodynamics and Sedimentary processes in a Hypertidal Salt Marsh Creek. *Earth Surface Processes and Landforms (in review).*

Paine, J., & Watt, W. (1992). Flood Risk Mapping in Canada: 2. Compatible Mapping . *Canadian Water Resources Journal* , 139-148.

Pappenberger, F., Beven, K., Horrit, M., & Blazkova, S. (2005). Uncertainty in the calibration of effective roughness parameters in HEC-RAS using inundation and downstream level observations. *Journal of Hydrology*, 46-69.

Pathirana, A., Tsegaye, S., Gersonius, B., & Vairavamoorthy, K. (2011). A simple 2-D inundation model for incorporating flood damage in urban drainage planning. *Hydrology and Earth System Science*, 2747-2761.

Pender, G., & Neelz, S. (2011). Flood Inundation Modelling to Support Flood Risk Management. In G. Pender, & H. Faulkner (Eds.), *Flood risk science and management* (pp. 235-255). Chichester: Blackwell.

Pietersma-Perrot, B., & van Proosdij, D. (2012). *Shore zone characterization for climate change adaptation on the Bay of Fundy.* Final Report presented to the Atlantic Climate Adaptation Solutions Association (ACASA), NS Department of Environment, Climate Change Secretariat, 61pp.

Pistrika, A., & Jonkman, S. (2010). Damage to residential buildings due to flooding of New Orleans after hurricane Katrina. *Natural Hazards*, 413-434.

Provincial Oceans Network. (2011, October). *Draft Coastal Strategy.* Retrieved from Coastal Management Nova Scotia: http://www.gov.ns.ca/coast/documents/draft-coastal-strategy2011oct.pdf

Public Service Canada. (2012, February). *The Canadian Disaster Database.* http://www.publicsafety.gc.ca/prg/em/cdd/index-eng.aspx

Pugh, D. (2004). *Changing Sea Levels: Effects of Tides, Weather and Climate.* Cambridge: Cambridge University Press.

Purvis, M., Bates, P., & Hayes, C. (2008). A probabilistic methodology to estimate future coastal flood risk due to sea level rise. *Coastal Engineering*, 1062-1073.

Richardson, J.R., & Julien, P.Y. (1994). Suitability of simplified overland flow equations. *Water Resources Research*, 665-671.

Roux, H., & Dartus, D. (2008). Sensitivity analysis and predictive uncertainty using inundation observations for parameter estimation in open-channel inverse problem. *Journal of Hydraulic Engineering*, 541-549.

SAGA GIS Development Team. (2011, November 23). *SAGA GIS.* Retrieved March 1, 2012, from http://sourceforge.net/projects/saga-gis/

Saul, A., Slobodan, D., Maksimovic, C., & Blanksby, J. (2011). Integrated Urban Flood Modelling. In G. Pender, & H. Faulkner (Eds.), *Flood risk science and management* (pp. 258-288). Chichester: Blackwell.

Scawthorn, C., Blais, N., Seligson, H., Tate, E., Mifflin, E., Thomas, W., et al. (2006). HAZUS-MH Flood Loss Estimation Methodology.I: Overview and Flood Hazard Characterization. *Natural Hazards Review*, 60-71.

Schumann, G., Matgen, P., Hoffmann, L., Hostache, R., Pappenberger, F., & Pfister, L. (2007). Deriving distributed roughness values from satellite radar data for flood inundation modelling. *Journal of Hydrology*, 96-111.

Sutherland, J., Walstra, D., Chesher, T. J., van Rijn, L., & Southgate, H. (2004). Evaluation of coastal area modelling systems at an estuary mouth. *Coastal Engineering*, 119-142.

Syme, W. (1991). *Dynamically Linked Two-Dimensional/One-Dimensional Hydrodynamic Modelling Program for Rivers, Estuaries & Coastal Waters (Master's Thesis).* Queensland, Australia: Dept of Civil Engineering, The University of Queensland .

Thompson, K. R., Bernier, N. B., & Chan, P. (2009). Extreme sea levels, coastal flooding and climate change with a focus on Atlantic Canada. *Natural Hazards*, 139–150.

Town of Windsor. (2010, July 16). *Town of Windsor Land Use By-Law.* Retrieved March 3, 2012, from http://www.town.windsor.ns.ca/index.php?option=com_docman&task=doc_download&gid=700&Itemid=190

TUFLOW BMT-WBM. (2010). *TUFLOW Manual 2010-10-AB.* BMT-WBM.

US Army Corps of Engineers Hydrologic Engineering Center (HEC). (2008). *HEC-RAS River Analysis System Hydraulic Reference Manual .* Davis, California: US Army Corps of Engineers.

van Proosdij, D. (2009). *Assessment of Flooding Hazard along the Highway 101 corridor near Windsor, NS using LIDAR.* Nova Scotia Department of Transportation.

van Proosdij, D. (2012). *Dykelands: Climate Change Adaptation.* Climate Change Issue Paper submitted to Atlantic Climate Adaptation Solutions Association, Climate Change Directorate, Nova Scotia Department of Environment 18 pp.

van Proosdij, D., Milligan, T., Bugden, G., & Butler, K. (2009). A Tale of Two Macro Tidal Estuaries: Differential Morphodynamic Response of the Intertidal Zone to Causeway Construction. *Journal of Coastal Research*, 772-776.

van Proosdij, D., Ollerhead, J., & Davidson-Arnott, R. (2006). Seasonal and annual variations in the volumetric sediment balance of a macro-tidal salt marsh. *Marine Geology*, 103-127.

van Proosdij, D and S. Page. (2012). *Best Management Practices for Climate Change Adaptation in Dykelands: Recommendations for Fundy ACAS sites.* Final report submitted to Atlantic Climate Adaptation Solutions Association, Climate Change Directorate, Nova Scotia Department of Environment. 151 pp.

Wamsley, T., Cialone, M., Smith, J., Atkinson, J., & Rosati, J. (2010). The Potential of Wetlands in Reducing Storm Surge . *Ocean Engineering*, 59-68.

Water Research Laboratory (WRL). (2010). *Australian Rainfall and Runoff*

Revision Project 10: Appropriate Safety Criteria for People.

Webster, T. (2010). Flood Risk Mapping Using LiDAR for Annapolis Royal, Nova Scotia, Canada. *Open Access Remote Sensing*, 2060-2082.

Webster, T. L., Mosher, R., & Pearson, M. (2008). Water Modeller: A component of a coastal zone decision support system to generate flood-risk maps from storm surge events and sea-level rise. *Geomatica*, 393-406.

Webster, T., Forbes, D., Dickie, S., & Shreenan, R. (2004). Using topographic lidar to map flood risk from storm-surge events for Charlottetown, Prince Edward Island, Canada. *Canadian Journal of Remote Sensing* , 64-76.

Webster, T., McGuigan, K., & MacDonald, C. (2011). *The Atlantic Climate Adaptation Solutions Association.* Retrieved 03 15, 2012, from http://atlanticadaptation.ca/sites/discoveryspace.upei.ca.acasa/files/Flood%20risk%20in%20ACAS%20municipalities_0.pdf

Werner, M., Hunter, N., & Bates, P. (2005). Identifiability of distributed floodplain roughness values in flood extent estimatio. *Journal of Hydrology*, 139-157.

Wicks, J., Lovell, L., & Tarrant, O. (2011). Flood Modelling in the Thames Estuary. In *Flood risk science and management* (pp. 473-483). Chichester: Blackwell.

Xia, J., Falconer, R., Lin, B., & Tan, G. (2011). Numerical assessment of flood hazard risk to people and vehicles in flash floods. *Environmental Modelling & Software, 26*(8), 987-998.

Zerger, A., & Wealands, S. (2004). Beyond Modelling: Linking Models with GIS for Flood Risk . *Natural Hazards*, 191-208.

Zhang, K., Xiao, C., & Shen, J. (2008). Comparison of the CEST and SLOSH models for storm surge flooding. *Journal of Coastal Research*, 489-499.

Glossary

Bathymetry –The measurement of the depth of water bodies

CGVD28- Canadian Geodetic Vertical Datum of 1928: Elevation relative to mean sea level collected at tide gauges on the east and west coasts.

DEM- Digital Elevation Model- A 'bare earth' representation of the ground surface where features such as buildings and trees are removed.

DSM- Digital Surface Model - A representation of the surface containing all features.

Easting and Northing – In a Cartesian coordinate system; easting refers to the eastward-measured distance (or the x-coordinate), while northing refers to the northward-measured distance (or the y-coordinate).

ESRI - Environmental Systems Research Institute, Inc. Makers of ArcGIS products.

Geodatabase - A database or file structure used primarily to store, query, and manipulate spatial data. Geodatabases store geometry, a spatial reference systems, attributes, and behavioral rules for data.

Geodetic Datum- Defines reference points on the Earth's surface against which position measurements are made. The coordinate system for these points is based on a mathematical representation of the earth known as a spheroid or ellipsoid.

GIS- Geographic Information System: A computer system for capturing, storing, querying analyzing and displaying geospatial data.

GRASS - Geographic Resources Analysis Support System. An open source GIS system originally developed by the US Army Corps of Engineers.

Higher High Water Large Tide (HHWLT)- The average of the highest high waters, based on CHS (Canadian Hydrographic Service) tidal level predictions from the last 19 years.

Hydraulic Radius- A term in the Manning formula defined as the ratio of a channel's cross sectional area to its wetted perimeter

Intertidal Zone- The area that is above water at low tide and under water at high tide.

Layer - A layer is a slice of the geographic reality in a particular area, analogous to a legend item on a map.

LiDAR- Light Detection And Ranging . A system of remote sensing whereby an aircraft emits laser pulses towards the ground and measures the return time and intensity of the pulse.

Macrotidal – A coastal system with a tidal range of over 4m.

Map projection- A method of representing the surface of earth on a plane.

Multibeam bathymetry- Bathymetry collected using a multibeam sonar system whereas multiple pulse of sound are sent simultaneously to obtain water depth readings along the path of a vessel. These readings tend to be high accuracy and are comparable to LiDAR.

Raster Data- A data model where a regular grid of pixels represents space. Values of grid cells correspond to the characteristic of a specific phenomenon (such as elevation) at the cell location.

SMS- Surface Water Modelling System: A software package created by Aquaveo LLC which contains tools (organized in modules) for pre and post processing data associated with a variety of hydrodynamic models.

TUFLOW – Two Dimensional Unsteady FLOW: A 1D/2D coupled hydrodynamic model which solves the full Shallow Water Equations using a finite difference scheme on a uniform grid in Cartesian coordinates.

Universal Transverse Mercator- A type of map projection where the surface of earth is divided into six-degree wide (longitude) zones and each zone has a unique Cartesian coordinate system based on eastings and northings.

Vector Data- A coordinate-based data model that represents geographic features as points, lines, and polygons. Each point feature is represented as a single coordinate pair, while line and polygon features are represented as ordered lists of vertices.

Water Returns – LiDAR elevations which correspond to the surface of a water body (since LiDAR is at a wavelength which does not penetrate the water column).

XMDF- eXtensible Model Data Format: A standard format for the geometry data storage of river cross-sections, 2D/3D structured grids, 2D/3D unstructured meshes, geometric paths through space, and associated time data. XMDF is a hierarchical data model which uses HDF5 for cross-platform data storage and compression (Aquaveo LLC, 2012).

XYZ- ASCII format for storing terrain data in columns corresponding to x,y coordinates and z-values correspond to elevations.

Appendices

Appendix A: Computational Procedure

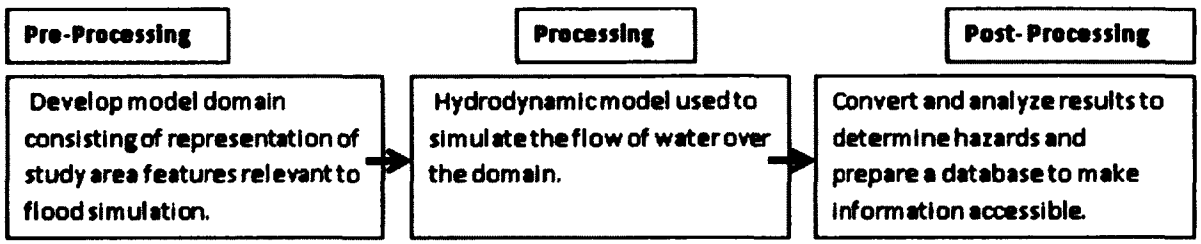

Figure A 1: Computational Procedure Steps.

Handling the data necessary for TUFLOW simulations followed the process shown in Figure A1.

1. Pre-Processing

1.1 GIS Tasks

Terrain data, based on a LiDAR survey of the study area, was used as the basis of elevations in the computational domain (Webster, McGuigan, & MacDonald, 2011). The LiDAR data was delivered to us in a raster grid consisting of pixel values corresponding to terrain elevations referenced to CGVD28 with a horizontal resolution of 2m. Two separate raster layers were used, a DSM and a DEM. The major difference between these layers is that LiDAR point returns in the DEM have been processed to remove non-ground features, thus the DEM is a bare-ground model of the terrain. A DEM is ideal for hydrologic/hydrodynamic modelling since it does not represent permeable features, such

as a forest, as solid barriers to flow (Webster, et al, 2004). The DSM contains elevations of important features, such as buildings, and was used to make modifications to the computational domain.

The raster needed to be transformed into a format usable in TUFLOW. ArcGIS was used to resample the raster data and transform it into an xyz format for use in SMS. Resampling is the method by which raster data may be transformed into different resolutions (cell sizes) or grid orientations. A bi-linear interpolation method was used to convert the 2 m resolution raster data to 3 m. The conversion was necessary to reduce the amount of data so as to make it readable by SMS for grid generation. Resampling from 2 to 3 m reduced the number of elevation values from 6,854,006 (2 m) to 3,046,417 (3 m).

1.2 Surface Water Modelling System

SMS is pre and post processing tool for different hydrodynamic surface water software packages including ADCIRC, FESWMS, and TUFLOW. It provides a Graphic User Interface (GUI) for setting up simulations and analyzing results. SMS was used for setting up TUFLOW as it contains tools for exporting processed data in the file structure and format required for TUFLOW simulations. SMS is composed of different modules for dealing with different data types. The map, mesh, grid, scatter, TUFLOW, GIS, and annotation modules were used.

The first step in setting up a TUFLOW simulation was importing the 3m horizontal resolution terrain data in the xyz file (Section A.1.1) as scatter data. Imported points were made into a uniform square grid in a Cartesian coordinate system (Universal Transverse

Mercator) using the 'Interpolate to Cartesian grid' tool which allowed grid boundaries and orientation to be set. Points inside the grid boundary were used to provide elevations to nodes on the Cartesian grid based on a linear interpolation method where node values were assigned based on a TIN surface created from scatter data (SMS Wiki). The interpolation method used to create the grid was the only one in SMS capable of working with the large number of points in the scatter set (SMS can also create grids using natural neighbour and inverse distance weighted interpolation methods). The final grid had a horizontal resolution of 5m, thus further error was introduced as the data was coarsened. Newer versions of TUFLOW allow input grids in ESRI Shapefile or ASCII format and ArcGIS seems more capable of working with large datasets so it may be better to generate the computational domain for large models within ArcGIS.

1.2.1 Geometry Modifications

To insure that features important to controlling water flow in the study were properly represented, the grid was modified after creation. TUFLOW can read GIS data which defines altered elevations for individual cells in a grid. Layers representing buildings and underpasses, line features representing dykes, culverts, channels, and the tide gate were used. By altering the grid directly, the error introduced through interpolation was mitigated. Dyke elevations were changed by importing surveyed points from the NS Department of Agriculture into SMS and converting them to a geometry modification layer for use in TUFLOW. There are multiple different methods of modifying grid geometry. Figure A2 shows modification through a 'GIS Zpts' layer where any domain Zpt falling within a building polygon was increased to the maximum

height of the building in the DSM. Overpasses were added in a similar way using polygons but elevations were lowered to the elevation of the road in front of the overpass

Figure A2: Grid modifications near Tregothic Creek. Red areas are where the pre-modified and final grids correspond. Green areas are where final grid values are higher. Buildings and dyke elevations were altered in this area.

rather than increased. Dyke elevations were altered using 'Z line' layers which act as 3D breaklines modifying the Zpts of the cells the line passes through. The entrances to culverts were also included as lines but a 'min' option was selected whereby only elevation values less than the specified line elevation were altered.

Lake Pisiquid was not represented properly in the LiDAR data as it was not fully drained at the time of the LiDAR survey. A tide gate under the causeway connects the lake to the Avon River and during a storm event it is expected that this gate would need to be opened to drain inland flooding. An older bathymetry survey showed the bottom of the lake to be -4.01 m (the same as the bottom of the tide gate). Areas within the 0m elevation contour of the lake were lowered to -4.01 m as there was no more detailed elevation data available. The tide gate itself is a uni-directional feature that would open only during the

low tide after the storm. An initial water level of 5.10 m was defined for the lake (bankful level), however this water was only allowed to drain after the storm tide passed and this was done through using a 'variable geometry' layer which was set to block drainage from the lake until the storm surge drains. Initial water level in the lake was different from the initial water level set for the channel which was based on water level from the WebTides time series at the beginning of the simulation (-6.7 m).

1.2.2 Adding 1D features and 1D/2D linking

After the 2D domain, the 1D domain consisting of underground culverts and the tide gate channel was set up. The 1D domain runs on the ESTRY hydrodynamic model which has been coupled with TUFLOW (Syme, 1991). The linking scheme (SX Link) used for pipes and culverts does not preserve momentum across domains but this is only an issue with large structures (TUFLOW Manual, 2010). Huxley (2004) showed that for most culvert types and flow regimes, TUFLOW/ESTRY is able to perform within accepted limits. Further modifications were made to the 2D domain to lower grid elevations to that of culvert inverts as it was required that inverts be above the channel bottom plus the model wet dry depth (Figure A3). Flow is transferred between the 2D domain and the 1D culvert through connection nodes which may be user or automatically defined. Since most culverts in the study area were linked to narrow channels (only 1 or 2 grid cells in width), the automatic method was used to specify the cells in the 2D domain linked to the 1D channel (Figure A3). Linking locations were checked before each model run to insure the proper cells were being selected. Due to the interpolation of the grid and lack of data about the precise elevations of some culvert inverts, the LiDAR DEM was

used to approximate the location of some inverts and modify the grid appropriately. For the aboiteaux and some of the culverts along Tregothic Creek, existing survey data was used. Whenever a computational grid of a different resolution was interpolated; the locations of the inverts needed to be updated and the connection cells checked. Figure A4 shows the 27 culverts and aboiteaux (added as unidirectional culverts) included in the model and the 1D channel representing the tide gate. Some of these features represent multiple barrel culverts which were included in the model but not shown here on the map. There are other important drainage features in the study area, such as storm sewers and storm water pumps as well as additional culverts only the features that there was available data for or that were surveyed for this thesis could be included.

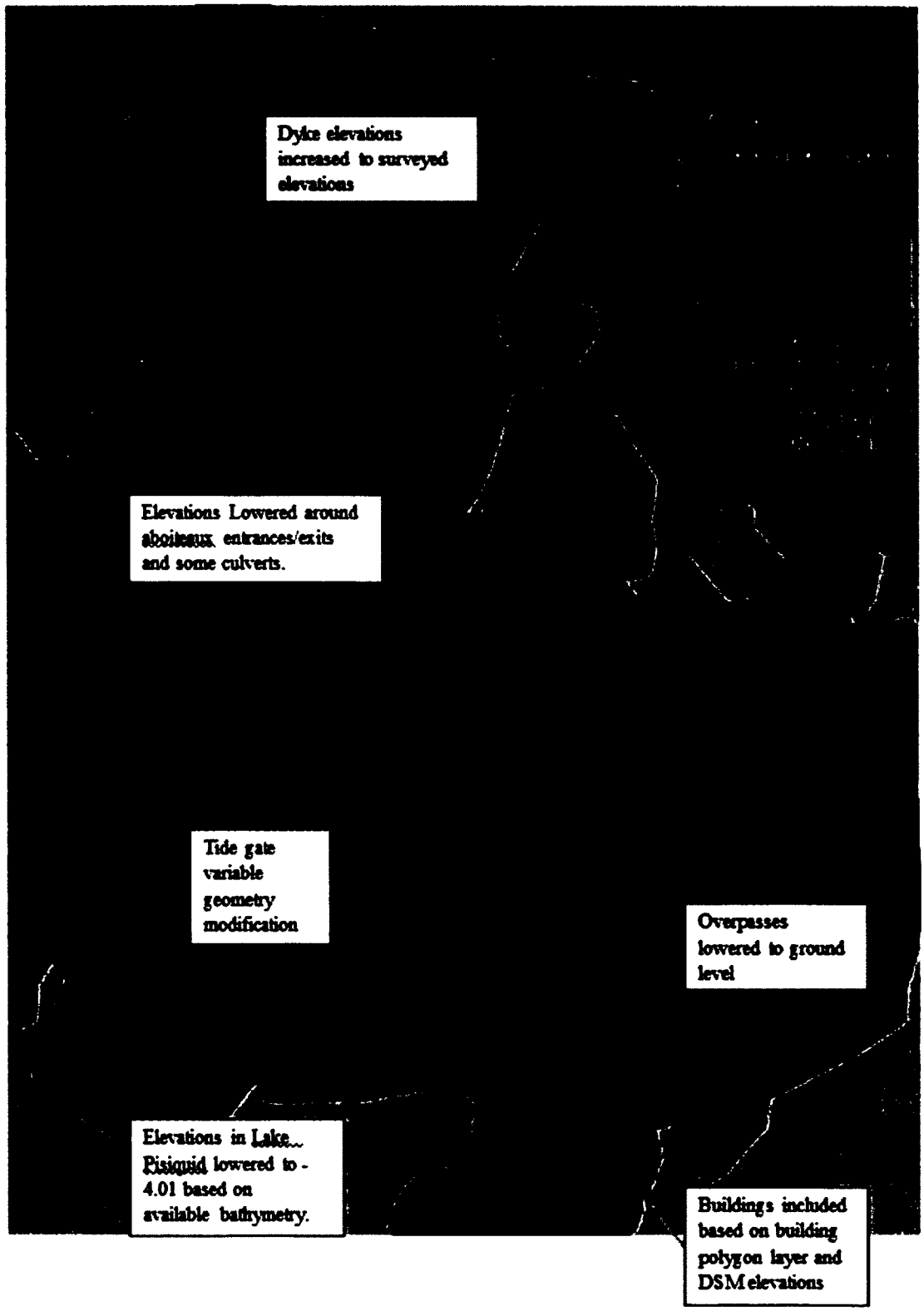

Figure A 3: Grid modifications applied after grid generation

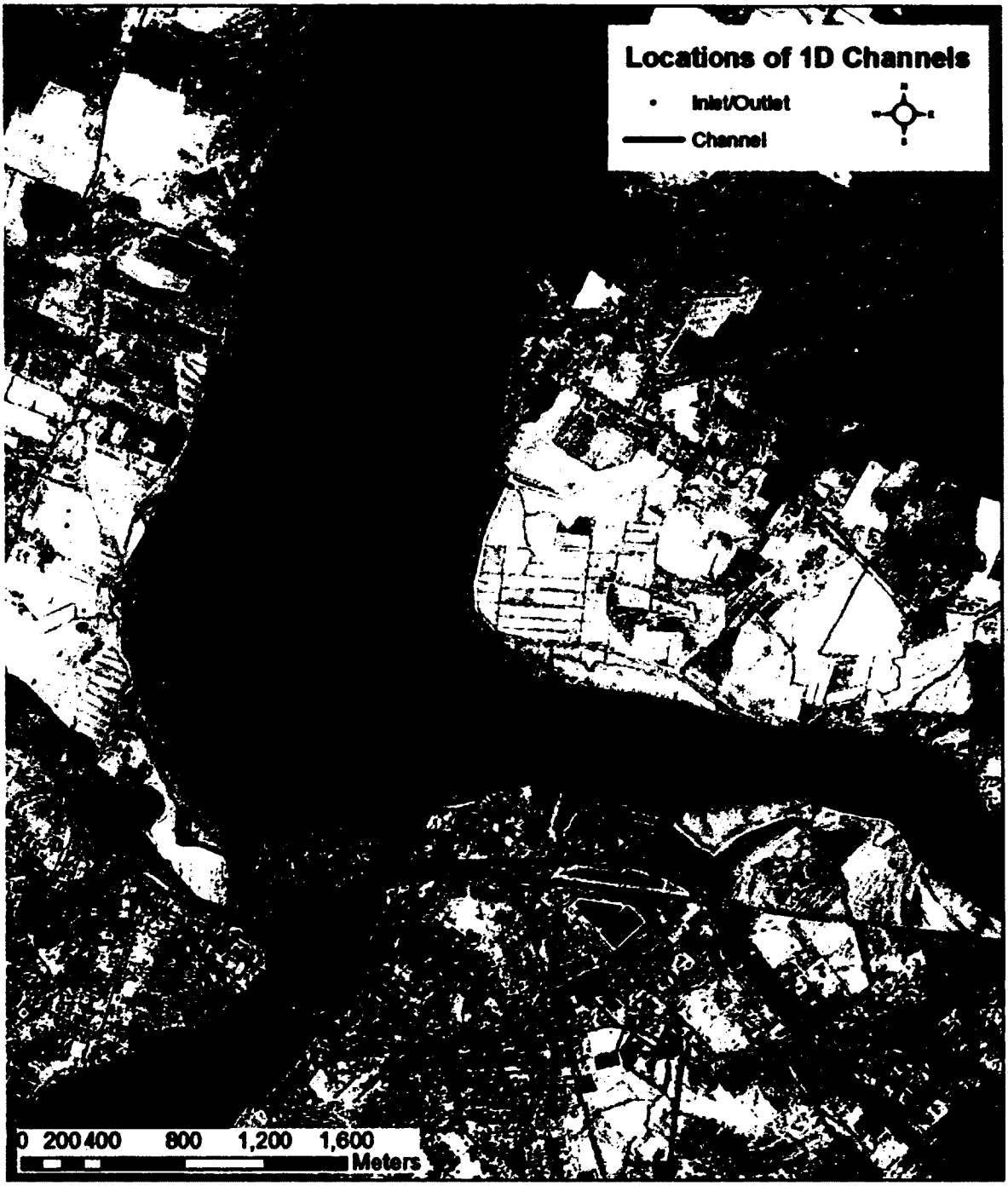

Figure A 4: Location of underground 1D features nested in the 2D grid.

1.2.3 Parameters and Boundary Condition

Model parameters included the computation timestep, surface roughness values, cell wet/dry depths, and the small scale turbulence dissipation scheme. For 1D culvert features, entrance and exit energy losses as well as roughness values needed to be specified. TUFLOW support advised us that the timestep for the study area should be ¼ the cell size (1.25 seconds). Surface roughness values were set using coverages in SMS with regions corresponding to areas of differing roughness (Figure 24). Surface roughness is represented in the governing equations of TUFLOW and can be represented as either a Chézy's C or Manning's n coefficient. The areas were determined based on aerial images and site visits and the coefficients from literature including Chow, (1959); French, (2009); and Wamsley et al, 2010. Sensitivity testing was carried out and it was determined that channel roughness had the largest effect on the tidal curve while inland areas of increased roughness, particularly in floodways, had some effect on inland flood depth and extent.

The boundary conditions were set using coverages defining the extents of the grid and the area of tidal inflow (Figure A3). The tidal curve time series was generated by WebTides (Dupont et al, 2005). The final computational domain was reduced to areas of interest and low elevation which was susceptible to flooding and where there was LiDAR data with minimal water returns. By reducing the size of the domain, the simulation run time was reduced; however the final boundary was oriented at an oblique angle to the computational grid (Figure A3). The orientation of the tidal boundary condition was important for the accuracy of a TUFLOW simulation. TUFLOW was created to be able to

use oblique boundaries (for 1D/2D linking primarily) as long as they are perpendicular to water flow (Syme, 1991).

The default values for the small scale turbulence dissipation scheme were used as the model results of concern did not show sensitivity to changing these values. Pender and Neelz, (2011) point out that viscosity is not usually an important parameter in open channel flows since it is small relative to friction. Cell wet/dry depths were set to 1 cm (0.01 m); this value controls the elevation when a cell is considered wet or dry in the model.

2. Processing (Simulation Runs)

After setting up the components necessary for running a TUFLOW simulation, the model was used in test mode to write out all of the files it would be using in its computation (geometry, timesteps, etc...). These were checked to insure that the set-up had created the expected results. TULFOW was set up to export to a XMDF format (all possible export formats were only SMS compatible). Since TUFLOW is a 1D/2D model, results are stored in a mesh format so output from both the 1D and 2D components can be displayed on the same surface. However the output types vary based on the interpolation method of results. A 5 minute output interval was used, meaning the state of the model every 5 minutes (300 seconds) was written to an output file. Maximums were also recorded for depth, water surface elevation, velocity and velocity depth product. A TUFLOW computational cell (Figure A5) is composed of multiple nodes; for the computation itself, the ZV, ZU and ZC points are important. The ZH points are where

values for output are interpolated from the four surrounding cells. The 2008 version of TUFLOW updated the output types so that values may be output at each node (called high resolution output). High resolution output provides much more data but also takes up much more storage space (60GB vs. 12GB for low resolution output from the same simulation). The results were output in low resolution format because of size constraints.

3. Post- Processing

3.1 Transfers to a GIS Compatible Format

The final goal was to make the results accessible in a GIS. Zerger and Wealands, (2004) achieved a similar goal using data from a hydrodynamic model by intersecting results from a model with exposed buildings and roads and transferring the intersecting values to tables in a database which could be queried and further analyzed. Their approach also reduced the amount of data since they reduced their data to just the exposed features. SMS does include some functionality for extracting values from mesh files, but this functionality was restricted to a small number of features (SMS was unable to extract values for the 500 dyke segments for instance). Furthermore, SMS does not provide a scripting interface to automate tasks. ArcGIS contains tools for storing and querying large datasets using a large number of features and a scripting interface for automating the execution of tools and the creation and querying of database tables. To get the data into ArcGIS it was transferred into raster catalogs within an ESRI File Geodatabase. A raster catalog is a collection of raster datasets defined in a table within a database. A file geodatabase is a format created by ESRI and is not a full object-relational

database (like PostGIS in PostgreSQL) but does provide some functionality for defining relationships (relationship classes) and limited SQL querying. It is also usable in freely available GIS programs which accommodate further use of the data.

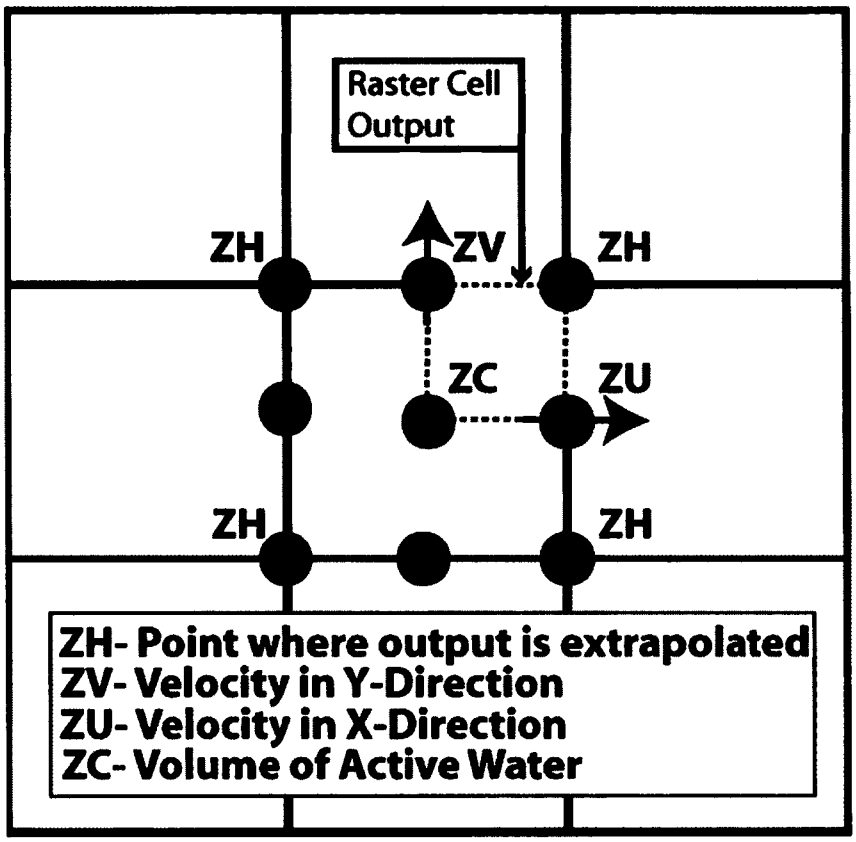

Figure A 5: TUFLOW Computational Cell

To transfer the data, the TUFLOW_to_GIS extension provided by TUFLOW developers was used. This extension converts the TUFLOW XMDF output mesh to a raster ASCII Grid file which can be read by most GIS programs. The conversion to a raster format resulted in four raster cells per ZH point (Figure A5). TUFLOW_to_GIS is a command line executable which allows the extraction of a single raster file corresponding to a single model output timestep of a single data type. There were 446 individual rasters (445

timesteps and 1 simulation wide maximum) created for each of the five output data types and this was repeated across 15 simulation runs resulting in a total of 33450 individual 32-bit rasters. Two scripts were written in Python to transform and analyze this data. The first created geodatabase structure to store the results and called TUFLOW_to_GIS to translate the XMDF files into rasters and then used the arcpy interface to copy these rasters into raster catalogs within the geodatabase. Each raster catalog contained the results from a single simulation stored in a tabular form. The columns in each catalog identified the original filename, timestep, and data type of each raster.

3.2 Analysis of Outputs

Once the geodatabase was filled, a second script was used to analyze drainage and the exposure of buildings and dykes to flooding. ArcGIS does not allow direct analysis of rasters stored in a raster catalog; therefore each raster needed to be extracted from the catalog, analyzed and then deleted (Figure A6). The script creates a list of all raster catalogs in a geodatabase and then loops through the list. First, the water surface elevation rasters were extracted (445 model outputs but not the maximum values). Then the Extract Values to Table tool in ArcGIS was called to extract raster values at each dyke point for each row in the raster catalog. The result was two tables; the main result table had three fields: the object id number of the dyke point from the dyke points layer,

the id number of the raster from a look-up table, and the value of the raster at that point and time. The second table was a look-up table which associated the raster id number with the name of the raster from the raster catalog. If no raster values intersected the points, then an empty table was written and the script skipped to analyze the next catalog. If raster values were found, the script continued to calculate the area of flooding in inland areas protected by the dykes. Inland areas were delineated by first using the lake flood

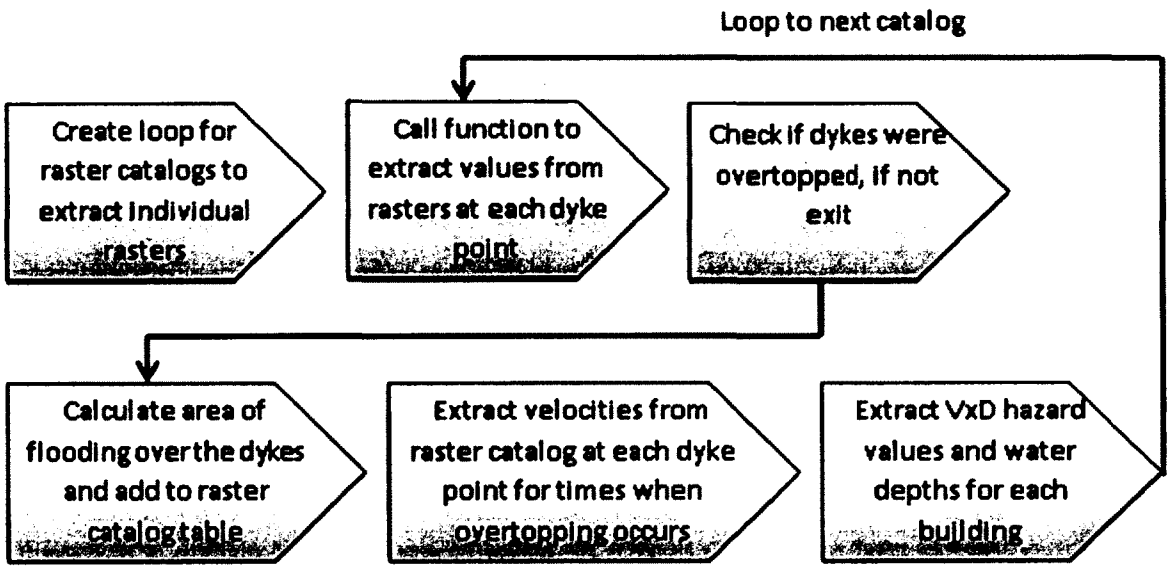

Figure A 6: Order of operations for the script used to associate raster values with vector features.

algorithm in SAGA GIS to delineate the channel and then Lake Pisiquid to the channel extent to create a 'wet' raster. By subtracting the wet raster from each result raster and counting the number of cells in each result, the flooding extent through time was calculated. Velocities at each dyke point with over 5cm of overtopping were then extracted using the same tool as before. Next, depth rasters and velocity depth product (VxD) values were extracted at each building using a version of the building polygon layer with a 2.5m horizontal buffer. When using the 'Extract Values to Table' tool with

polygons, all cell values intersecting a polygon are written to the table. The buffer was necessary so that after removing redundant tables and deleting extracted rasters; what was left were tables containing overtopping heights and velocities for each dyke segment, depth and VxD hazard values for each building polygon and raster catalogs updated with areas of inland flooding.

The output from extracting values did not contain the geometry of each point and polygon on which it was based. There are many values in the tables for each point and polygon so in order to be able to associate them with geometry, the outputs needed to be summarized using the Summary Statistics tool in ArcGIS. With this tool, the range of time a feature was exposed to a hazard could be found along with the hazard values through time and placed into a time series for plotting. Analysis of the distribution of hazard to structures was based on this output.

Analysis of rasters was also carried out in SMS. While SMS did not allow for running tools through scripts and automating processes, the timestep based mesh and scatter analysis tools were useful as all timesteps could be examined at once. Information about maximum areas and depths was produced using the SMS data calculator and zonal classification tools. As well as comparisons between results were carried out in SMS.

3.2.1 Methods for Examining Dyke Overtopping

Because dykes were included as breaklines, it was difficult to determine when the top of the dyke was overtopped. The points were on the corner of the output raster cells and in the mesh output, values were based on the ZH points while the ZV and ZU points

were altered by the geometry modification layer. Within TUFLOW, a plot output file can be specified which collects values at points as the model is running; however these values are also interpolated. The available tools were useful where the dyke point was definitively overtopped by flood waters but at the beginning and the end of a flood, neither the Extract Values to Table nor the Plot Output tools produced reliable results.